University of South Carolina

Scholar Commons

Fall 2020

A Novel Analytical Method for Studying Pharmacological Treatments for Affective Disorders in Neuroscience

Shane N. Berger

Recommended Citation

A NOVEL ANALYTICAL METHOD FOR STUDYING PHARMACOLOGICAL TREATMENTS
FOR AFFECTIVE DISORDERS IN NEUROSCIENCE

by

Shane N. Berger

Bachelor of Science
The Pennsylvania State University, 2015

_____

Submitted in Partial Fulfillment of the Requirements

For the Degree of Doctor of Philosophy in

Chemistry

College of Arts & Sciences

University of South Carolina

2020

Accepted by:

Parastoo Hashemi, Major Professor

Timothy J. Shaw, Committee Member

Ken D. Shimizu, Committee Member

Geoffrey I. Scott, Committee Member

Cheryl L. Addy, Vice Provost and Dean of the Graduate School

ii

DEDICATION

I would like to dedicate this dissertation to my family members for their steadfast support, always believing in me and pushing me to achieve my goals. I could not have done it without you all.

I would also like to dedicate this to the animals who have sacrificed their lives for science.

ACKNOWLEDGEMENTS

First and foremost, I would like to thank my advisor, Parastoo Hashemi, for her incredible support throughout my time in her lab. I have learned so much about myself over these years and your input and thoughtful discussions on science, life, and of course the intricacies of US and UK politics have helped me grow into a better person.

I would like to thank my committee members, Dr. Ferry, Dr. Scott, and Dr. Shimizu, for their thoughtful discussions and for pushing me to become a better scientist throughout graduate school. I would also like to thank Dr. Shaw for being able to sit in on my committee on such short notice; I really appreciated that.

The past few years have been wonderful getting to know past and present members of the Hashemi lab. Everyone has had a profound impact on me. I credit all my learning and development to the great people of this lab: Pavithra terrified me into learning electrochemistry; Rachel taught me innumerable things about science but most importantly, not to trust a 'ground wire' you found in a drawer; Thushani taught me if the elevator is broken, sometimes that's a sign to just turn around and go home; Srimal taught me everything I know about histamine experiments and how to 'just be good' at FSCV; Aya took me under her wing to ensure I learned everything about FSCV surgeries; Ou helped me think critically about data and experiments and I learned an incredible amount on our walks to and from work. Thoughtful discussions and venting with Melinda, Alyssa, Jordan, and Rhiannon made the highs and lows of the past years bearable and completely worth it. Anna Marie, Colby, Brenna, Lauren, and Melissa I cannot thank you enough for

iv

www.manaraa.com

the support over the years and helping me learn how to become a better mentor. There have been many undergraduate researchers during my time, Bruce, Evan, Ian, and Navid have all done an incredible amount of work in helping with histology and the consistent, tedious production of electrodes. Thank you all for everything.

I owe an immense amount of gratitude to my family for their support and dedication during these past few years. The endless phone calls of encouragement from my parents, my sister, my grandparents, and aunts, uncles, and cousins helped me stay motivated. The friends I've made along the way in Columbia and friends back home kept me grounded and reminded me there was always time for a hike or a beer. Emily, I cannot thank you enough for your unwavering support throughout the lows and celebrating the highs. Graduate school would not have been the same for each of us if we were not there for one another.

ABSTRACT

Histamine and serotonin are important neurochemicals that maintain crucial brain functions. Both are thought to be altered in affective and neurodegenerative disorders such as depression and Parkinson's disease. Histamine and serotonin are thought to modulate one another but the exact relationship remains unknown and this gap in knowledge makes diagnosing and treating disorders involving the transmitters difficult. The Hashemi lab studies serotonin neurochemistry to understand serotonin's role in psychiatric disorders. However, histamine has remained an understudied neurotransmitter due to a lack of analytical tools. In 2015 and 2016, the Hashemi lab pioneered a novel detection method utilizing fast-scan cyclic voltammetry (FSCV) for the real-time detection of histamine and serotonin *in vivo*. Using this method, we are able to visualize the real-time modulation of serotonin by histamine through H_3 receptors. The work herein furthers our understanding of the histaminergic system in the brain and its modulation of serotonin. First, we provided a review of analytical methods for monitoring neurotransmitters in the brain (Chapter 2). Then we pharmacologically challenged various aspects of the histaminergic systems of male and female mice and show the highly conserved nature of the brain (Chapter 3). This study also revealed that female mice may have a more tightly regulated brain histamine system controlled by cycling hormones. Next, we investigated the synaptic transport mechanisms of histamine and utilized a genetically modified mouse model to rule out the contribution of the serotonin transporter towards histamine clearance (Chapter 4). After we characterized the histamine system and its clearance mechanism, we applied histamine

FSCV to a chronic stress mouse model of depression (Chapter 5). We found brain histamine was elevated during chronic stress and inflammation; this has large implications given the comorbidity of psychiatric disorders and chronic inflammation. Finally, we investigated the effect of ketamine, the newly approved antidepressant and anti-inflammatory compound, on histamine transmission and subsequent serotonin modulation (Chapter 6). Collectively, this dissertation furthers our understanding of histamine and serotonin modulation and the mechanisms governing their transmission. Novel discoveries will provide necessary the insight to develop more efficient and targeted therapies for brain disorders.

TABLE OF CONTENTS

LIST OF FIGURES

x

LIST OF ABBREVIATIONS

BBB..Blood Brain Barrier

CFM ....Carbon Fiber Microelectrode

CMS .... Chronic Mild Stress

CNS.. Central Nervous System

CV ....Cyclic Voltammetry

DAT .... Dopamine Transporter

ERα/β..Estrogen Receptor α/β

FSCAV... Fast-Scan Controlled Adsorption Voltammetry

FSCV..Fast-Scan Cyclic Voltammetry

GABA .... γ-Aminobutyric Acid

HA...Histamine

HDC .... Histidine Decarboxylase

NET...Norepinephrine Transporter

NMDA .... *N*-Methyl-D-Aspartate

OCT.. Organic Cation Transporter

PMAT ....Plasma Membrane Monoamine Transporter

SERT.. Serotonin Transporter

SSRI.. Selective Serotonin Reuptake Inhibitor

TMN... Tuberomammillary Nucleus

VMAT.. Vesicular Monoamine Transporter

CHAPTER 1

INTRODUCTION

1.1 Brain Signaling *via* Chemical Transmission

A major paradigm shift occurred in the late 1950s and 1960s when the understanding of brain communication shifted from electrical signaling to chemical signaling.[1] The chemical messengers responsible for relaying signals from the brain to the periphery would come to be known as neurotransmitters. Histamine is a bioaminergic neurotransmitter responsible for myriad processes in both the peripheral and central nervous systems and is capable of modulating other chemicals in the body. One key neurotransmitter that histamine modulates is serotonin (5-hydroxytryptamine; 5-HT). The dysregulation of both histamine and serotonin have been implicated in psychiatric and neurodegenerative diseases like depression and Parkinson's disease.[2-5] Understanding the underlying chemical miscommunication is a critical component of diagnosing and accurately treating diseases of the brain and the absence of robust tools to do so hinders treatment advances. The Hashemi lab specializes in developing and using electrochemical tools to understand the unique neurochemistry of histamine and serotonin *in vivo* in rodents. Relative to the serotonergic system, the histaminergic system remains understudied in the context of psychiatric and neurodegenerative diseases, especially when studied simultaneously. The Hashemi lab optimized an electrochemical technique that allowed for simultaneous, real-time, in vivo detection of histamine and serotonin in rodent brains. This current work furthers our understanding of the CNS histaminergic system and

the implications in inflammatory states. The focus of this dissertation will be analyzing and understanding the modulatory effects of histamine on serotonin in healthy and inflammatory states using electroanalytical chemistry. This will be accomplished in several chapters: 1) Reviewing analysis methods for neurotransmitters; 2) Investigating differences between the male and female histaminergic system in the context of pharmaceutical challenges in mice; 3) Studying the transport mechanisms of histamine in the CNS; 4) Determining how histamine is altered in models of inflammation and neurodegeneration; and 5) Investigating how an atypical antidepressant affects histaminergic signaling.

1.1.1 The Histaminergic System

Histamine is a key bioamine neurotransmitter that has roles in circadian rhythm, arousal, appetite, and inflammation. [6-9] The enzyme L-histidine decarboxylase (HDC) is responsible for transforming histamine's precursor molecule, the amino acid L-histidine, into histamine in the tuberomammillary nucleus (TMN) located in the hypothalamus. [6-7] Similar to other monoamine neurotransmitters (i.e. serotonin, dopamine, or norepinephrine), histamine is stored neuronally until its release, at which point it is packaged into vesicles *via* the vesicular monoamine transporter protein (VMAT). [10-13] Whereas serotonin, dopamine, and norepinephrine each have their own active, high-affinity transport mechanisms (serotonin transporter, SERT; dopamine transporter, DAT; norepinephrine transporter, NET), an analogous transport protein for histamine has not yet been identified. [14-16] Brain histamine is thought to be exclusively degraded to *tele*-methylhistamine by the intracellular histamine *N*-methyltransferase enzyme. [17] It can then be further degraded into *tele*-methylimidazoleacetic acid *via* monoamine oxidase B and

2

aldehyde dehydrogenase.[18-19] It is worth noting that this metabolic route is only available for central histamine; peripheral histamine undergoes its own specific degradation through diamine oxidase.[14]

From the cell bodies in the TMN, histamine neurons project widely throughout the brain and spinal cord with the densest innervations ascending to the hypothalamus.[20-21] There have been four receptors identified associated with the histaminergic system: H_1R, H_2R, H_3R, and H_4R, all of which belong to the rhodopsin-like family of G protein-coupled receptors.[6] Receptors H_1, H_2, and H_3 are expressed in large amounts throughout the brain and while there is some recent evidence for H_4R mRNA expression in neuronal cells and microglia, the science remains unsettled.[6, 22-25] However, it is important that H_4R are widely expressed in mast cells which can cross the blood brain barrier (BBB).[26-27]

The H_1 receptor is post-synaptically located and activation leads to neuronal excitation. Arousal and feeding behavior have been linked to H_1R activation using knockout models to visualize behavioral deficits associated with H_1 impairment.[28-32] Common over-the-counter antihistamines (diphenhydramine and loratadine; brand names Benadryl® and Claritin®, respectively) target this receptor to block H_1 activation and signal propagation. H_2R is expressed throughout the brain and localized post-synaptically similar to H_1R, but is more consistently localized with HA projections.[33-34] Particularly high expression is found in the amygdala and hippocampus where H_2R deficient mice display cognitive impairments.[35] Additionally, H_2R targeted therapies are commonly prescribed for the alleviation of gastric disorders as H_2R has been shown to mediate gastric secretion.[36-37] The H_3 receptor, identified in 1983[38] and cloned in 1999[39], is unique in its location and ability. It is located presynaptically on HA neurons and functions as an

3

inhibitory autoreceptor controlling the release and synthesis of histamine.[40-41] H$_3$R is also able to exert modulatory control over other neurotransmitter systems through locations on presynaptic terminals of serotonin[42], dopamine[43], norepinephrine[44], glutamate[45], GABA[46], and acetylcholine.[47] As such, the H$_3$ receptor rapidly became a target for various therapeutic strategies.[48-50] Animals lacking H$_3$R show enhanced susceptibility to CNS inflammatory disease[51] and behavior abnormalities.[52] H$_4$R are the most recently identified receptor subtype and subsequently the least understood as briefly discussed in the previous paragraph.[53] The majority of H$_4$R expression is confirmed in the peripheral nervous system in mast cells, basophils, and hematopoetic cells playing a critical role in the recruitment and activation of inflammatory cells.[54-55] With similar function to H$_3$R, H$_4$R has also been highlighted for its therapeutic potential.[56]

1.1.2 Histamine's Role in Neurodegenerative and Psychiatric Diseases

Dysfunctions of the histaminergic system have been linked to physiological and behavioral abnormalities. In post-mortem analyses of patients diagnosed with Huntington's disease, a significantly lower H$_3$ receptor density was observed in areas of the dorsal striatum suggesting indirect impaired control of motor function neurons.[57] Significant decreases in tuberomammillary neurons and H$_1$ receptor binding are observed in Alzheimer's disease patients.[58-60] H$_1$R knockout mice show pronounced impairment of spatial learning and memory and reduced neurogenesis.[61] Decreased histamine throughout the CNS paired with blunted neurogenesis may partially explain the cognitive decline seen in AD patients. Parkinson's disease (PD) patients have significantly higher histamine levels in the brain compared to age matched controls and show alterations in histamine receptor expression density.[62-63] Similar results have been found in a rodent model of PD.[64-65]

4

Growing evidence highlights histamine's role in psychiatric disorders like depression and anxiety. Histamine receptor binding was significantly less in patients with major depressive disorder compared to age-matched controls *via* positron emission tomography.[66] Recently, an HDC knockout mouse revealed that chronic histamine depletion induced depression-like phenotypes and impaired memory analyzed by the tail suspension, elevated zero maze, and Y-maze tests.[67]

1.1.3 Histamine's Role in Inflammation

Histamine is most well-known for its role in the immune system and inflammatory state. It is a critical signaling molecule that recruits pro-inflammatory proteins and markers to the site of a foreign body response.[68] The foreign body response can range from something as common as the immune reaction to a splinter to oxidative stress in Parkinson's disease. These examples highlight two distinct locations, the splinter in the peripheral nervous system – systemic inflammation – and oxidative stress – neuroinflammation. Systemic inflammation is marked by upregulation of microglia, recruitment of proinflammatory cytokines and a local increase in histamine levels.[69] While neuroinflammation produces similar chemical markers, the effect on local levels of histamine remains unclear for several reasons. First, the brain is a unique, dynamic medium that is analytically challenging to probe. Secondly, histamine is present in the brain at extremely low concentrations (nM-µM), therefore, techniques must possess the selectivity and sensitivity to capture these low concentrations. Third, histamine, itself, presents a distinct fundamental challenge to overcome due to 'the observer effect' – meaning, to measure histamine a probe must be inserted into the area of interest (*eg*. brain). This action inevitably causes a disruption of tissue and cellular communication and registers a foreign

5

body response. The inflammation resulting from probe insertion causes an inherent perturbation in histamine levels in the surrounding tissue that can result in techniques reporting varying concentrations of histamine.

1.1.4 Sex Mediated Differences in the Histaminergic System

In 2015 the National Institutes of Health (NIH) ruled that all NIH funded research involving pre-clinical animal models must consider sex as a biological variable.[70] Previously, the majority of pre-clinical research was conducted using only the male sex to avoid complications from the female estrous cycle.[71] This has led to several instances of untranslatable research between animal models and humans.[72] Estrogen is shown to be a major regulator of eating behavior, lordosis, and anxiety through estrogen receptor alpha and beta (ERα; ERβ) in the ventromedial nucleus (VMN) of the hypothalamus.[73-75] In the VMN, H$_1$R and ERα mRNA are co-expressed in histaminergic neurons.[73, 76] ERβ is not as strongly expressed in the VMN as ERα but is expressed in the TMN where histaminergic projections originate.[77] The localization of estrogen receptors on histamine projections highlights the potential role estrogen plays in regulating immune response. Indeed, estrogen and progesterone have been shown to mitigate the acute inflammatory response to lipopolysaccharide exposure.[78-81] Additionally, inflammatory diseases and the susceptibility to the occurrence of diseases are more likely in post-menopausal women than pre-menopausal women and age matched males.[82-83]

1.1.5 Classical Versus Atypical Antidepressants

Since the discovery that the main therapeutic effects of early antidepressants were due to targeting the monoaminergic systems of dopamine, norepinephrine and serotonin, the field has remained focused on optimizing strategies to increase levels of these in the

6

brain.[84] Broadly, these monoamine targeting antidepressants are grouped into 'classical' antidepressants adhering to the monoamine hypothesis, but research drive for these classic antidepressants has steadily weaned.[85-86] At the turn of the century a revised monoamine hypothesis was being constructed that brought the glutamatergic system to the forefront.[87] The modulatory roles that glutamate and GABA play on the monoamines is being explored as a new potential therapeutic route for antidepressants.[88] Ketamine, an NMDA receptor antagonist, became a molecule of interest for its rapid acting antidepressant activity when administered in subanesthetic doses.[89] The exact mechanism(s) of the new rapid acting antidepressants are still unknown and its clear they involve several complicated biochemical pathways.[90-95] As an antidepressant and anti-inflammatory, we are interested in understanding ketamine's effects on central histamine.

1.1.6 Motivation for this Dissertation

Given the information above, exploring the fundamental neurochemical actions of histamine within the brain presented a unique and challenging opportunity. The Hashemi lab is deeply focused on the chemical underpinnings of psychiatric diseases, specifically depression, and the nexus of histamine and serotonin holds the potential of being a rich body of information. Therefore, my work herein, focuses on furthering the community's understanding of the relationship between the histaminergic and serotonergic systems and their co-modulation. As mentioned above, measuring chemicals in the brain is a great challenge; requiring technical ability in addition to niche tools that fulfill strict criteria. An ideal method must have the *selectivity* to discern between structurally and chemically similar neurotransmitters and metabolites, high *sensitivity* to monitor the low extra-synaptic analyte concentrations, a high *temporal resolution* to capture the sub-second

7

neurotransmission process, and the micro- *dimensions* to target specific brain regions of interest while causing minimal disruption to the surrounding tissue *in vivo*. Electrochemical methods utilizing carbon electrodes are promising for such a challenging task.

1.2 Analysis of Neurotransmitters in the Brain

The brain is a dynamic medium in a delicate homeostasis. As stated above, monitoring the chemicals present in the brain necessitates *selectivity, sensitivity, temporal,* and *size* requirements. Detection and quantification methods can be delineated into two main categories: microdialysis (followed by separation and detection) and direct electrochemical analysis, each with their respective benefits and drawbacks. For the purposes of this dissertation, only electrochemical methods will be discussed.

Electroanalytical methods are favorable for neurochemical analyses due to the ability to quantify species through direct oxidation and reduction. Carbon electrodes have proven to be the most commonly used implantable electrochemical probe due to its relative inertness, abundance, cost efficiency, wide potential window, and rich surface chemistry.[96-97] Specifically, carbon fiber microelectrodes (CFMs) are extensively used in the field of monitoring neurotransmitters as they are biocompatible, stable, minimally invasive, and have favorable electrochemical properties.[98] The CFM surface is an electrochemically rich environment covered in striations and electrostatically charged oxygen functionalities (-OH, C=O, COOH/COO$^-$) that result in an adsorptive substrate.[99] Thus, the CFM is a go-to tool for direct electrochemical analysis of neurotransmitters *in vivo*.

1.2.1 Electrochemical Methods Utilizing CFMs

CFMs are covered in striations that create a rich surface for electrochemical activity. The obvious drawback of electroanalytical methods is the key criterion that an

8

analyte of interest must be readily oxidizable in the given potential window of the electrode material. Several key bioamines in the brain, dopamine, serotonin, and histamine, are in fact oxidizable within the potential window for carbon. In the 1960s, Ralph Adams conducted his seminal work using crudely fabricated carbon paste disc electrodes constructed from graphite powder mixed with mineral oil packed into Teflon tubing.[100] These electrodes were used to carry out foundational electrochemical analyses of catecholamines.[101-102]
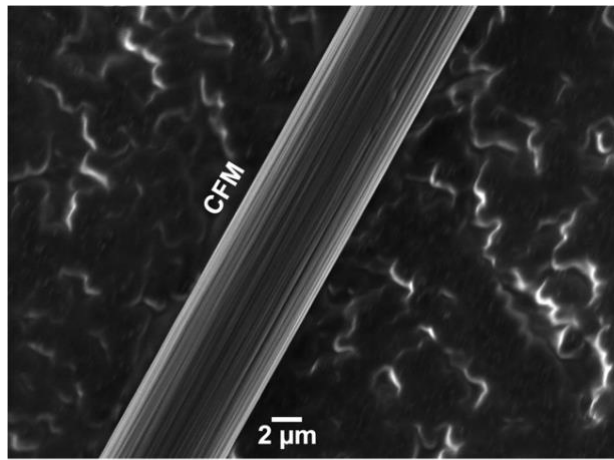
Figure 1.1: A scanning electron micrograph of a carbon fiber microelectrode.

Amperometry involves holding an electrode at a constant potential while measuring the current from analytes undergoing oxidization at the surface. This method excels at temporal resolution (< 1 ms) as oxidation is only limited by diffusion to the electrode surface since potential is constant.[103] Unfortunately, holding at a specific voltage oxidizes all analytes with oxidation potentials under that voltage and, thus, amperometry suffers from a lack of chemical specificity which is critical when probing the brain. Amperometry at carbon disks, fibers, and microelectrode arrays has been used extensively to study the vesicular events of single cells *ex vivo*.[104-105] These studies aim to further the understanding

9

of neurotransmission by studying vesicle fusion pore size, duration, and the amount of contents release during an event.[106-107]

Chronoamperometry was developed to increase the selectivity afforded by amperometry. Chronoamperometry uses a square wave step function between an upper and lower potential limit. The ratio of peak oxidative current to peak reductive current is able to yield information about the analyte identity. There is a large capacitive (non-faradiac) current associated with potential pulse that decays rapidly, while the faradiac current decays more slowly over time. Analyte information is obtained through the relationship of redox current over time. This technique has been used to study psychiatric models[108], transport kinetics[109-110], and drugs of abuse.[111] Despite its improvements over amperometry, chronoamperometry is still limited in scope and selectivity.

1.2.2 Fast-Scan Cyclic Voltammetry

Pioneered by R. Mark Wightman and Julian Millar in the mid 1980s, fast-scan cyclic voltammetry (FSCV) (originally termed fast cyclic voltammetry) emerged as a new, selective method to monitor the release and reuptake of dopamine *in vivo* by direct electrochemical means at CFMs.[112-113] FSCV has become a primary technique used by electrochemists, neuroscientists, and pharmacologists to monitor neurochemicals in the brain. As in traditional cyclic voltammetry, FSCV uses the combination of 2 or more linear voltammetric sweeps (*eg*. A → B → A) while measuring the current from redox processes occurring at the working electrode. This set of instructions that dictates how the potential of the working electrode is changed with respect to time is called a waveform and is the primary source of selectivity. FSCV employs significantly faster scan rates (100s – 1000s V s^{-1}) than traditional cyclic voltammetry (typically <100 mV s^{-1}) that result in a large

10

capacitive current. This necessitates background subtraction to remove it. Therefore, FSCV is only capable of recording changes in a system and reports data as a change from baseline. *In vivo,* this change is typically induced through electrical, pharmacological, or optical stimulation of neurotransmitter release.[114-116]

An FSCV data set is collected on a sub-second timescale. The fast scan rate results in the potential window being traversed in <10 ms, and the application frequency of 10 Hz allows for analytes to preconcentrate on the electrode surface at the holding potential for >90 ms, thereby increasing sensitivity. Scanning from the resting potential to the positive limit is called the anodic scan, where oxidation of the analyte will occur. Once the limit is reached, the scan direction is switched, and the cathodic scan begins, during which reduction occurs, until the negative limit is reached. The rapid switch in scan direction results in the aforementioned large capacitive current due a phenomenon known as the electrical double layer.[117-118] Data obtained through a complete scan of the waveform is plotted as current vs voltage to create an analyte-specific cyclic voltammogram (CV) used for both qualitative and quantitative analysis. FSCV software collects the CVs and stacks them in chronological order to construct a 3D plot of current vs voltage vs time. For ease of interpretation, 3D plots are visualized from a bird's-eye view, termed color plots, where current is assigned a false color as seen in **Figure 1.2A**. Importantly, a vertical line through the color plot provides the CV and a horizontal line will detail how current is changing over time.

It was only recently that FSCV was expanded for the analysis of neurochemicals other than dopamine *in vivo*. Serotonin detection *via* FSCV is very difficult due to low extracellular concentrations and the metabolite, 5-hydroxyindoleacetic acid, is present at

11

much higher concentrations and fouls the electrode surface.[119] To overcome the surface fouling, a thin layer of Nafion, a cation exchange polymer, is electrodeposited onto the CFM.[119]
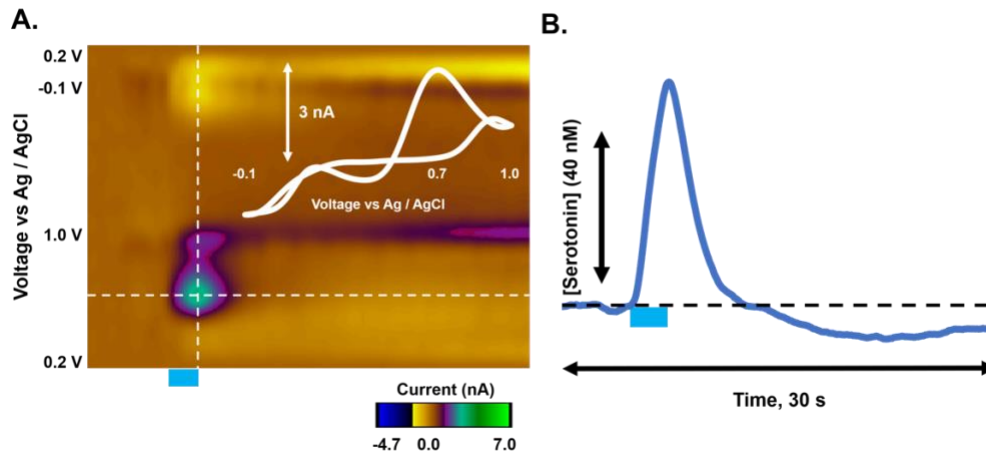
Figure 1.2: Serotonin FSCV(**A**) Representative serotonin color plot with a characteristic serotonin CV inset. The green event corresponds to serotonin oxidation occurring around 0.7 V. Abstracting the vertical dashed line will reconstitute the inset CV. (**B**) Concentration vs time profile for the stimulated release and reuptake of serotonin. **B** is obtained by following the horizontal dashed line in **A**. The light blue bar at the bottom represents the 2 s electrical stimulation.

We measure serotonin dynamics in the CA2 region of the hippocampus by stimulating a dense tract of nerves that innervate numerous brain regions called the medial forebrain bundle (MFB). **Figure 1.2** shows a typical data set obtained for the stimulated release of serotonin in the CA2. **Figure 1.2A** is a representative serotonin color plot with an inset CV in the right corner. Interpretation of the color plot is described in detail elsewhere.[120] Briefly, time is on the x-axis, voltage is on the y-axis, and current is represented in false color. The green event corresponds to the oxidation of serotonin around 0.7 V. **Figure 1.2B** shows a typical profile of stimulated serotonin release and reuptake over time as [5-HT] vs time. Background is collected for 5 s followed by a 2 s stimulation, denoted by the light blue bar, resulting in the release of serotonin which reaches a

12

maximum amplitude around 7.5 s where the rate of reuptake now overtakes the rate of release following the end of the stimulation and the curve decays to baseline as serotonin is reuptaken into the cells.

In 2015, the Hashemi lab expanded the scope of FSCV once again by pioneering a novel, selective waveform for the detection of histamine *in vivo* that scans from -0.5 V to -0.7 V to 1.1 V to -0.5 V at 600 V s^{-1}.[121] This method is not only able to detect histamine but also serotonin simultaneously due to the potential window encompassing both neurotransmitters' oxidation potentials.[122] Using this technique, we showed that the stimulated release of histamine results in the rapid inhibition of serotonin release in the posterior hypothalamus of mice.[122] Shown in **Figure 1.3A** is a representative color plot of the stimulated histamine release and subsequent serotonin inhibition. The green event corresponds to the release and reuptake of histamine and the blue/black event corresponds to the inhibition of serotonin. What is important to reiterate here is that FSCV is background subtracted and therefore only captures changes. The serotonin event is shown in blue, or negative current, which is only denoting that serotonin is decreasing with respect to its pre-stimulation levels. It is still occurring around 0.7 V, which is serotonin's oxidation potential for FSCV. The stimulated release of histamine is shown in green because it is increasing with respect to its ambient concentration. Histamine FSCV uses a stimulation of the MFB to elicit the release of neurotransmitters, albeit a different placement along the tract to minimize serotonin release. **Figure 1.3B** shows the corresponding concentration vs time plots for both histamine and serotonin together to better visualize the release-inhibition relationship. Following stimulation (light blue bar) [histamine] increases (blue; top trace) and returns to baseline while the inhibition of [serotonin] (red; bottom trace) can

13

be seen as it reaches peak inhibition slightly after histamine's peak release and returns to around 20 nM. Figure **1.3C** is a representative CV collected for histamine FSCV. It is visually very different than a serotonin CV and difficult to interpret. The broad peak around 0.2-0.3 V represents HA oxidation and the inverted peak around 0.7-0.8 V represents the serotonin oxidation (the oxidation peak is inverted due to serotonin levels decreasing with respect to ambient levels).
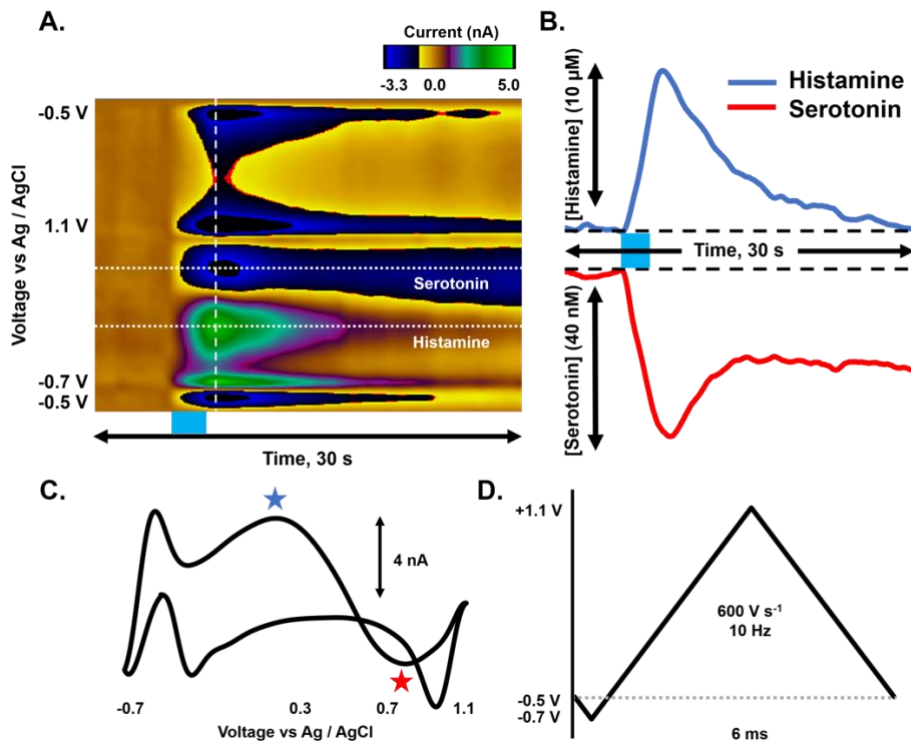
Figure 1.3: Histamine fast-scan cyclic voltammetry in the mouse posterior hypothalamus. (**A**) Representative histamine FSCV color plot. The green event is stimulated histamine release (labeled 'histamine') and the blue even is the subsequent inhibited serotonin (labeled 'serotonin'). (**B**) Release and inhibition vs time profiles of histamine (blue) and serotonin (red), respectively. Stimulation is shown as the light blue bar. (**C**) Characteristic histamine CV. Blue star shows the typical histamine peak around 0.3 V and red star shows the inverted serotonin oxidation peak around 0.7-0.8V. (**D**) Histamine FSCV waveform.

The development of this novel waveform that enables the monitoring of two neurotransmitter systems simultaneously provides a tool to obtain critical information

14

about the modulatory relationship between histamine and serotonin and widens the scope of questions we are able to ask about the brain.

1.3 Scope of the Dissertation

In this dissertation, I first provide a review of analysis methods for neurochemicals in the brain (Chapter 2). I then use histamine FSCV to characterize the male and female histaminergic system and their respective response to pharmaceutical challenge *via* voltammetry (Chapter 3). I then further investigated the reuptake mechanisms of histamine in male and female mice through use of a genetic mouse model (Chapter 4). After gaining an understanding of the functionality of the histaminergic system, I apply histamine FSCV to a model of chronic inflammation: behaviorally depressed mice (Chapter 5). Finally, I used histamine FSCV to understand the effects of a new 'atypical' antidepressant on the modulation of histamine and serotonin (Chapter 6). An outline of this dissertation is described below:

Chapter 1: Introduction

Chapter 2: Review of methods for neurochemical analysis in the brain.

Chapter 3: This chapter describes the voltammetric investigation of the histaminergic system. I pharmacologically challenged receptors, synthesis, packaging, and metabolism of histamine to determine how synaptic histamine responds in male and female mice. Additionally, I investigated histamine release throughout the estrous cycle of female mice and sexual differences in H_3R targeting drugs.

Chapter 4: This chapter builds upon previous work that investigated the transport mechanisms of histamine. We determined SERT, NET, and OCT may all play a role in

histamine uptake. I used a genetically altered mouse model (Met172) with a SERT that is insensitive to certain SSRIs to rule out SERT's contribution to histamine uptake.

Chapter 5: This chapter covers the application of histamine FSCV to an animal model of inflammation. I analyzed the evocable histamine levels in behaviorally depressed mice (chronic mild stress paradigm) and compared that to age matched controls.

Chapter 6: This chapter describes the response of histamine and its modulation of serotonin in response to a new 'atypical' antidepressant, ketamine. Ketamine doesn't directly target the monoaminergic systems like traditional antidepressants (*eg*. SSRIs). I found that ketamine caused a rapid and sustained inhibition of stimulated histamine release and greatly alleviates the inhibition of serotonin levels in the posterior hypothalamus.

Chapter 7: The final chapter summarizes the conclusions of my work and highlights future directions of research for histamine FSCV.

CHAPTER 2

BRAIN CHEMISTRY | NEUROTRANSMITTERS[1]

---

[1] Berger, S.N.; Hashemi, P. (2019). Brain Chemistry | Neurotransmitters. In Worsfold, P., Poole, C., Townshend, A., Miró, M. (Eds.), Encyclopedia of Analytical Science, (3rd ed.). vol. 1, pp 316-331, Elsevier.
Reprinted with permission from Elsevier.

2.0 Abstract

This chapter focuses on analytical detection methods for measuring neurotransmitters *in vivo*. The discussion begins by outlining the challenges of *in vivo* neurotransmitter analysis. Then, microdialysis, an *in vivo* sampling method, is critically described. Subsequently, three methods of direct detection of neurotransmitters are presented in terms of their advantages and disadvantages. Finally, future directions of monitoring brain chemistry are prospectively explored.

2.1 Introduction

Neurotransmission is the essential mechanism *via* which brain cells communicate. This process is fundamental to all aspects of brain function. Briefly, biochemical impulses arrive at the initiating, or presynaptic, cell that cause neurotransmitter-filled vesicles to fuse with the cell's membrane. The neurotransmitter contents of these vesicles are then expelled into the small gap preceding the receiving or postsynaptic cell, called the synapse. The neurotransmitter then interacts with a postsynaptic protein (receptor), relaying the biochemical message from the presynaptic cell *via* initiation of a signaling cascade. The neurotransmitter is subsequently inactivated in the synapse either through reuptake back into the presynaptic cell *via* transporter proteins and/or enzymatic catabolism directly in the synapse. This process is fast (sub-second), the levels of transmitters are low in the extracellular space (nanomolar) and the synaptic space is tight (nanometers). Taken together, these characteristics immediately render an investigation of neurotransmission a difficult analytical challenge.

Meaningful analytical measurements of neurotransmitters are highly significant, since there is a clear gap in the understanding of the chemical underpinnings of brain

pathophysiology. This shortcoming makes it almost impossible to accurately diagnose and treat disorders of the brain. A clearer definition of the roles of neurotransmitters in health and disease would greatly enhance the ability to improve diagnostic and therapeutic approaches to the brain.

Analytical chemists have developed a suite of tools for analysis of the low concentration of neurotransmitters within the dynamic and harsh environment of the brain. Each method possesses inherent advantages and shortcomings. This module represents an overview of cutting-edge analytical approaches for neurotransmitters. The discussion begins with an outline of the analytical challenges for monitoring neurotransmitters. Two major classes of analytical methods, microdialysis, an *in vivo* sampling technique, and direct detection at microelectrodes, are highlighted in the context of their pros and cons. While the majority of work cited focuses on *in vivo* analysis, we chose to include work on single cell exocytosis. We believe there is much value in understanding fundamental mechanisms of neurotransmitter function *via* these single cell models. Cutting-edge advances in development or applications of these methods are showcased. Finally, the future of neuro-analytical chemistry is prospectively discussed.

2.2 Analytical Challenges for Measuring Neurotransmitters

Neurotransmission occurs as a function of many simultaneous processes that control extracellular neurotransmitter levels. To characterize the chemistry of neurotransmission, ideally two types of measurements are necessary. First, is the ambient extracellular neurotransmitter concentrations that depict the system at rest. Second, is the much faster, neurotransmitter release and reuptake events that define receptor, transporter

19

and catabolic activity. In the proceeding text we refer to these measurements as slow and fast measurements.

While slow and fast chemical measurements of neurotransmitters are the targets of analysis, there are several, chemical and non-chemical, criteria that need to be addressed for successful neuro-analytical measurements. These criteria are discussed below.

2.2.1 Biocompatibility

Chemical measurements, for the most part, involve direct implantation of a probe into the tissue. Implantation of foreign objects into the brain cause rapid and severe immune responses that serve to isolate the object from surrounding tissue.[1-2] This renders electrochemical measurements during immune attack very challenging.

Metal substrates, such as Ag and Pt, are excellent laboratory probes because they are inert. However, these materials are not ideal for implantation into the brain because of a robust immune response arising primarily because Ag or Pt are not readily found in mammalian bodies.[3-4]

One strategy being explored to alleviate the immune response occurring from implantation is the controlled release of therapeutic compounds through polymer coatings. For example, the Schoenfisch lab at the University of North Carolina has been developing methods to control the release of nitric oxide, an immune mediator, from polyurethane coated glucose biosensors.[5-7] Another approach is to utilize a fundamentally biocompatible material, which the body does not immediately perceive as foreign. A good example of this is carbon. Carbon has been shown to be biocompatible and maintain its measurement capabilities over days to weeks.[8] This material has been fashioned into innumerable forms, the most popular of which in neuroanalysis are carbon fiber electrodes.[9-10] Furthermore,

20

carbon electrode surfaces can easily be manipulated with polymer coatings or structural moieties (e.g. carbon nanotubes and nanotube yarns) to increase selectivity to a specific analyte.[11-15]

2.2.2 Invasiveness

Damage created by insertion of a probe is a profound consideration. The distance through which neurotransmitters relay their biochemical messages are 10s of nanometers, thus, the measuring probe must retain its dimensions as small as possible.

Capillaries are responsible for blood transport throughout the brain and create the blood-brain barrier *via* their connection with astrocytes. If the blood-brain barrier is compromised, brain homeostasis can be severely disrupted. The intercapillary distance dictates the size of probe that can be introduced into brain tissue without rupturing the blood-brain barrier. This distance varies between brain regions in rodents but does not exceed ~30 μm.[16-17] Intercapillary diameter is inextricably linked with the biocompatibility of a probe, as any material large enough to compromise the blood-brain barrier will induce an immune response. Therefore, microelectrodes with one dimension under ~30 μm show the most promising outlook to qualify as minimally invasive. When met, the criteria of biocompatibility and minimal invasiveness allow for probes to remain in tissue for weeks or months without evidence of gliosis.[8] Currently, sample methods are not typically able to employ < 30 μm probes but the miniaturization of standard techniques like microdialysis is actively being pursued. One of the limiting factors in the size of microdialysis probes is the sample membranes are prefabricated. Decreasing probe size is limited by perfusate channels and reasonable flow rate. Microfabricated silicon microdialysis probes have been created with 70 µm x 85 µm and 45 µm x 180 µm thick sampling areas.[18-19] While

21

microdialysis is limited in its size, the technique is widely applicable and recently a method has been developed to alleviate the inevitable penetration injury response. Retrodialysis with an anti-inflammatory compound, dexamethasone, has been shown to drastically reduce symptoms of probe damage.[20]

2.2.3 Temporal Resolution

To study slow vs. fast changes fundamentally different time scales are required. Slower shifts in ambient neurotransmitter levels can be captured with measurements every minute to 10s of minutes. However, the fast changes that correspond to transmission necessitate sub-second temporal resolution analysis. Of the methods surveyed below, microdialysis serves to provide information about slower ambient level shifts while fast voltammetric methods indicate the sub-second neurochemistry of the analyte. In recent years, however, fast voltammetric methods have been modified to provide ambient level information.[21-23]

For exocytosis analysis, amperometric methods at single cells provide microsecond temporal resolution that resolves mechanistic information about exocytotic events.[24-27]

2.2.4 Sensitivity and Selectivity

Chemical messengers in the brain are present at very low concentrations, typically in the nanomolar to low micromolar range.[21, 23, 28-29] Additionally, there are many structurally and chemically similar analytes (precursors and metabolites). Thus, a high degree of sensitivity and selectivity (i.e. the ability to discern between analytes) is necessary for neurotransmitter analysis. For sampling methods such as microdialysis these criteria are less of a challenge since the ability to prepare the sample *ex-vivo* provides many opportunities to improve sensitivity and selectivity. With direct analysis, however, it is

much more challenging to acquire both a high level of sensitivity and selectivity. Thus, most direct analysis is limited to one, at most, two analytes.[12, 30-33]

2.3 Neurochemical Analysis Methods

For the purposes of this section, we chose to breakdown neurotransmitter analysis into two main factions: **1)** A technique based on sampling, followed by detection, namely microdialysis and **2)** direct detection at microelectrodes.

2.3.1 Microdialysis

Microdialysis utilizes a probe that is implanted into brain tissue. This is a sampling method that uses a semi-permeable membrane to allow the selective diffusion of analytes into a collection stream, the dialysate. Microdialysis sampling can be used to study the effects of pharmacological agents on various endogenous systems or metabolism of the agents themselves. The method can also be utilized for delivery of pharmaceutical agents. Following sample collection, the dialysate is coupled to a secondary analysis system such as liquid chromatography - mass spectrometry[34-37] or biosensors.[38-40] A key advantage of microdialysis is its ability to monitor multiple analytes.

2.3.1.1 Microdialysis Probes; Mitigating Tissue Damage and Immune Response

Microdialysis probes are typically between 200 and 300 μm in diameter, because recovery rate is directly proportional to porosity and surface area.[18, 41-44] These dimensions cause significant damage to brain tissue.[2, 45] This damage creates two primary issues; first, emanating from the probe is a concentric gradient of damaged cells extending around 250 μm[46] and sampling from this compromised tissue confounds data.[47] Secondly, microdialysis sampling devices greatly exceed the intercapillary distance in rodent brains (~30 µm). This means that when implanted into brain tissue, these probes damage blood

vessels, compromise the blood-brain barrier and induce a rapid inflammatory response. As such, profound gliosis has been observed around the microdialysis implantation site which reduces probe stability over time and impedes analyte diffusion into the dialysate stream.[20, 48-49]

To improve the integrity and longevity of microdialysis measurements, researchers have sought to a) mitigate the initial penetration damage *via* probe miniaturization and b) lessen the brain's immune response to probe implantation. We briefly discuss these two strategies below:

a) A good approach for reducing tissue damage caused by the microdialysis probe is to decrease the overall size. A significant dimension is the intercapillary diameter of ~30 µm in the mouse brain *(vide supra)*. To this end, Kennedy and colleagues are miniaturizing microdialysis probes. For example, a silicon microdialysis probe (45 µm x 180 µm) was microfabricated with a nanoporous membrane embedded onto the probe that functions as the sampling membrane.[18-19] A key disadvantage of probe miniaturization is the loss of recovery. At flow rates of 100 nL/min, Lee *et al.* only observed 2-21% recovery rates with the microfabricated silicon probe, which has been attributed to pore blockage.[18]

b) To reduce the brain's immune reaction to implanted probes, Michael and colleagues have shown that retrodialysis of an anti-inflammatory glucocorticoid, dexamethasone, greatly reduces glial scarring typically seen at microdialysis probe tracks.[50-51] Without dexamethasone treatment, electrically evoked dopamine release was not observable in tissue ~100 µm from probe

24

implantation nor at the dialysate outflow within 4 hours of implantation. However, following dexamethasone retrodialysis, dopamine release was restored in surrounding tissue and in the dialysate. Additionally, immunohistochemistry confirmed that dopamine transporters surrounding the probe track were preserved after dexamethasone treatment.[51] Furthermore, beneficial effects were observed for up to 5 days after cessation of dexamethasone perfusion.[49]

2.3.1.2 Improving the Temporal Resolution of Microdialysis

Perfusion rates through the microdialysis probe must be slow enough (typically 1-2 μL min^{-1}) to allow analytes to reach equilibrium with the solution inside the probe, facilitating sufficient recovery. This slow perfusion rate is one of the factors limiting the temporal resolution of microdialysis experiments to slower, ambient level changes, on the order of 10s of minutes.[46, 52] Increasing the perfusion rate would provide better temporal resolution, however this strategy is a trade off with sensitivity since a faster rate of perfusion would mean less time for analyte diffusion into the probe. Innovative solutions to this tradeoff are discussed below.

2.3.1.2.1 Liquid Chromatography Coupled to Electrochemical Detection

Ngo *et al.* reported *in vivo* monitoring of striatal dopamine in awake-behaving rats with under one-minute resolution *via* on-line liquid chromatography coupled to electrochemical detection. To achieve this sub-minute analysis, a previous separation[53] was modified by using an 8-port, 2-loop separation setup, increasing the sample volume from 500 nL to 600 nL and decreasing HPLC flow rate from 9.0 μL min^{-1} to 7.5 μL min^{-1}. This higher temporal resolution allowed a detailed view of the dopaminergic response to

25

pharmacological manipulation.[47] In a similar progression of experiments, serotonin was measured at 1-3 minute time resolution.[52, 54-56]

2.3.1.2.2 Microchip Electrophoresis

An alternative method to rapidly analyze microdialysis samples is microchip electrophoresis.[57-60] Microchip electrophoresis uses nL sample volumes and an applied electrical potential to separate analytes in dialysate that travels a series of conduits etched into a silicon-based wafer. Due to the small volume used and fast separation technique, microchip electrophoresis limits the band broadening of sample plugs.[61] This approach has pushed the temporal resolution of microdialysis sampling to under 60 s[62-63], reaching < 15 s.[64-67] In 2008, Wang *et al.* reported a microfluidic device that preserved sampling resolution *via* segmentation of the dialysate flow into nL droplets by introducing an immiscible oil.[68] The oil partitioned the sample stream into discrete pockets that minimized band broadening while allowing for <15 s temporal resolution. Recently, segmented flow has been applied to measurements of acetylcholine[69] and glutamine, glutamate and gamma-aminobutyric acid, simultaneously *via* nano-electrospray ionization mass spectrometry with 6 second time resolution at 100 nL min^{-1}.[70]

2.3.1.2.3 Enzyme Biosensing

Microdialysis has also been coupled to enzyme biosensing for rapid (30 s) analysis. An on-line rapid sampling microdialysis method was developed and applied to clinical microdialysate to visualize biochemical changes during patient surgery.[40, 71] In 2018, the resolution of clinical dialysate that had been collected off-line was compared to on-line dialysate. Samples stored at -80°C for up to 72 days showed good time alignment with

26

samples collected on-line.[38] A schematic of sampling from the brain to analysis by the biosensors is shown in **Fig. 1** below.
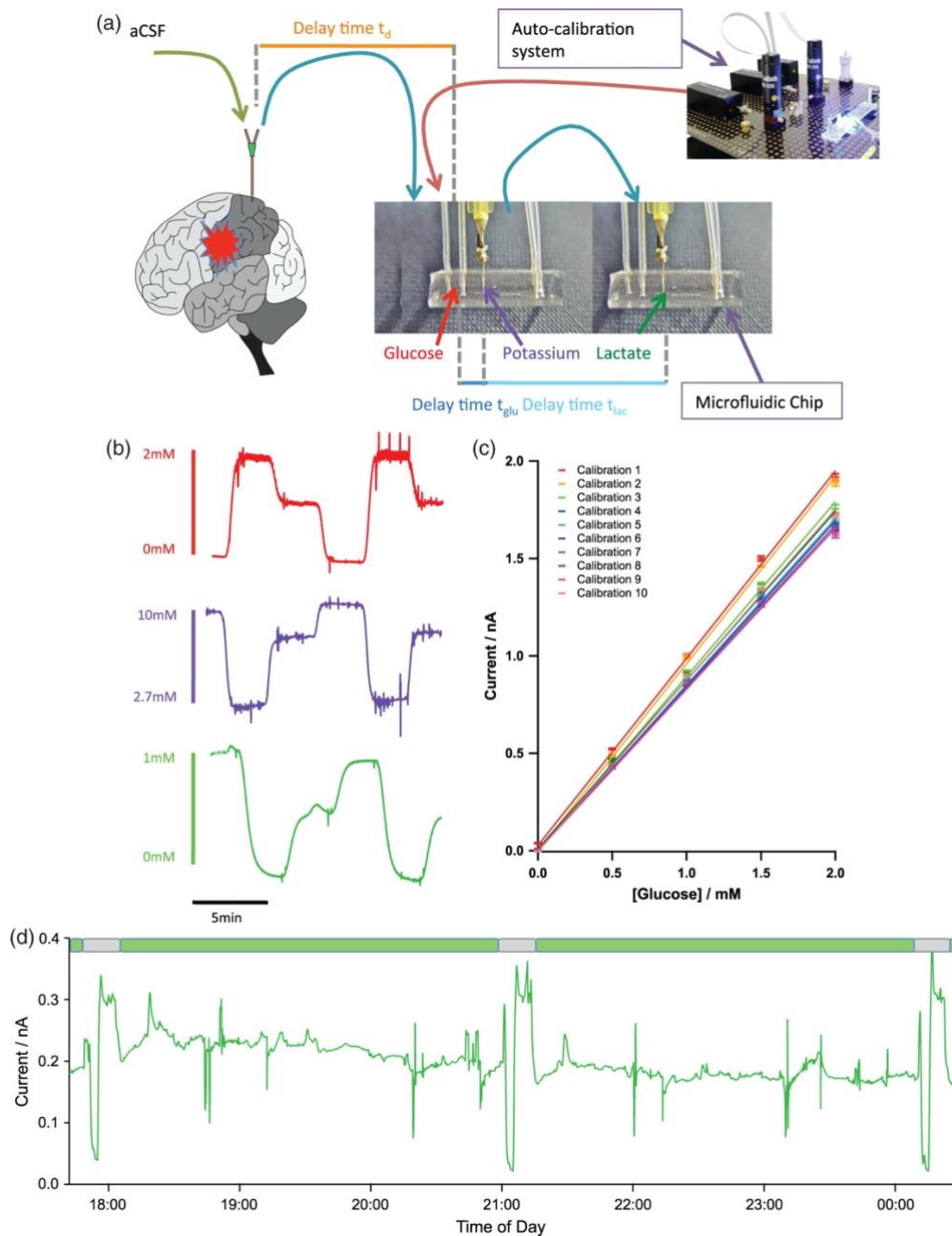
Figure 2.1: Continuous online microdialysis analysis system for bedside monitoring using microfluidic chips containing biosensors for glucose and lactate and a potassium ion selective electrode. (a) shows the overall setup. (b) Raw traces from glucose (red), potassium (purple) and lactate (green) during a computer-controlled three-point automatic calibration run. Concentrations indicated by legend. (c) Sequential analysis of sensor performance over 12 h

using automatic calibration. (d) Raw data for microdialysate brain lactate levels collected at the bedside with three automatic calibrations. The green boxes indicate sections of clinical data and the grey boxes indicate calibrations. Clinical data were collected from patient 2. Reproduced from Rogers, ML. *et al. J. Cereb. Blood Flow Metab.* **2017**, *37* (5), 1883-1895.

A method utilizing microdialysis sampling with on-line electrochemical detection for acetylcholine monitoring was reported by Lin *et al*. in 2015.[39] Dialysate flowed through a bioreactor with choline oxidase and prussian blue immobilized onto iron nanoparticles. The enzyme-catalase pair removed choline (and subsequent peroxide) present in the dialysate thus ensuring accurate quantification of acetylcholine at the detector.

2.3.2 Direct Detection of Neurotransmitters

In the following section we outline three methods of direct neurotransmitter analysis: enzyme biosensors, amperometry, and fast-scan cyclic voltammetry (FSCV). The biosensor and FSCV studies included here measure *in vivo* neurotransmitter concentrations while the amperometry studies investigate exocytosis at single cells *ex vivo*.

2.3.2.1 Biosensors

Biosensors play a powerful role in the toolbox of neuro-analytical methods as they are capable of monitoring traditionally non-electroactive molecules. Biosensors are chemical detection platforms that produce a quantifiable signal proportional to a specific analyte following an enzymatic reaction at a sensor surface.

The majority of biosensors designed for neurotransmitter analysis rely on oxidation of enzymatically generated hydrogen peroxide as a direct proxy of analyte concentration.[72-74] Inclusion of a size exclusion polymer is necessary to isolate the electrode surface from interferences while still allowing hydrogen peroxide diffusion. Two commonly used polymers are a Nafion-polypyrrole combination or 1,3-phenylenediamine.[72-74]

28

Microfabrication of biosensors produces microarray electrodes composed of multiple individual sensing sites on one ceramic substrate. A microarray of four electrodes can be isolated to create two enzyme sensors and two *in situ* control sensors.[75]

There have been many biosensors created for a myriad of substrates since their introduction in the late 1960s[76-79] Neurotransmitter biosensors utilize enzymes that are responsible for the endogenous break down of the analyte, *i.e.* glutamate oxidase for the metabolism of glutamate. These sensors often exhibit promising results *in vitro* but *in vivo* applications of biosensors in the brain are severely limited.[1, 80-81] The two primary challenges for *in vivo* biosensing are a) biosensors are large (typically >300 µm) relative to brain tissue (see above for issues with large probes and neurotransmitter measurements) b) biosensors rely on immobilized enzymes which have poor stability. We next discuss these issues briefly.

Biosensors are typically hundreds of microns in 2 or all 3 dimensions.[82-85] Furthermore, metals like platinum (Pt) often serve as the electrode platform. Both the large dimensions and presence of metals like Pt serve to trigger inflammation and gliosis around the implantation site, that creates analysis limitations as described above.[86] This foreign body reaction dramatically reduces device stability. Two strategies are being explored to decrease the probe size and reduce local inflammation. First, the Sombers lab at NC State has been pioneering the immobilization of glucose oxidase onto carbon fiber microelectrodes for successful *in vivo* glucose measurements.[87] The probe that is utilized has a *substantially* smaller footprint than traditional biosensors at 25 µm diameter and 100 µm length. These probes were further optimized to simultaneously detect glucose and dopamine.[88] Second, the Schoenfisch lab at UNC are on the forefront of increasing the

29

longevity of *in vivo* placement of biosensors by applying nitric oxide releasing polymers. There are analytical challenges associated with nitric oxide loading into polymers, undesired leaching over time and controlling the release parameters of the polyurethane coating.[7, 89] Despite current working challenges, this technique has shown promising results in swine *in vivo* implantation for several days.[5-6]

Enzymes have a small window of efficiency in which they best function. Enzyme activity drops off exponentially when the it is not in conditions that mimic the enzyme's ambient environment (*e.g.* temperature and pH). This means pre- and post-calibrations/preparations likely denature enzymes and reduce probe activity. Moreover, enzyme loading on the electrode is a balancing act; a high load is necessary for adequate response. However, this comes at the expense of production of high concentrations of metabolic products of analysis (*e.g.* hydrogen peroxide) that inhibit and/or denature the enzyme. Ongoing work is to optimize this balance.[90-92]

2.3.2.1.1 In Vivo Measurements

As stated above, direct *in vivo* analysis with biosensors is limited. In the past five years there are a handful of studies that have been successful *in vivo*. Measurements of glutamate are common. In the rat cortex, studies have been carried out using a platinum electrode array to reveal acetylcholine and kynurenic acid's dependence on glutamate release.[73, 93] A new glutamate sensor that benefits from sensing platforms on each side of the ceramic substrate was reported for investigating distinct areas of the brain simultaneously.[94] Glutamate release has also been monitored in the nucleus accumbens and ventral tegmental are in rats using a commercially available glutamate oxidase coated Pt-Ir wire, 180 μm diameter.[95] Malvaez *et al.* were able to demonstrate that glutamate release

in the basolateral amygdala encodes outcome-specific motivation.[74] Outside of glutamate, an enzyme-linked microelectrode array was reported for the detection of adenosine in the rat cerebral cortex.[96] The effects of learned behavior and cue detection on acetylcholine transients have been analyzed in the rat frontal cortex using a Pt electrode with immobilized acetylcholinesterase and choline oxidase embedded on a ceramic substrate, similar in fabrication to the glutamate sensors detailed above.[97-98]

2.3.2.2 Amperometry

Although the methods discussed in this module focus on the *in vivo* detection of neurotransmitters, we chose to include this section on amperometric detection of single cell vesicular events (*ex vivo*) because of the fundamental importance exocytotic events play in understanding the mechanisms of neurotransmission.

Exocytosis, the process by which neurotransmitter-filled vesicles fuse with and expel their contents out of the cell, is a primary mechanistic player in neurotransmission. Understanding exocytosis in terms of fusion pore size, duration, and the amount of content released during fusion is critically important to neurotransmission studies. When applied to single cell measurements at carbon microdisc electrodes, amperometry is a unique technique to investigate the release dynamics of exocytosis. This is because in amperometry an electrochemical potential is applied to the electrode and held at a constant value thus sampling frequency can be very high and time resolution can be on the order of microseconds.

2.3.2.2.1 Electrode Platforms; Carbon Disc, Short Cylinders, & Microelectrode Arrays

Carbon discs are the most common platform on which to perform single cell amperometry.[99] These disc electrodes are fabricated by filling a glass capillary a single

31

carbon fiber and then pulling the capillary apart under heat and gravity to form a carbon-glass seal. To form the disc shape, the microelectrode is beveled at a 45-degree angle. Oftentimes, to reinforce the carbon-glass seal, a small application of epoxy resin is applied to the electrode before experimentation. Despite variations among individual carbon fibers, it was found that factors such as charge and maximum current were independent of surface area and remained constant for disc electrodes made with 7 μm fibers.[100] Surface modification of carbon discs to increase sensitivity is ongoing.[101]

Although most amperometry at cells utilizes carbon discs, carbon fibers are also employed, although they tend to be etched to decrease their size. The cylindrical shape enables insertion into the cell to monitor intracellular chemistry. Cylinders can also be used for vesicle impact electrochemical cytometry (VIEC).[102] VIEC utilizes the immediate interaction of vesicle and carbon surface to explore direct vesicle release processes. VIEC has been used to model the vesicle membrane fusion and pore opening of PC12 cells[103] as well as modeling the percentage of vesicle content oxidized with respect to cell location on the electrode surface.[104]

Application of similarly designed carbon microelectrode arrays of 2, 3, and 7 disc electrodes were used to improve spatial and temporal resolution of cellular exocytosis measurements.[105] Electrode tips were spaced 7 μm apart, which demonstrated the ability to resolve simultaneous release events. Electrode crosstalk was analyzed for fast-scan cyclic voltammetric and amperometric detection using a 7-disc microarray.[106] Crosstalk was minimal for amperometric detection because amperometric reactions occur rapidly. By contrast, oxidative processes measured with FSCV (described below) are slower since analysis involves redox cycling. Here, molecules can diffuse to adjacent electrodes

32

permitting substantial crosstalk. A 30 μm x 30 μm microelectrode array with 36 2-μm-width microelectrodes was fabricated *via* photolithography. Cells were adhered to the surface to spatially analyze the heterogeneity of exocytosis.[107]
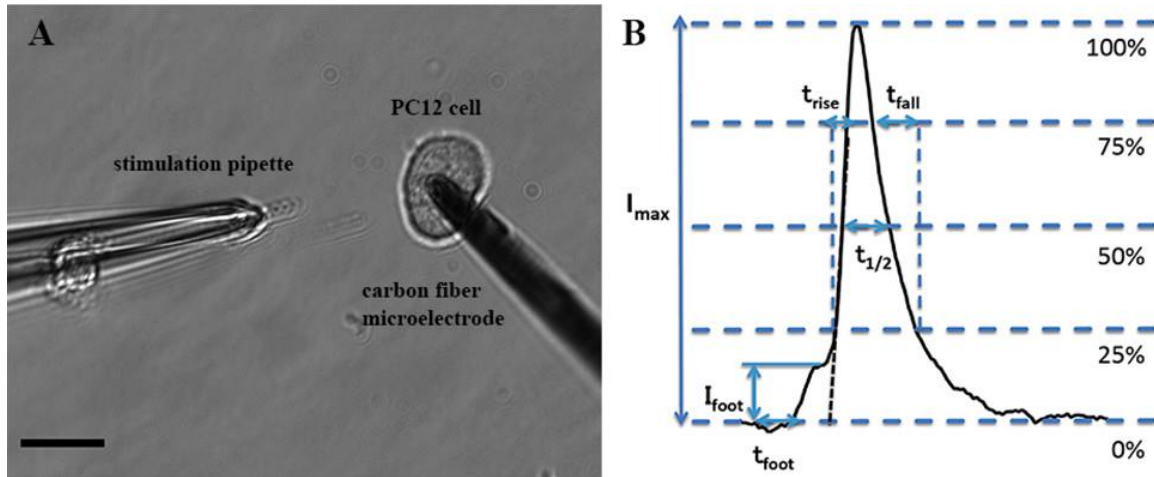

Figure 2.2: Vesicle impact electrochemical cytometry. (**A**) Optical micrograph of the experimental setup for exocytosis. Scale bar: 20 μm. Detection of exocytosis was carried out by applying 700 mV (versus Ag/AgCl reference electrode) to the electrode. (**B**) Scheme to show the different parameters for event analysis. Reprinted (adapted) with permission from Ye, D., Gu, C., Ewing, A. *ACS Chem. Neurosci.* **2018**, *9*(12), 2941-2947. Copyright 2018 American Chemical Society.

2.3.2.2.1 Key Studies in the Mechanisms of Exocytosis

An ongoing debate on the key mechanisms of vesicular release continues to date.[26] Dynamin, an enzyme involved in the late stages of endocytosis, has been shown to have contrasting effects during exocytosis, namely being necessary in stabilizing the fusion pore and increasing fusion duration.[108] When dynamin was inhibited, a shorter release duration and smaller pore size were observed supporting proposed the 'kiss-and-run' hypothesis.[108] Additionally, there is evidence that inhibiting actin, a transport mediating polymer, influences the closing mechanisms of pore fusion and results in larger pore size and fractional release supporting the 'kiss-and-run' hypothesis of release.[109] Alpha-synuclein, a protein localized at nerve endings, was shown to increase fusion duration reducing 'kiss-

and-run' characteristics pointing towards partial release fusion dynamics as being the normal function.[110] Experimental and mathematically modeled exocytosis provided evidence that fusion pores do not exceed $\frac{1}{5}$ of the radius of the vesicle, strongly detracting the notion of full fusion.[111] Recently, Ye et *al*. showed mechanistic evidence of pore size and fusion duration fluctuations may explain the neuroprotective and neurotoxic effects of lidocaine.[27]

Evidence of full vesicle fusion has been shown to be dependent on cell membrane tension where, amperometric and imaging data revealed that both partial release and full fusion were found to occur.[112]

2.3.3 Fast-Scan Cyclic Voltammetry

FSCV at carbon fiber microelectrodes (CFMs) can directly, electrochemically measure certain electroactive analytes with sub-second temporal resolution.

2.3.3.1 Carbon Fiber Microelectrodes

Carbon fiber microelectrodes (CFMs) are most often used when applying FSCV to the detection of neurotransmitters for their excellent biocompatibility and electroactive surface and their small size. Typical CFMs used in FSCV experiments are ~7 μm in diameter and range in length from 20-150 μm and benefit from small sampling areas, or 'hot spots' of neuronal activity.

Carbon has a wide-ranging chemical reactivity that allows for numerous paths to surface modification. Stable polymer deposition has been achieved.[11, 13] Scanning to high positive potential limits has been shown to increase surface oxide density and adsorptive properties[113-115] and carbon nanotube deposition has increased sensitivity towards bioamines.[15, 116-117]

34

2.3.3.2 Scan Rate

FSCV utilizes fast scan rates (400 - 1000 V s^{-1}) to detect fast changes in neurotransmitters. The electrical double layer at the CFMs charges and discharges, like a capacitor, into the electrode. At high scan rates, this 'charging current' is much larger in amplitude than the Faradaic processes that define neurotransmitter redox reactions. Thus, FSCV is background subtracted to remove the background charging or capacitive current. As different species adsorb to the CFM, the charge and discharge profile of the double layer capacitor changes and as such, this current cannot be subtracted out, appearing on FSCV color plots (raw data) as narrow peaks at switching potentials. Switching peaks cannot be easily be utilized to identify substrates since any adsorbed species on the CFM can create a switching peak. Thus, there has been significant efforts to remove this erroneous signal.[118]

2.3.3.3 Waveforms

The waveform is an integral part of FSCV analysis. A waveform is the combination of 2 or more linear voltammetric sweeps and a set of instructions that dictates how the potential changes with time at the electrode. Waveforms have been modified to increase the selectivity of analyte detection based on electrostatic and electron transfer differences between analytes. Commonly used FSCV waveforms are illustrated in **Figure 2.3** below.

2.3.3.4 Ambient Neurotransmitter Measurements with FSCAV

Because FSCV is background subtracted, it is necessary to induce a change in neurotransmitter concentration, this has been achieved electrically[119], pharmacologically[120], and optically.[121] Thus, the baseline, or ambient level concentrations, are unknown with FSCV recordings. This was, for decades, a key disadvantage of the

35

method. A great deal of information can be garnered from ambient level neurotransmitter measurements concentrations.
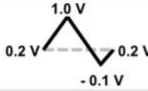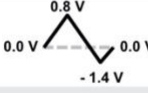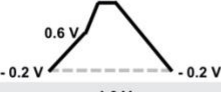

Analyte	Waveform	Scan Rate	Modifications	Reference
Dopamine	1.3 V -0.4 V / \ -0.4 V	400 Vs⁻¹		Keithley, RB. *et al. Anal. Chem.* **2011**, *83* (9), 3563-3571
Serotonin	1.0 V 0.2 V / \ 0.2 V -0.1 V	1000 Vs⁻¹	Nafion Electrodeposition	Hashemi, P. *et al. Anal. Chem.* **2009**, *81* (22), 9462-9471
H_2O_2	1.4 V -0.4 V / \ -0.4 V	400 Vs⁻¹	1,3-phenylenediamine Electrodeposition	Wilson, LR. *et al. Anal. Chem.* **2018**, *90* (1), 888-895
Histamine	1.1 V -0.5 V / \ -0.5 V -0.7 V	600 Vs⁻¹	Nafion Electrodeposition	Samaranayake, S. *et al. Analyst* **2015**, *140* (11), 3759-3765
Adenosine	1.45 V -0.4 V / \ -0.4 V	400 Vs⁻¹	Nafion & CNT Deposition	Ross, AE., Venton, BJ. *Analyst* **2012**, *137* (13), 3045-3051
Oxygen	0.8 V 0.0 V / \ 0.0 V -1.4 V	400 Vs⁻¹		Hobbs, CN. *et al. Analyst* **2017**, *142* (16), 2912-2920
Octopamine & Tyramine	1.3 V 0.1 V / \ 0.1 V	600 Vs⁻¹		Cooper, SE., Venton, BJ. *Anal. Bioanal. Chem.* **2009**, *394* (1), 329-336
Met-Enkephalin	1.2 V 0.6 V -0.2 V / \ -0.2 V	100Vs⁻¹, 400 Vs⁻¹, 3 ms hold, 100 Vs⁻¹		Schmidt, AC. *et al. Anal. Chem.* **2014**, *86* (15), 7806-7812
Melatonin	1.3 V 0.2 V / \ 0.2 V	600 Vs⁻¹		Hensley, AL., Colley, AR., Ross, AE. *Anal. Chem.* **2018**, *90* (14), 8642-8650

Figure 2.3: Outline of current FSCV waveforms for various species and any modifications to the CFM.

In 2013 Atcherley *et al*. introduced a method to quantify the absolute concentrations of dopamine at CFMs utilizing a FSCV-like technique that relies on waveform selectivity and a controlled adsorption step.[22] This method, fast-scan controlled-adsorption voltammetry (FSCAV), represents a significant analytical breakthrough for the field of voltammetric monitoring of neurotransmitters.[23] Pairing FSCV and FSCAV analysis enables a researcher to elucidate both the fast and slow chemical changes that define neurotransmission. Briefly, a dopamine-specific waveform is applied to the electrode, but

36

at a high enough frequency (100 Hz) that dopamine adsorption to the electrode is minimized. The waveform is then *'switched off'* and a constant potential is applied instead for 5-15 seconds to allow dopamine to come to an adsorption equilibrium on the electrode surface. The dopamine waveform is then reapplied, resulting in rapid oxidation/reduction of the adsorbed dopamine, essentially quantifying the ambient dopamine surrounding the CFM. FSCAV was expanded to ambient serotonin measurements in 2017 by Abdalla *et al.* with slight modifications to the electrode surface, specifically, electrodeposition of Nafion prior to the experiment.[21]
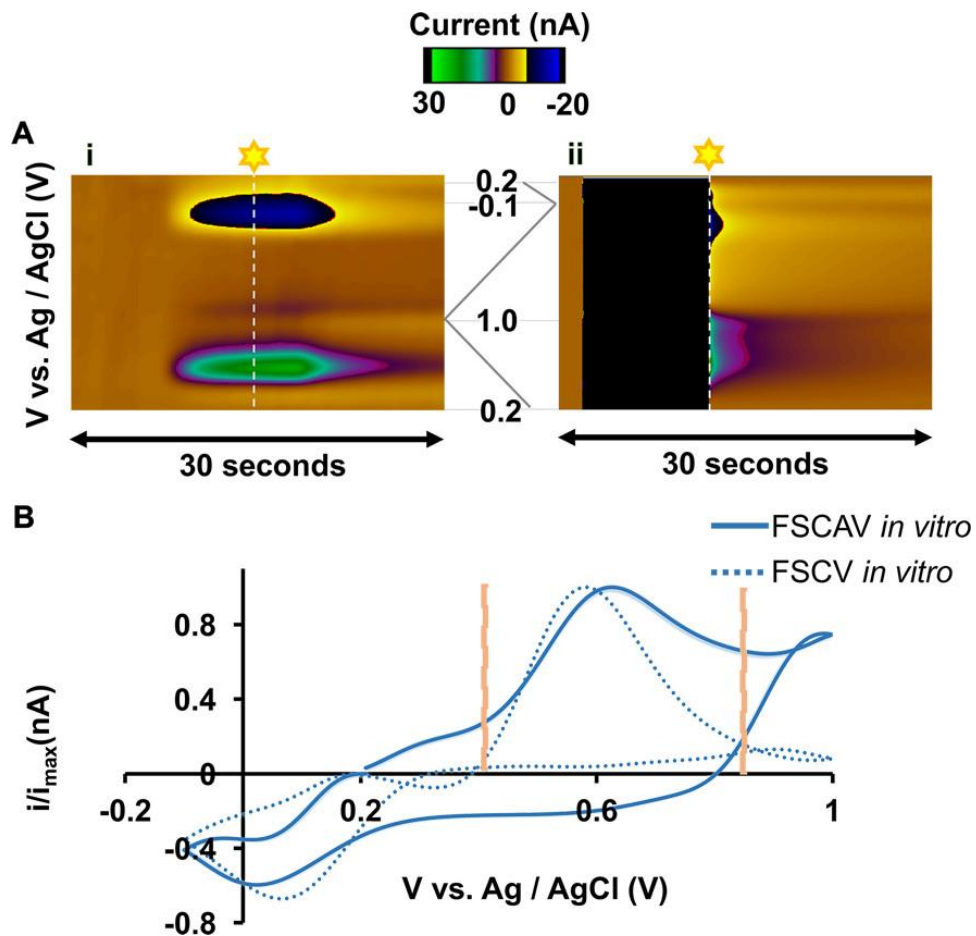
Figure 2.4: Serotonin FSCAV (**A**) Representative FSCV (**i**) and FSCAV (**ii**) color plots of 100 nM serotonin *in vitro*. (**B**) Cyclic voltammograms extracted from the vertical dashed lines in **A(i)** and **A(ii)** after normalization (current/maximum current). Vertical orange dashed lines represent

integration limits. Reprinted (adapted) with permission from Abdalla, A. *et al. Anal. Chem.* **2017**, *89* (18), 9703-9711. Copyright 2017 American Chemical Society.

2.3.3.5 Chronically Implanted Electrodes

Typical FSCV experiments will last 3-8 hours with an acutely implanted electrode. Uncertainties regarding the long-term stability of and the foreign body reaction to chronically implanted microelectrodes were eased in 2010 when the Phillips lab reported stability and minimal tissue disruption, confirmed by immunohistochemical staining, up to four months post-implantation of a CFM.[8] Chronically implanted CFMs have also be applied to awake-behaving studies of non-human primates with successful detection occurring up to 100 days post-implantation.[122] A key feature to highlight is the fact that CFMs renew their surface when the applied potential is sufficiently high to oxidize carbon (*i.e.* >1.1 V vs Ag/AgCl). While this method likely contributes to long term stability in response, long-term waveform application may steadily etch the carbon electrode, decreasing the overall size of the electrode and compromising the carbon-glass seal.[115]

2.3.3.6 Expanding Beyond Dopamine; Increasing the Scope of FSCV

For several decades, *in vivo* FSCV measurements were limited to dopamine. A serotonin selective waveform was established in 1995[123] and optimized with electrode modification in 2009 for selective *in vivo* serotonin analysis in rats.[11] Two factors were crucial for the optimization of *in vivo* serotonin FSCV. First, a thin layer of Nafion, a cation exchange polymer, is necessary to block the electrode fouling effects of serotonin metabolites. Second, a high scan rate (1000 Vs^{-1}) exploits the more favorable electron transfer kinetics for serotonin redox reactions vs. dopamine, enabling more sensitivity towards serotonin. *In vivo* serotonin FSCV has revealed evidence of dual transport mechanisms in the

38

serotonin synapse and discrete circuitry dependent on sublayer morphology within the medial prefrontal cortex.[124-125]
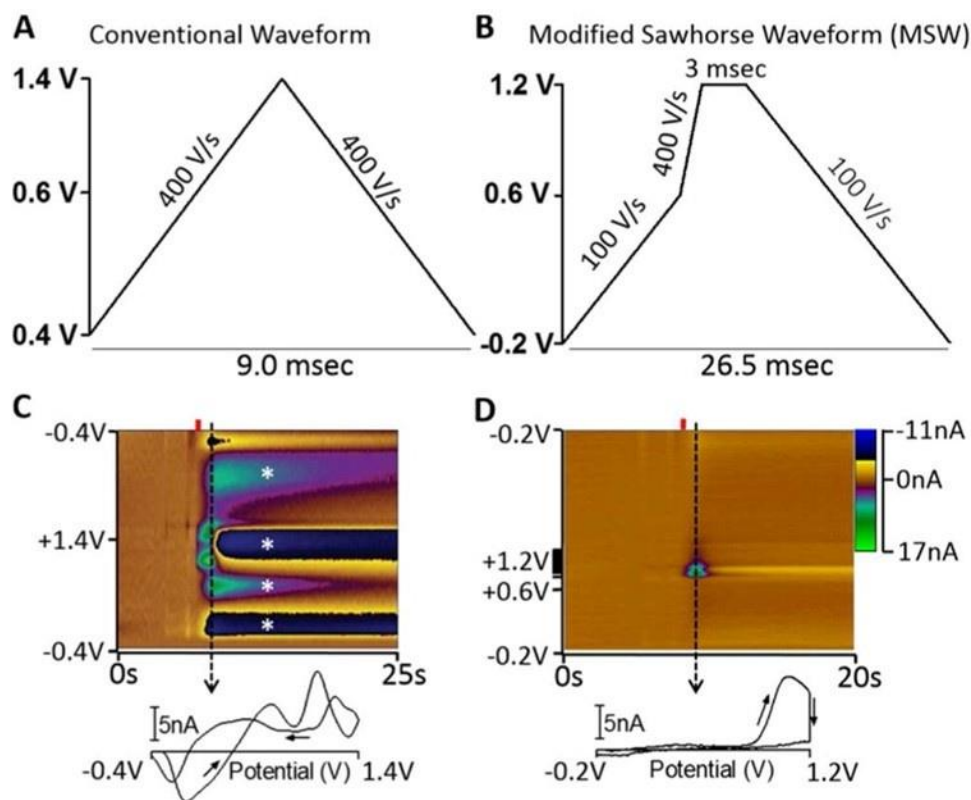
Figure 2.5: Met-enkephalin FSCV (**A**) Triangular waveform (TW). (**B**) Modified sawhorse waveform (MSW). (**C, D**) Representative *in vitro* voltammetric data collected using the waveforms depicted in parts A and B, respectively, where the ordinate is the potential applied to the carbon-fiber electrode, the abscissa is time in seconds, and the current (nA) is depicted in false color. 2 μM M-ENK was introduced to the microelectrode at the time indicated by the red bar. Displayed voltammograms were extracted at the time indicated by the dashed line. Asterisks indicate electrode fouling. Reprinted (adapted) with permission from Schmidt, AC. *et al. Anal. Chem.* **2014**, *86* (15), 7806-7812. Copyright 2014 American Chemical Society.

Fast-scan cyclic voltammetry has been expanded to include hydrogen peroxide[126-127], adenosine[12, 117], octopamine[128], tyramine[129], histamine[130], norepinephrine[131-132], molecular oxygen[133-134], methionine-enkephalin[135] and most recently, melatonin.[30]
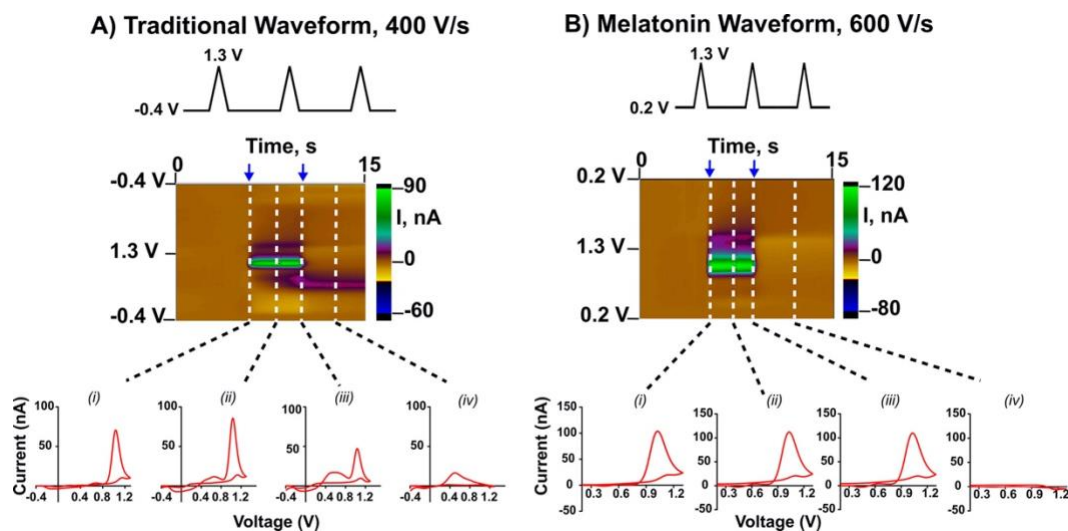
Figure 2.6: Melatonin fouls the surface of the carbon-fiber microelectrode using the traditional FSCV waveform. The traditional waveform for FSCV detection is defined as a −0.4 V holding potential scanned to 1.3 V switching potential and back at a rate of 400 V/s and 10 Hz frequency (**A**). A three-dimensional color plot represents the change in current as a function of both voltage and time. Melatonin (5 μM) is manually injected at approximately 5 s and washed away at approximately 10 s (denoted by blue arrows). For the traditional waveform, a secondary oxidation product remains even after melatonin has been flushed away by buffer. The CV for melatonin is not stable over time (**i–iv**). (**B**) A waveform for melatonin that eliminates fouling at the electrode surface is shown (0.2 to 1.3 V at 600 V/s). CVs remain stable during the length of the injection (**i–iii**) and are not present after the analyte was washed away (**iv**). Reprinted (adapted) with permission from Hensley, AL., Colley, AR., Ross, AE. *Anal. Chem.* **2018**, *90* (14), 8642-8650. Copyright 2018 American Chemical Society.

Another key disadvantage of FSCV is that it is traditionally limited to detection of individual analytes. Simultaneous detection of dopamine and oxygen in anesthetized rats was reported in the early 1990s[133-134] while simultaneous dopamine and glucose detection was recently reported.[88] The approach of multi-monitoring has been applied to studies of oxygen and dopamine changes in response to spreading depolarization.[31] In 2016 Samaranayake and colleagues published a report detailing pharmacological and mathematical evidence of histaminergic modulation of serotonin in the mouse hypothalamus.[32] FSCV's fast measurements captured an increase in the concentration of

40

extracellular histamine coincided with a decreased release of serotonin. Evidence pointed towards activation of H_3 receptors on presynaptic serotonin terminals functioning as a negative feedback loop to inhibit serotonin release. From this study, it is clear that expanding the ability of FSCV to monitor multiple analytes simultaneously can resolve questions surrounding the interaction of neurotransmitters in the synaptic area. Appreciating the connection of neurotransmitters can be used to better design and understand therapeutic effects of drugs.
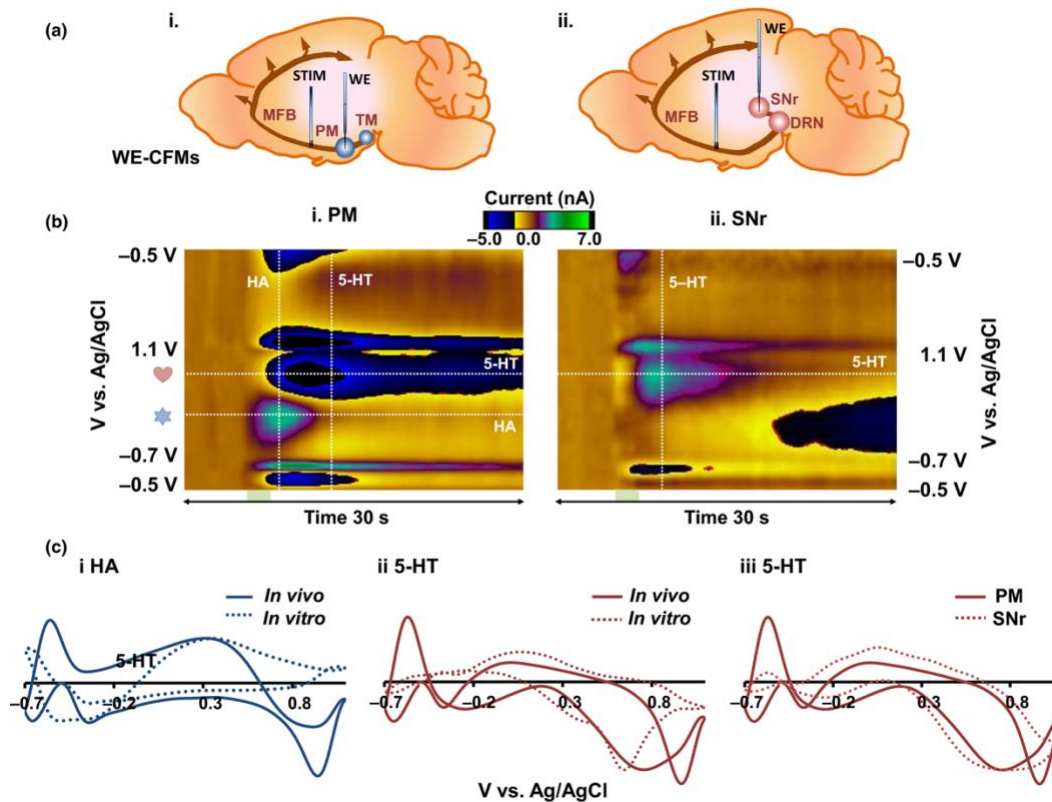
Figure 2.7: Histamine FSCV**. (ai & aii)** The position of electrodes (stimulation and carbon fiber microelectrodes) in the mouse brain. **(bi & bii)** Representative color plots of the stimulated release of histamine and serotonin in the premammillary nucleus (PM) and stimulated release of serotonin in the substantia nigra pars reticulata (SNr), respectively. **(ci & ii)** Superimposed cyclic voltammograms of *in vivo* and *in vitro* histamine and serotonin signals taken from vertical dashed lines in the PM. **(ciii)** Comparison of normalized cyclic voltammograms of *in vivo* serotonin signals taken from vertical dashed lines in both PM and SNr. HA, histamine; 5-HT, serotonin. Reprinted with permission from Samaranayake, S., *et al. J. Neurochem.* **2016**, *138* (3), 374-383. Copyright 2016 John Wiley and Sons

41

2.3.3.7 Instrumentation

FSCV instrumentation has long been sourced from prominent academic labs, whose electronics facilities assemble systems (e.g., University of North Carolina's UEI potentiostat, University of Washington's FSCV system, etc.). Limited technical and customer support, long purchasing lead times, and significant costs involved with such academic systems led to the emergence of commercial FSCV instrumentation options (e.g., Pine Research Instrumentation WaveNeuro, Pinnacle Technologies, Inc.), which have supported growth in the area of electroanalytical neurochemistry. The Dagan Corporation is an additional supplier of FSCV potentiostats as well.

Data analysis software is available from several commercial or academic entities. Pinnacle Technologies, Inc. includes their FSCV software package with purchase of a system. The HDCV software package can be purchased from UNC at Chapel Hill, the WCCV software package can be purchased from Knowmad Technologies, LLC (Tuscon, AZ) or the Demon Voltammetry & Analysis software suite is freely available to academics and non-profits. (Wake Forest)

2.4 Prospects and Conclusions

Analytical neurotransmitter measurements is a thriving and cutting-edge field. Conventional limits of microdialysis are continuing to be pushed further to allow for less invasive, faster, more efficient sampling and separation methods. Decreasing the footprint of microdialysis probes through microfabrication will allow for more reliable sampling from intact tissue. With the increasing body of work demonstrating the advantages of locally perfusing anti-inflammatory agents, the field of microdialysis sampling, as a whole, stands to benefit from adopting this method. Along with smaller membranes, the resolution

42

of microdialysis is now steadily under the one-minute mark for on-line analysis with some methods reaching single second resolution. The trend is expected to continue with the joining of efficient microfabricated probes and single-second on-line detection.

Recent developments in biosensor technology have explored the use of substrate anchored aptamers for the selective detection of molecules. Aptamers are short chained single stranded DNA or RNA that have a unique 3D conformation. They are synthetically produced and can therefore be tailor-made for various molecules. DNA based aptamer sensors that selectively bound to dopamine have been explored for their applications in dopamine monitoring.[136-137] Additionally, the Andrews lab at UCLA has been exploring the use of DNA aptamer-based sensors for dopamine[138] and have been expanding the applicability by detecting glucose, serotonin and dopamine in mouse serum with tailor-made field-effect transistors.[139]

A new class of multimodal monitoring has recently emerged as a promising method to stimulate and monitor numerous processes simultaneously. In a 2017 *Nature Neuroscience* report, Park and colleagues described a miniature device consisting of six individual electrodes, two microfluidic channels and a fiber optic channel for photostimulation.[140] *In vivo* proof of concept was demonstrated by implantation in the medial prefrontal cortex of a mouse. There, viral injections were delivered through the device's microfluidic channels followed by photostimulation and electrophysiology recordings. This device demonstrated favorable chronic stability in awake-behaving mice. Additionally, Patriarchi and colleagues introduced a novel fluorescence intensity-based genetically encoded dopamine indicator coined "dLight1."[141] Transfection of a viral protein into the striatum permitted two-photon imaging of dopamine response to an

electrical stimulation and cocaine challenge in slice preparations in addition to optogenetically stimulated dopamine release. Fluorescence data were also collected from awake-behaving mice in response to pharmacological administration and visuomotor learning tasks. Multimodal monitoring represents a substantial advancement in the field of neuroanalysis and the growing field of optogenetics.

Recently a novel method has been developed, by Mei Shen's group, to detect non-electroactive neurotransmitters that utilizes ionic transfer across an immiscible liquid-liquid interface (ITIES).[142] A nanopipet filled with 1,2-dichloroethane was submerged into an aqueous solution of acetylcholine, tyramine, and serotonin. Electrodes placed in each phase allows the interface to function as the working electrode (WE). A voltammetric sweep is applied to one of the electrodes that can detect ionic transfer when charged molecules are polarized and cross the interface (WE). This method was applied to the detection of gamma-aminobutyric acid (GABA) in aqueous solution in 2018 with slight modification.[143] Due to GABA being neutral at pH ~ 7, it required the addition of octanoic acid in the organic phase (nanopipet filling) to facilitate transfer of GABA through the liquid-liquid interface. Linear current increases were shown for serial additions of GABA concentrations for a small range. However, these experiments show the exciting first steps of a new analytical strategy to quantify non-electroactive neurotransmitters in aqueous solutions.

Single cell amperometric recordings of exocytosis appears to be focusing on a consensus of 'kiss-and-run' release as being the main or only method of release. Investigations of proteins regulating the fusion pore size will continue to shed light on possible reasons for impaired neurotransmission during neurodegenerative disease and

other psychiatric disorders. Vesicle impact electrochemical cytometry and microelectrode

arrays are essential tools for investigating intracellular vesicle dynamics and heterogeneous

exocytotic events, respectively.
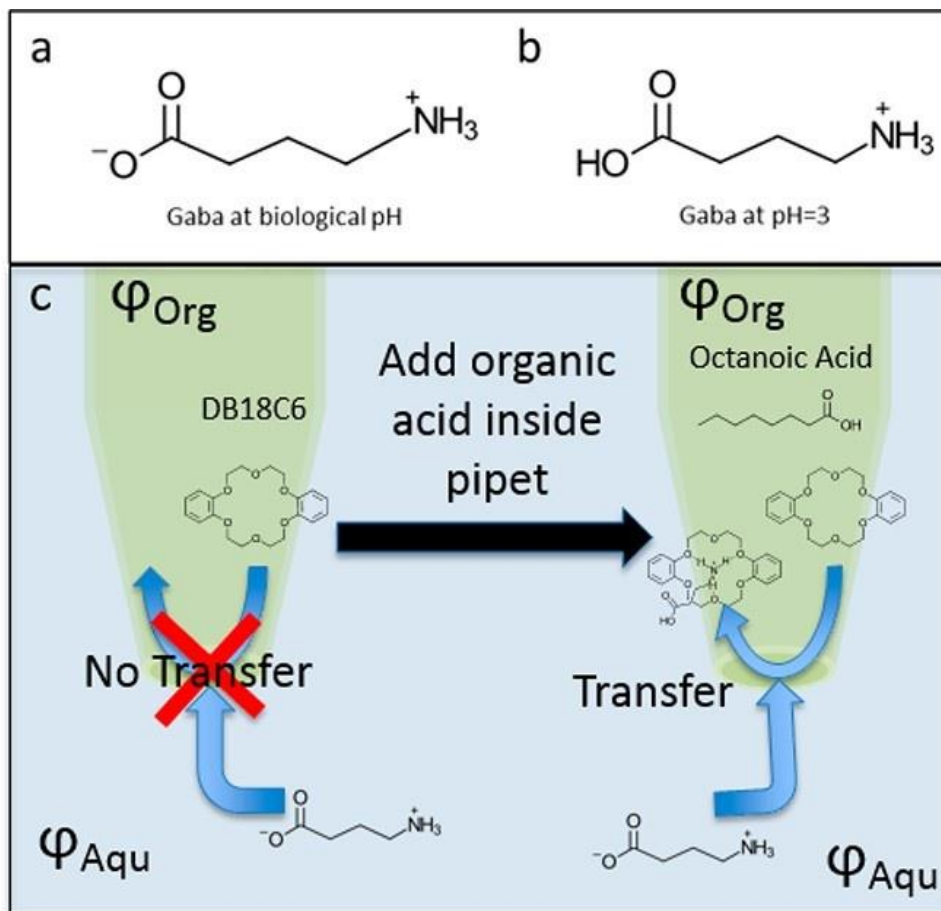
Figure 2.8: Newly introduced detection mechanism based on pH modulation from an organic acid in the oil phase. This mechanism enables the direct electrochemical detection of γ-aminobutyric acid (GABA), an important neurotransmitter and a zwitterion, with nanoITIES pipet electrodes. Chemical structures of GABA at pH ≈ 7 (**a**) and pH ≈ 3 (**b**). The pKa of the amine and carboxylic acid moieties of GABA are 10.22 and 4.53, respectively. Without organic acid modulation, GABA is not detected; in contrast, after adding an organic acid, octanoic acid, to the oil phase contained inside the pipet, GABA is detected (**c**). Reprinted (adapted) with permission from Iwai, NT., *et al*. *Anal. Chem.* **2018**, *90* (5), 3067-3072. Copyright 2018 American Chemical Society.

FSCV continues to be a leading method for neurotransmitter analysis in the quality

and accuracy of data it delivers. The scope and quantity of analytes are continually being

www.manaraa.com

improved. Additionally, new brain regions are being explored as they are implicated in emerging disease states. We anticipate *in vivo* monitoring of trace metals with FSCV in the very near future. Trace metals, such as Cu^{2+}, act as important cofactors in several synaptic processes and will help create a more thorough understanding of neurotransmission. FSCV analysis will continue to play a foundational role in determining the synaptic underpinnings of neurotransmitter regulation.

In conclusion, a clear gap persists in understanding the fundamental chemistry of the brain with emphasis placed on obtaining meaningful analytical measurements of neurotransmitters. Targeted brain diagnoses and therapeutics are very difficult without these paired measurements. Understanding the role and function of neurotransmitters in healthy and diseased states would serve to greatly improve approaches to clinical treatment.

This module served to outline the most recent, cutting edge analytical advancements in neurotransmitter analysis spanning primarily the last five years. There is a rich literature of important developments and applications for monitoring molecules in neuroscience. The discussion began with an outline of the analytical challenges encountered when monitoring neurotransmitters. Two major classes of analytical methods, *in vivo* microdialysis sampling and direct detection at microelectrodes, were highlighted with their respective advantages and disadvantages. Cutting edge advancements, applications and prospects of these methods were showcased.

CHAPTER 3

VOLTAMMETRIC CHARACTERIZATION OF THE CENTRAL

NERVOUS HISTAMINERGIC SYSTEM IN MALE & FEMALE MICE[1]

---

[1] Berger, SN., Hersey, M., Baumberger Altirriba, BM., Samaranayake, S., Bain, I. Hashemi, P. Voltammetric characterization of the ventral nervous histaminergic system in male and female mice. In preparation. *J. Neurochem.*

3.0 Abstract

Histamine is an important molecule that plays a key role mediating inflammation throughout the body. In the central nervous system (CNS), histamine has a demonstrated ability to function as a neuromodulator. Historically, a substantial amount of pharmacological testing was carried out using only male animal models, however, in 2015 the National Institutes of Health mandated that sex be included as a biological variable. Histamine remains understudied in the CNS especially with respect to how the male and female histaminergic systems respond to pharmacological treatments. In this chapter, we first compare the male and female systems and the influence the estrous cycle has on the histamine system under control conditions. Next, we target histamine receptors, vesicular packaging, synthesis, and histamine metabolism to explore differences between the sexes. We found robust similarities between male and female evoked histamine levels and no difference throughout the estrous cycle. Additionally, we found similar responses across sexes regarding receptors H_1 and H_2 antagonism, inhibition of vesicular packaging, and inhibition of synthesis and metabolism. Our data revealed that sex should be considered when evaluating the effectiveness of H_3 targeting compounds as antagonism *via* thioperamide did not elevate histamine levels above control in female mice, even when pretreated with an H_3 agonist to first decrease histamine. We posit that cycling hormones in pre-menopausal females provide a crucial anti-inflammatory role and regulate histamine levels in the brain as an evolutionary trait. Our study demonstrates the highly conserved nature of neurological systems and will aid in designing therapeutic strategies for both male and female sexes.

3.1 Introduction

Histamine is a biological amine with a well-established role in mediating inflammation, found in immune cells including glia[1], mast cells[2-3], and T-cells.[4] In addition to its roles in the immune system, histamine has also been identified as a neuromodulator.[1, 5] In the central nervous system, histamine cells bodies reside in the tuberomammillary nucleus (TMN) with projections that innervate throughout the brain.[6-8] Studies have shown that histamine is able to modulate the release of other neurotransmitters such as serotonin, dopamine, acetylcholine, glutamate and GABA.[5] The majority of previous literature has been based on experimentation of male animal models (typically mouse or rat) and that data is then extrapolated to female models assumed to behave and respond in sufficiently similar ways. In 2015, the NIH mandated that all animal-based experiments carried out under their funding would have to consider sex as a biological variable.[9] Differences in the peripheral histamine systems of male and female mice have been shown,[10-11] along with previous suggestions that histamine may be present at higher basal levels in females.[12-14] Additionally, hypothalamic concentrations of histamine and its associated enzymes are found to vary through the estrous cycle.[15-18] However, due to the difficulties with measuring histamine in the brain, there is a clear lack of information regarding central histamine chemistry between the sexes and if peripheral histamine relates to central.

CNS histamine has been previously studied using brain homogenates[15, 19], *in vivo* microdialysis coupled to high-performance liquid chromatography[20-21], and electrophysiology.[22-23] More recently, the Hashemi lab developed a fast-scan cyclic voltammetry (FSCV) method to selectively detect histamine *in vivo*.[24-25] The power of our technique is that it creates minimal inflammatory response and directly measures both

histamine and serotonin at a single carbon fiber microelectrode (CFM).[24] We showed that evoked histamine resulted in an inhibition of serotonin release due to H_3 receptors present on 5-HT terminals; this data was in agreement with previous findings.[26-27]

In this study we investigated potential sex differences of the central histaminergic system between male and female. We first use FSCV to characterize the release and reuptake characteristics of histamine release of both sexes and the effects of this release on serotonin under control conditions. We then compared the evoked release of histamine throughout the four stages of the mouse estrous cycle, namely estrus, metestrus, diestrus, and proestrus. Next, an extensive pharmacological screening is undertaken to target histamine receptors H_1R, H_2R, H_3R, H_4R, histamine synthesis, vesicular packaging, and metabolism in both male and female mice and compare the effects of each. Interestingly, the only significant differences we find were when targeting H_3R in females, leading us to explore the possibility of cycling hormones playing a key role in the female mouse's ability to mitigate immunologic signaling. Finally, we compared the release and reuptake profiles of stimulated histamine with electrode placement in the posterior hypothalamus and found that regions receiving significant input from hormones, (i.e. ventromedial nucleus) are more likely to have variable profiles. This study provides broad insight into the histaminergic system of male and female mice and will yield better understanding of how an understudied neurochemical system functions.

3.2 Materials and Methods

Chemicals and Reagents

All chemicals were used as received from the supplier. Diphenhydramine hydrochloride (20 mg kg^{-1}; Sigma Aldrich, St. Louis, MO, USA), zolantidine dimaleate

50

(10 mg kg^{-1}; Tocris, Minneapolis, MN, USA), immepip dihydrobromide (5 mg kg^{-1}; Sigma Aldrich), thioperamide maleate (20 mg kg^{-1} or 50 mg kg^{-1}; Sigma Aldrich and Tocris), tacrine hydrochloride (2 mg kg^{-1}; Tocris), and α-fluoromethylhistidine (20 mg kg^{-1}; Toronto Research Chemicals, North York, ON, CAN) were all dissolved in sterile saline (0.9% NaCl solution, Mountainside Medical Equipment, NY, USA) at 5 mL kg^{-1}. Reserpine (10 mg kg^{-1}; Sigma Aldrich) was dissolved in 0.1 % acetic acid (Sigma Aldrich) in sterile saline at 5 mL kg^{-1}. Tetrabenazine (Sigma Aldrich) was dissolved in 10 % DMSO (Sigma Aldrich) in sterile saline with 1 M HCl (10 µL mL^{-1} injection volume). All solutions were made fresh at the time of injection and all injections were given *via* intraperitoneal (*ip*) injection. Urethane (Sigma Aldrich) was dissolved in sterile saline as a 25 % w/v solution and administered at 7 µL kg^{-1}.

Electrode Fabrication

All electrodes are made in house. A single carbon fiber is aspirated into a borosilicate capillary (0.6 mm x 0.4 mm x 10 cm; OD x ID x L) (A-M Systems, Sequim WA, USA) and sealed under gravity and heat by a vertical pipette puller (Narishige, Amityville, NY, USA) to create two separate electrodes. The protruding fiber is trimmed under light microscope to ~150 µm by scalpel. An electrical connection is forged with the fiber through a stainless-steel connecting wire (Kauffman Engineering, Cornelius, OR, USA) and silver epoxy. Finally, a thin layer of Nafion (LQ-1105, Ion Power, New Castle, DE, USA) is electrodeposited onto the fiber surface at 1 V for 30 s; the coated fiber is dried for 10 min at 70 °C.[28]

Data Collection and Analysis

Fast-scan cyclic voltammetry was performed on anesthetized mice using a Chem-Clamp potentiostat (Dagan Corporation, Minneapolis, MN, USA), custom built hardware interfaced with PCIe 6341 & PCI 6221 DAC/ADC cards (National Instruments, Austin, TX), and a Pine Research headstage (Pine Research Instruments, Durham, NC, USA). WCCV 3.06 software (Knowmad Technologies LLC, Tucson, AZ, USA) was used to control the hardware and perform data analysis. The histamine waveform (-0.5 V to -0.7 V to +1.1 V to -0.5 V at 600 V s^{-1}) was applied at 60 Hz for 10 min, then at 10 Hz for 10 min prior to data collection. Data were collected at 10 Hz. Histamine was evoked *via* biphasic stimulation applied through a linear constant current stimulus isolator (NL800A Neurolog, Digitimer North America LLC, Fort Lauderdale, FL, USA) with stimulations at 60 Hz, 360 µA, 2 ms in width, and 2 s in length.

Data were collected and filtered on WCCV software (zero phase, Butterworth, 3 kHz low pass filter). Four control evoked files, 10 min apart, were averaged for the control evoked histamine signal after which one compound from **3.2.1** was administered and files were collected at 0 min, 5 min, 10 min, and every 10 min thereafter until 120 min. For immepip-thioperamide experiments, data were collected for 60 min as described followed by administration of thioperamide immediately after the 60 min file was collected. Files were then collected for an additional 60 min in the same fashion as described above. Currents obtained were converted to concentrations through previously generated calibration factors for both histamine (2.825 µM nA^{-1}) and serotonin (11 µM nA^{-1}).[24-25] At the completion of each experiment, a large voltage (~10 V; ~2 min) was applied to the CFM to lesion the surrounding tissue for histological analysis. Mice were euthanized,

brains were rapidly harvested and stored in 4% paraformaldehyde solution. Prior to sectioning, brains were transferred to 30% sucrose solution for 24 h minimum. Brains were rapidly frozen and sectioned into 25 µm slices (Thermo Scientific Cryotome FSE, Thermo Scientific, Waltham, MA, USA) and visualized under light microscope to confirm electrode placements.

Statistical Analyses

Average control response was generated from four current vs time traces per animal and averaged to create an overall group average. To determine the $t_{1/2}$, a code was custom written in Excel to fit the reuptake component of the curve and calculate the time taken to reach half the maximum amplitude. Exclusion criteria were based on outliers (*via* Grubbs test) and animals that did not survive the experimental paradigm. Standard error of the mean (SEM) was calculated using the average response of each animal (n = # animals). Significance between two points was determined by 2-tailed paired t-test and taken as $p < 0.05$. For non-normally distributed data (*via* Shapiro Wilk test), the Kruskal-Wallis H test was used to determine significance and taken as $p<0.05$. All error bars represent the standard error of the mean (SEM).

Animals and Surgical Procedure

Animal procedures and protocols were in accordance with the regulations of the Institutional Animal Care and Use Committee (IACUC) at the University of South Carolina, accredited through the Association for Assessment and Accreditation of Laboratory Animal Care (AAALAC). Male and female C57BL/6J mice aged 6-12 weeks were used. Animals were group housed with *ad libitum* access to food and water and were kept on a 12 h light/12 h dark cycle (lights on 0700/lights off 1900).

Stereotaxic surgery (David Kopf Instruments, Tujunga, CA, USA) followed induction of deep and sustained anesthesia from an intraperitoneal injection of urethane (above). Mouse body temperature was maintained using a thermal heating pad (Braintree Scientific, Braintree, MA, USA). All surgical coordinates were taken in reference to bregma.[29] A Nafion coated CFM was lowered into the posterior hypothalamus (AP: -2.45, ML: 0.50, DV: -5.45 to -5.55) and a stimulating electrode (insulated stainless-steel, diameter: 0.2 mm, untwisted, Plastics One, Roanoke, VA, USA) was placed into the medial forebrain bundle (AP: -1.07, ML: +1.10, DV: -5.00).[24] A pseudo-Ag/AgCl reference electrode, created by chloridizing a polished silver wire in HCl (15 s in 1 M HCl at 5 V), was placed in the contralateral hemisphere.

For the analysis of sex and estrous cycle differences control histamine and serotonin data were pooled. Due to the sensitivity of the measurements being made, we are unable to determine the estrous cycle stage prior to the experiment as we have observed in previous animals that doing so influences release and reuptake characteristics. For cycle determination, vaginal lavage was performed following the conclusion of data collection. Briefly, approximately 10 µL of sterile saline was administered and quickly removed from the vagina and then visualized under low power light microscope to determine estrous cycle stage *via* cytological examination.[30] (**Figure B1**)

3.3 Results

3.3.1 Control Evoked Histamine and Serotonin Inhibition Does Not Vary Between Sexes

The stimulated histamine release and the resulting serotonin inhibition is shown in **Figure 3.1**. Panel **A** is a representative color plot of histamine FSCV with a CV inset in the top right corner. Averaged male stimulated histamine release (Amp_{max}: $7.54 \pm 1.20\,\mu M$)

and serotonin inhibition (Amp_{max}: 42.53 ± 4.74 nM) is shown in blue in **(B)**. In **(C)**, the female stimulated histamine release (Amp_{max}: 7.11 ± 1.10 µM) and serotonin inhibition (Amp_{max}: 45.33 ± 4.72 nM) is shown in red. Tabulated in **(D)** are the max amplitude values for overall histamine peak release (Amp_{max} male-female: $p = 0.80$) and serotonin inhibition (Amp_{max} male-female: $p = 0.98$), the ratio of peak release to peak inhibition (HA/5HT: male: 0.19 ± 0.02; female: 0.16 ± 0.02; $p = 0.34$), and the rate of decay for the stimulated histamine release ($t_{1/2}$: male: 3.1 ± 0.4 s; female: 3.9 ± 0.7 s; p=0.34). The sample size was equal for male and female mice at n=20.

	Male	**Female**	**p-value**
HA Amp_{max}	7.54 ± 1.20 µM	7.11 ± 1.10 µM	0.80
$t_{1/2}$	3.1 ± 0.4 s	3.9 ± 0.7 s	0.34
5HT Amp_{max}	42.53 ± 4.74 nM	45.33 ± 4.72 nM	0.98
Inhibition (HA/5HT)	0.19 ± 0.02	0.16 ± 0.02	0.34
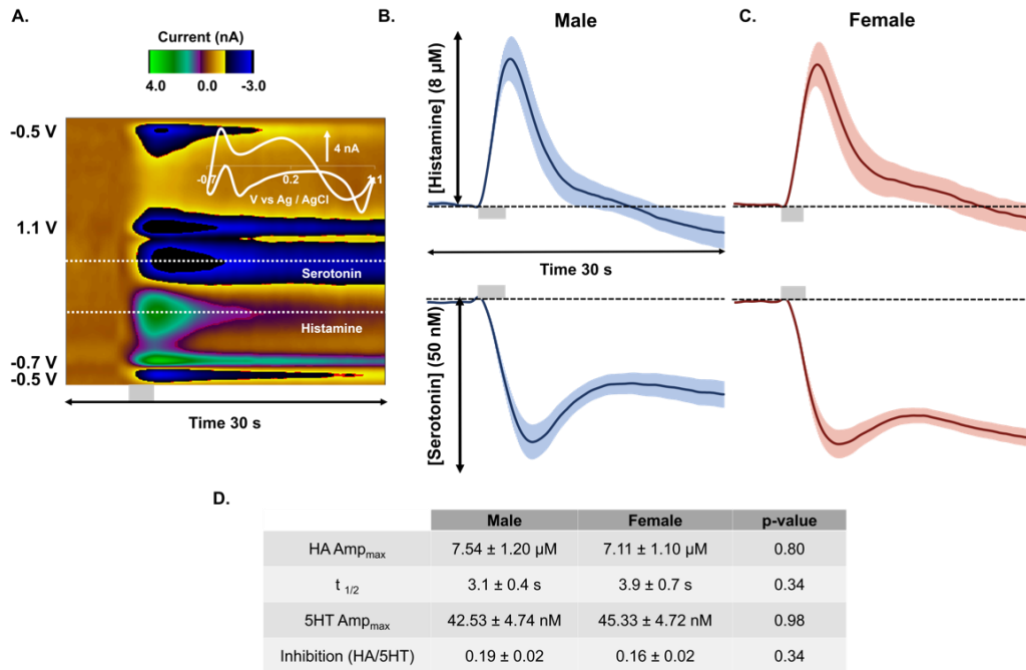
Figure 3.1: Control evoked histamine is not significantly different between male and female mice. **A)** representative color plot shows the stimulated release and reuptake of histamine as the green event and the blue event is the inhibition of serotonin. Inset in the top right corner is the characteristic CV with peaks occurring around 0.2 V for histamine and 0.7 V for serotonin oxidation. The concentration vs time traces for the release of histamine and inhibition of serotonin is shown for **B)** male and **C)** female mice. The electrical stimulation (2 s) is represented by the grey bar. **D)** tabulated data of release and inhibition.

3.3.2 Control Evoked Histamine and Serotonin Inhibition Does Not Vary Throughout the Estrous Cycle

We next evaluated the effect of estrous cycle stage on stimulated histamine release and inhibition of serotonin. **Figure 3.2A** shows the stimulated histamine release throughout estrus, metestrus, diestrus, and proestrus. We found no significant difference in the evoked histamine amplitude (Amp_{max}: estrus (blue; n=23): 6.58 ± 0.55 µM; metestrus (orange; n=16): 6.82 ± 0.74 µM; diestrus (yellow; n=10): 7.86 ± 1.33 µM; proestrus (green; n=10): 5.80 ± 1.83 µM; p = 0.84 Kruskal-Wallis H-test) or $t_{1/2}$ (estrus: 3.9 ± 0.7 s; metestrus: 5.4 ± 1.1 s; diestrus: 3.8 ± 0.9 s; proestrus: 4.3 ± 1.1 s; p = 0.79 Kruskal-Wallis H-test) of reuptake curve across estrous stages. The peak serotonin inhibition is shown across cycle stages in **Figure 3.2B** (Amp_{max}: estrus (blue; n=23): 44.70 ± 4.04 nM; metestrus (orange; n=16): 40.76 ± 5.93 nM; diestrus (yellow; n=10): 37.04 ± 4.92 nM; proestrus (green; n=10): 31.74 ± 5.17 nM; p = 0.27 Kruskal-Wallis H-test). These data are tabulated in Figure **3.2C**.

C	Estrus	Metestrus	Diestrus	Proestrus	p value
[HA] Amp_{max}	6.58 ± 0.56 µM	6.82 ± 0.74 µM	7.86 ± 1.33 µM	5.80 ± 1.83 µM	0.84
[HA] $t_{1/2}$	3.9 ± 0.7 s	5.4 ± 1.1 s	3.8 ± 0.9 s	4.3 ± 1.1 s	0.79
[5HT] Amp_{max}	44.70 ± 4.04 nM	40.76 ± 5.93 nM	37.04 ± 4.92 nM	31.74 ± 5.17 nM	0.27
[HA]/[5HT]	0.17 ± 0.02	0.20 ± 0.02	0.21 ± 0.02	0.21 ± 0.02	0.18

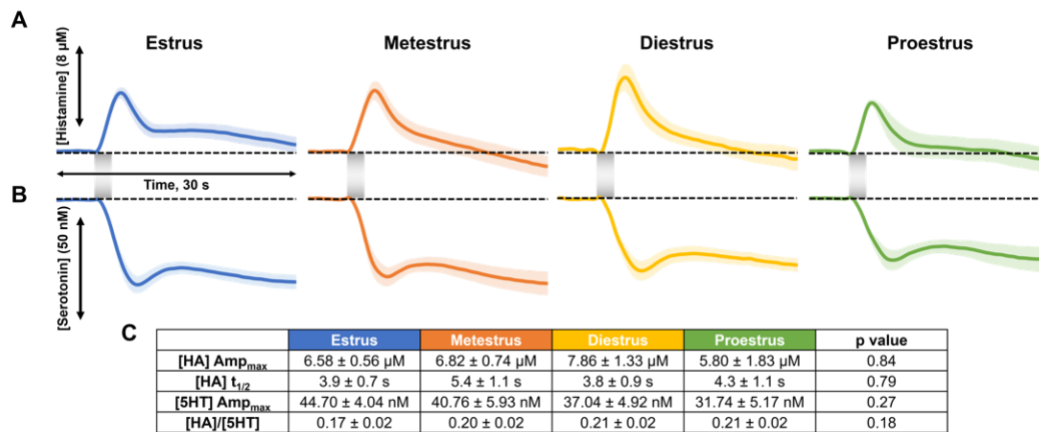**Figure 3.2:** Evoked histamine release does not significantly differ throughout estrous. (**A**) Evoked histamine release and (**B**) serotonin inhibition for female mice in estrous (blue, n=23), metestrus (orange, n=16), diestrus (yellow, n=10), and proestrus (green, n=10). The shaded grey bar represents the 2 s electrical stimulation. (**C**) Tabulated data covering the maximum amplitude of [histamine]

56

release, $t_{1/2}$ of histamine clearance, maximum inhibition of [serotonin], and the ratio of [histamine]/[serotonin]. Data were analyzed *via* Kruskal-Wallis H-test. Significance was taken as $p<0.05$.

We observed the occurrence of two distinct release profiles in female mice that occurred exclusively while in estrus. **Figure 3.3** shows the single (**A**), double (**B**), and combined (**C**) release profiles for evoked histamine. There was not a significant difference in the peak histamine amplitude (Amp_{max}: single (red; n=13): 6.70 ± 0.94 µM; double (purple; n=10): 6.42 ± 0.47 µM; $p = 0.83$ unpaired t-test) or in peak serotonin inhibition (Amp_{max}: single (red; n=13): 39.85 ± 5.65 nM; double (purple; n=10): 50.97 ± 5.38 µM; $p = 0.88$ unpaired t-test) between the single and double release events. At the end of data collection, a large voltage was passed through the electrode to lesion the tissue from which our measurements are made. This allows for histological verification of the electrode location placement. We hypothesized that the single and double release events were region specific. We found that electrode placements anterior to the target coordinates were more likely to result in a double peaked release. (**Figure B2**)

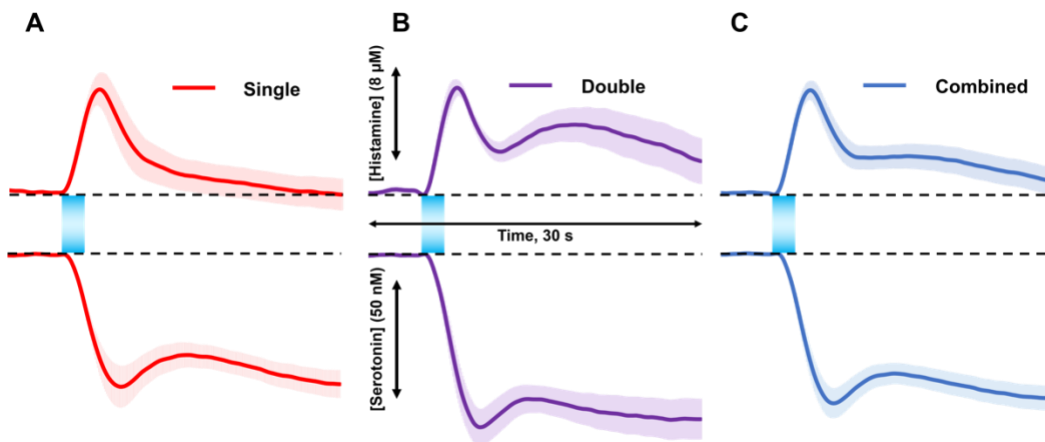**Figure 3.3:** Comparison of evoked histamine and serotonin signals during estrus. The different release profiles obtained for [histamine] vs time in female mice during estrus are shown in (**A**) single release (red), (**B**) double release (purple), and (**C**) the combined average of the single and double profiles. Maximum amplitude of histamine release ([HA]Amp_{max}: single (red; n=13): 6.70 ± 0.94 µM; double (purple;

57

n=10): 6.42 ± 0.47 µM; p = 0.83 unpaired t-test) and serotonin inhibition ([5HT]Amp_{max}: single (red; n=13): 39.85 ± 5.65 nM; double (purple; n=10): 50.97 ± 5.38 µM; p = 0.88 unpaired t-test) were not significantly different. Significant was taken as p<0.05.

3.3.3 H_1R and H_2R Pharmacology

First, we investigated how the antagonism of post-synaptic receptors H_1 and H_2 would affect the release and reuptake of hypothalamic histamine. **Figure 3.4** shows the male and female response to diphenhydramine (DPH) (20 mg kg^{-1}), an H_1 antagonist, and zolantidine (10 mg kg^{-1}), an H_2 antagonist. In column (**A**) the administered compound and sex is given, (**B**) a representative color plot of histamine release and serotonin inhibition, (**C**) cyclic voltammograms confirming the electrochemical identities of histamine and serotonin, (**D**) concentration vs time plots of control evoked histamine release (blue) and following drug administration (green). No significant change in evoked histamine release was seen in male mice given DPH (**Di**) (n=5; Amp_{max}: control: 9.22 ± 3.06 µM; post-drug: 9.38 ± 2.66 µM; p = 0.83 paired t-test) or zolantidine (**Diii**) (n=5; Amp_{max}: control: 5.84 ± 0.55 µM; post-drug: 4.90 ± 0.60 µM; p = 0.33 paired t-test). Significant slowing of histamine reuptake was obtained 50 min following administration of DPH (**Di**) ($t_{1/2}$: control: 2.7 ± 0.4 s; post-drug: 7.2 ± 1.1 s; p = 0.014 paired t-test) but not following zolantidine (**Diii**) ($t_{1/2}$: control: 4.2 ± 1.3 s; post-drug: 3.2 ± 1.0 s; p = 0.46 paired t-test). In (**Dii**), female mice respond to DPH with a slight decrease in histamine amplitude (n=4; Amp_{max}: control: 6.78 ± 0.16 µM; post-drug: 5.34 ± 0.56 µM; p = 0.077 paired t-test) and a slowing of reuptake ($t_{1/2}$: control: 3.3 ± 0.8 s; post-drug: 12.0 ± 2.6 s; p = 0.042 paired t-test). Female response to zolantidine was similar to male with no change in histamine amplitude (n=5; Amp_{max}: control: 5.40 ± 0.65 µM; post-drug: 5.45 ± 0.87 µM; p = 0.96

58

paired t-test) or clearance profile ($t_{1/2}$: control: 2.7 ± 0.7 s; post-drug: 3.8 ± 1.6 s; p = 0.59 paired t-test).
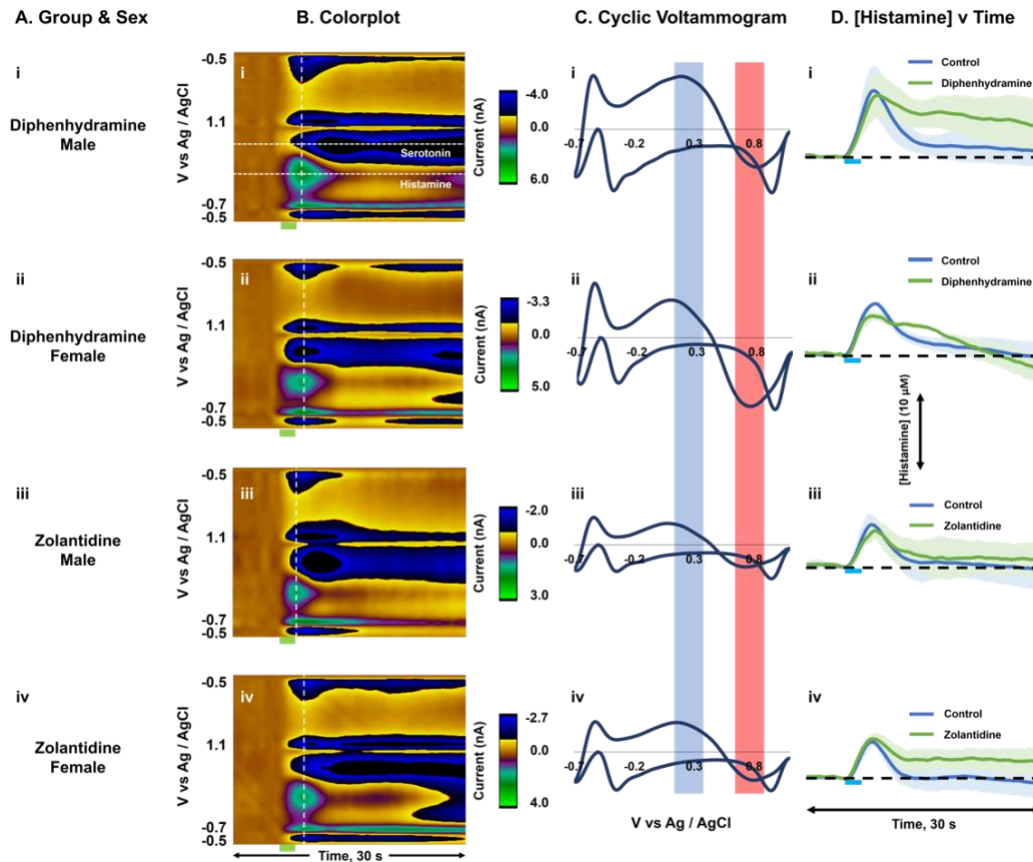
Figure 3.4: Post-synaptic H_1 and H_2 receptor targeting highlights differential receptor-release communication mechanisms. (**A**) the drug and mouse's sex are listed. (**B**) a representative color plot for each grouping of animals is shown. The green bar represents the 2 s electrical stimulation. (**C**) a representative cyclic voltammogram from each cohort of animals. The CV is obtained from the vertical dashed line in each color plot in **B**. The blue shading covers the oxidation peak of histamine and the red shading highlights the oxidation serotonin. (**D**) concentration versus time traces for control (blue) and post-drug (green) evoked histamine. Traces are obtained from the horizontal dashed lines in color plot in **Bi-iv**.

3.3.4 Distinctive H₃R Autocontrol Between Males and Females

We established there was no difference between histamine release, serotonin inhibition, or the ratio of HA/5HT between male and female mice in **3.3.1.** We wanted to further investigate the regulatory role of H_3 receptors in male and female mice by

المنارة للاستشارات

www.manaraa.com

administering an H_3R agonist, immepip (5 mg kg^{-1}), and an H_3R antagonist, thioperamide (20 mg kg^{-1}).

In **Figure 3.5**, male (**Di**) and female (**Dii**) mice respond similarly to H_3R agonism with an overall decrease in max amplitude (male, n=5: Amp$_{max}$: control: $7.72 \pm 1.55\ \mu M$; post-drug: $4.77 \pm 1.56\ \mu M$; $p = 0.024$; female, n=5: Amp$_{max}$: control: $6.20 \pm 0.86\ \mu M$; post-drug: $3.58 \pm 0.51\ \mu M$; $p = 0.005$) and no change in histamine clearance (male: $t_{1/2}$: control: 4.5 ± 1.7 s; post-drug: 2.9 ± 0.6 s; $p = 0.4$; female: $t_{1/2}$: control: 5.6 ± 1.8 s; post-drug: 5.6 ± 2.6 s; $p = 1$ paired t-test).

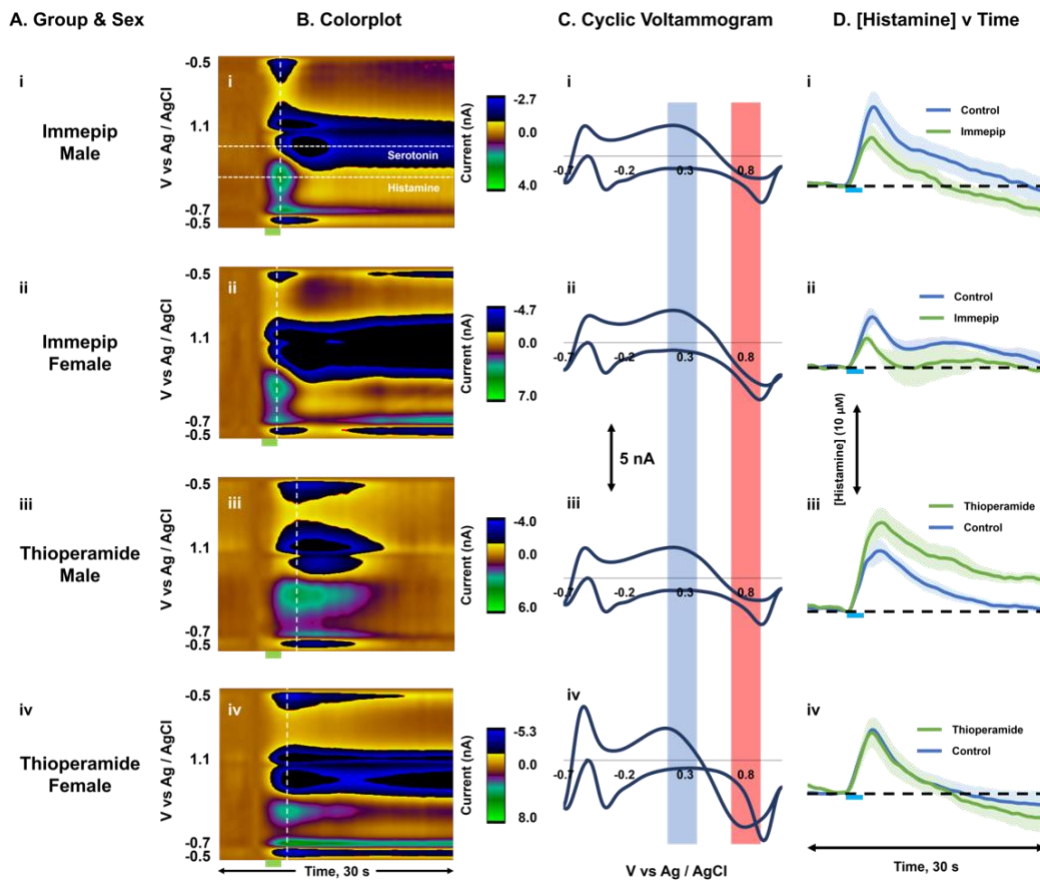**Figure 3.5:** H_3 targeting drugs highlight distinct response of male and female mice. (**A**) the drug and mouse's sex are listed. (**B**) a representative color plot for each grouping of animals is shown. The green bar represents the 2 s electrical stimulation. (**C**) a representative cyclic voltammogram from each cohort of animals. The CV is obtained from the vertical dashed line in each color plot in **B**.

The blue shading covers the oxidation peak of histamine and the red shading highlights the oxidation serotonin. (**D)** concentration versus time traces for control (blue) and post-drug (green) evoked histamine. Traces are obtained from the horizontal dashed lines in color plot in **Bi-iv**.

Thioperamide administration resulted in a significant increase in evoked hypothalamic histamine in male mice (**Diii**) (n=5; Amp_{max}: control: 8.83 ± 1.35 µM; post-drug: 12.10 ± 1.75 µM; p=0.046) while trending toward a significant slowing of reuptake ($t_{1/2}$: control: 4.5 ± 1.7 s; post-drug: 9.9 ± 2.2 s; p = 0.051). However, in the female mice, no such change in amplitude was observed. Female mice (**Div**) exhibit no change in histamine amplitude (n=5; Amp_{max}: control: 7.37 ± 1.40 µM; post-drug: 7.01 ± 1.65 µM; p=0.39) or rate of reuptake ($t_{1/2}$: control: 4.2 ± 1.6 s; post-drug: 3.9 ± 1.3 s; p = 0.48) following the same dose of thioperamide.
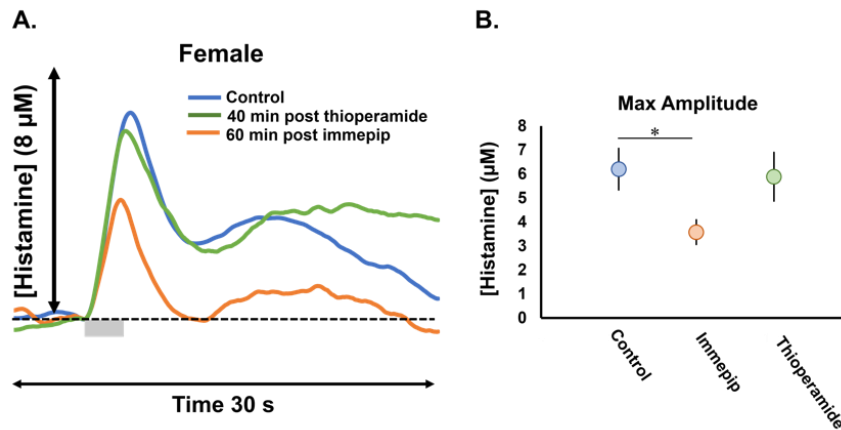
Figure 3.6: Thioperamide raises histamine to control levels following immepip pretreatment. (**A**) FSCV [HA] vs time profiles of evoked histamine for control (n=5, blue), 60 min following immepip (n=5, orange), and 40 min following thioperamide after 60 min immepip (n=4, green). Error bars have been eliminated for clarity. (**B**) max amplitude of evoked histamine for control (blue), 60 min immepip (orange), and 40 min following thioperamide after initial 60 min immepip (green). Significance between two points was taken as p < 0.05

61

Given that females did not respond to 20 mg kg^{-1} thioperamide but did respond to the H$_3$ agonist, immepip, we hypothesized there was a threshold level of extracellular histamine that female mice were unable to surpass. Therefore, we administered immepip (5 mg kg^{-1}) for 60 min to decrease evoked histamine and then administered thioperamide (20 mg kg^{-1}) to determine if histamine levels would increase to control or exceed control levels. **Figure 3.6A** shows the [HA] vs time profiles of control (blue), 60 min post-immepip (orange), and 40 min post-thioperamide (green). Error bars have been omitted for clarity. Following a significant decrease from immepip (*vida supre*), we show that thioperamide elevates stimulated histamine only to around control level (Amp$_{max}$: immepip: 3.58 ± 0.51 µM; post-immepip-thioperamide: 5.89 ± 1.13 µM; p=0.13); we were unable to increase evoked histamine in female mice to above control (Amp$_{max}$: control: 6.20 ± 0.86 µM; post-immepip-thioperamide: 5.89 ± 1.13 µM; p=0.83 paired t-test).

3.3.5 Histamine is Packaged via the Vesicular Monoamine Transporter

We investigated the packaging mechanisms of histamine in the brain using two vesicular monoamine transporter (VMAT) inhibitors with different affinities for VMAT1 and VMAT2 (tetrabenazine (TBZ): 10 mg kg^{-1}; reserpine: 10 mg kg^{-1}). Each compound functions by inhibiting packaging of histamine (and other neurochemicals) into vesicles prior to exocytosis which results in the intracellular neurochemicals being enzymatically metabolized in the cytosol. Both reserpine and tetrabenazine required modification to the saline vehicle to fully dissolve the compounds. Reserpine was dissolved in 0.1 % AcOH in saline and tetrabenazine required 10% DMSO in saline with 1 M HCl (10 µL mL^{-1}). Vehicle solutions were administered (5 mL kg^{-1}) to each mouse for 30 min between control files and drug files to determine any vehicle effects on the evoked histamine and serotonin

profiles. Vehicle injections did not significantly change the evoked release in males or females; however, female mice did have a more obvious change in release amplitude following vehicle.

Reserpine vehicle (0.1% AcOH in saline) injection did not significantly change histamine amplitude from control (male, n=5: Amp_{max}: control: 5.41 ± 1.01 µM; AcOH vehicle: 5.43 ± 0.64 µM; p=0.98) (female, n=5: Amp_{max}: control: 9.17 ± 1.22 µM; AcOH vehicle: 7.76 ± 1.01 µM; p=0.053). However, 60 min following reserpine injection, a significant decrease in evoked histamine amplitude was observed in both male (**Figure 3.7 Di**) (Amp_{max}: AcOH vehicle: 5.43 ± 0.64 µM; reserpine: 2.72 ± 0.47 µM; p=0.009) and female (**Figure 3.7 Dii**) mice (Amp_{max}: AcOH vehicle: 9.17 ± 1.22 µM; reserpine: 6.53 ± 1.01 µM; p=0.016). There was no change in the rate of reuptake of histamine for either sex (male: $t_{1/2}$: control: 2.4 ± 0.7 s; reserpine: 2.8 ± 0.7 s; p=0.51) (female: $t_{1/2}$: control: 6.3 ± 2.5 s; reserpine: 4.4 ± 1.6 s; p=0.23).

Tetrabenazine vehicle (acidified 10% DMSO) administration did not significantly change control evoked histamine (male, n=5: Amp_{max}: control: 7.51 ± 1.32 µM; DMSO: 7.08 ± 1.42 µM; p=0.18) (female, n=5: Amp_{max}: control: 9.02 ± 1.45 µM; DMSO: 7.56 ± 0.75 µM; p=0.27). After the mice received TBZ, a significant decrease in evoked histamine was observed for both sexes (male: Amp_{max}: DMSO: 7.08 ± 1.42 µM; TBZ: 5.49 ± 1.44 µM; p=0.023) (female: Amp_{max}: DMSO: 7.56 ± 075 µM; TBZ: 3.83 ± 0.40 µM; p=0.008)

3.3.6 Pharmacological Manipulation of Histamine Synthesis and Metabolism

Finally, we targeted the beginning and end of histamine's metabolic life cycle in the central nervous system. We used tacrine, an *N*-methyltransferase inhibitor, and α-fluoromethylhistidine, an L-histidine decarboxylase inhibitor, to accomplish this.

63
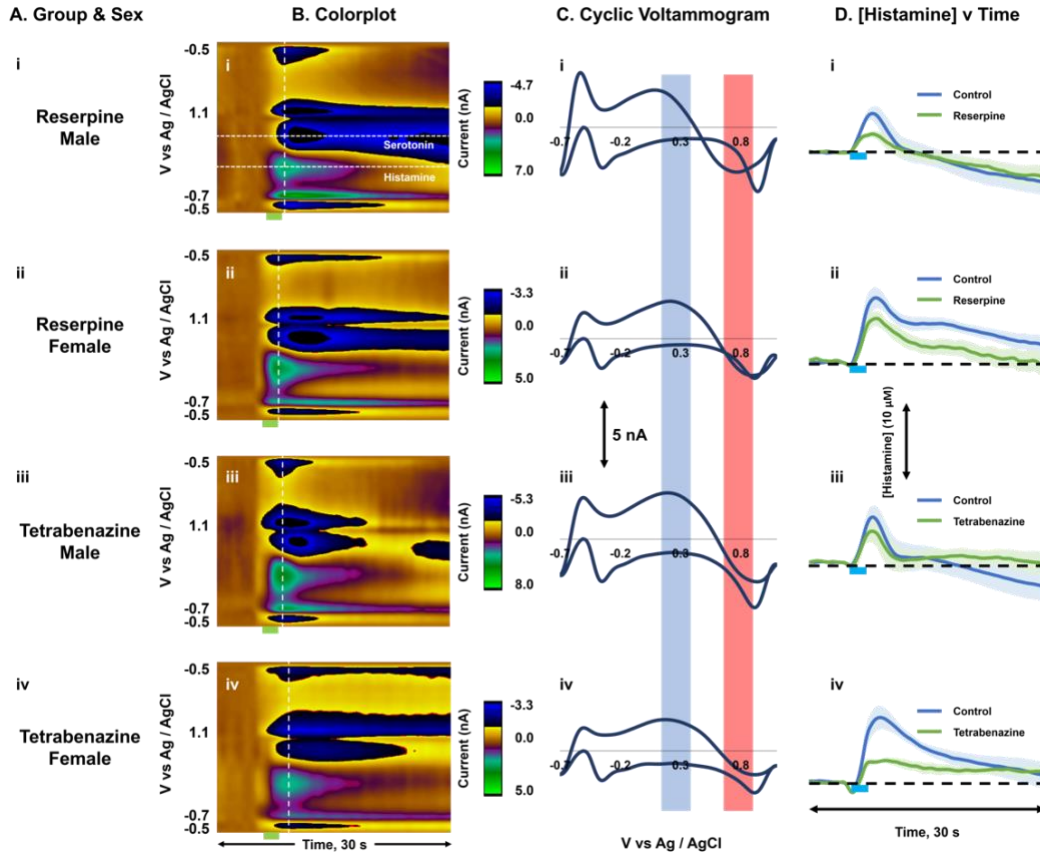
Figure 3.7: VMAT inhibition lowers evoked histamine release. (**A**) the drug and mouse's sex are listed. (**B**) a representative color plot for each grouping of animals is shown. The green bar represents the 2 s electrical stimulation. (**C**) a representative cyclic voltammogram from each cohort of animals. The CV is obtained from the vertical dashed line in each color plot in **B**. The blue shading covers the oxidation peak of histamine and the red shading highlights the oxidation serotonin. **D**) concentration versus time traces for control (blue) and post-drug (green) evoked histamine. Traces are obtained from the horizontal dashed line 'histamine' in color plots in **Bi-iv.**

Administration of tacrine to male mice (**Figure 3.8 Di**) resulted in no change in histamine amplitude (n=5, Amp_{max}: control: 9.56 ± 0.89 µM; tacrine: 9.41 ± 1.22 µM; p=0.92) and a slowed clearance of histamine from the extracellular space ($t_{1/2}$: control: 2.8 ± 0.8 s; tacrine: 6.0 ± 0.7 s; p=0.025). Female mice (**Figure 3.8 Dii**) displayed no amplitude change following tacrine (n=4, Amp_{max}: control: 7.01 ± 1.79 µM; tacrine: 7.74 ± 1.85 µM; p=0.22) and had a slowing of reuptake that trended towards a significant change ($t_{1/2}$: control: 4.8

± 1.4 s; tacrine: 4.9 ± 2.4 s; p=0.095). It's clear that in both male and female mice, inhibiting the intracellular metabolic enzyme results in no change in overall release of histamine but does cause histamine to remain in the synapse for a prolonged amount of time due to the concentration gradient created intracellularly.
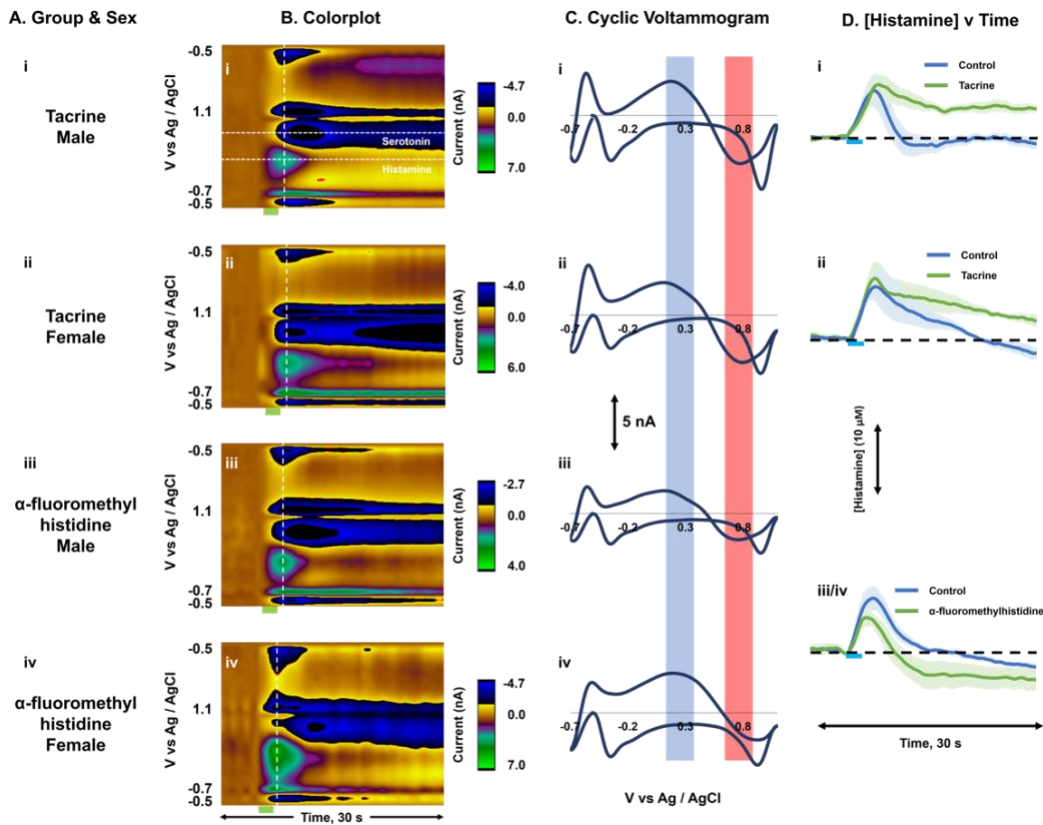
Figure 3.8: Inhibition of histidine decarboxylase lowers evoked histamine release while inhibiting histamine *N*-methyltransferase results in histamine remaining in the extracellular space. (**A**) the drug and mouse's sex are listed. (**B**) a representative color plot for each grouping of animals is shown. The green bar represents the 2 s electrical stimulation. (**C**) a representative cyclic voltammogram from each cohort of animals. The CV is obtained from the vertical dashed line in each color plot in **B**. The blue shading covers the oxidation peak of histamine and the red shading highlights the oxidation serotonin. (**D**) concentration versus time traces for control (blue) and post-drug (green) evoked histamine. Traces are obtained from the horizontal dashed line 'histamine' in color plots in **Bi-iv.**

Due to the limited amount of FMH we had available, we combined the male and female responses into one grouping. We have shown that 60 min following inhibition of

histamine synthesis *via* FMH, a significant decrease in stimulated histamine was observed (**Figure 3.8 Diii/iv**) (n=2 male, 2 female; Amp_{max}: control: 8.59 ± 1.86 µM; post-FMH: 5.83 ± 1.24 µM; p=0.038). There was no change in histamine clearance (($t_{1/2}$: control: 2.4 ± 0.2 s; FMH: 2.3 ± 0.4 s; p=0.82)

3.4 Discussion

3.4.1 Histamine FSCV in male and female mice

The exclusion of females from pharmacological testing can have serious consequences for the health and safety of patients.[31] Estrogen has been shown to be an important regulator in the ventromedial nucleus (VMN) of the hypothalamus.[23, 32-33] H_1R and estrogen receptor alpha (ERα) mRNA are co-expressed in histaminergic neurons[23, 34] and ERβ are expressed in the TMN.[35] The localization of estrogen receptors on histamine projections highlights the potential role estrogen plays in regulating immune response. Indeed, estrogen and progesterone have been shown to mitigate the acute inflammatory response to lipopolysaccharide exposure.[36-39] Additionally, inflammatory diseases and the susceptibility to the occurrence of diseases are more likely in post-menopausal women than pre-menopausal women and age matched males.[40-41]

In this study we set out to investigate the machinery of the central histaminergic systems of male and female mice *via* response to various pharmaceutical challenges. Under control conditions, we did not find any differences in the release of hypothalamic histamine in male and female mice (**Figure 3.1**). This finding is in agreement with our previous work that compared hippocampal serotonin between sexes and found no statistical differences.[42] Our results differed from some literature reports that suggested histamine turnover and histamine cerebrospinal fluid concentration are higher in females[43] or show lowered

histamine in females.[22] FSCV is accompanied by a large aphysiological stimulation which releases a substantial amount of neurochemicals and is a fundamentally different type of measurement than other sampling techniques. *In vivo* measurements keep brain circuits intact and are often different than data obtained from *ex vivo* brain slices.[44] Our data are unnormalized and highlight the high level of conservation in neurochemical regulatory mechanisms across individual mice.

There is an intrinsic belief that there may be neurochemical differences between the different stages of the estrous cycle that has limited the use of females in research.[45] Due to histamine's potential role in neuroinflammation, this belief may be even stronger; the extent of immune reactivity has been thought to depend on the different stages of the estrous cycle.[46-47] Therefore, we compared evoked histamine in female mice during different stages of the estrous cycle and found that histamine was not significantly different throughout (**Figure 3.2**). This finding is not surprising given our prior experience with measuring neurotransmitters with FSCV where we have had to employ aggressive means to affect a significant but small change from homeostasis[24, 42], such as high doses of SSRIs which correspond to profound behavioral alterations.[48] Interestingly, we observed a double release event that occurred during the estrus stage of the female cycle. We have previously observed a similar phenomenon in the prefrontal cortex (pFC) regarding stimulated serotonin release.[49] West *et al* determined that the occurrence of a single release or double release was dependent upon the specific region of the pFC the CFM was located. We applied that assumption to the posterior hypothalamus as well and found that double peaks were most likely to occur when the CFM was located anterior to our target coordinates. The ventromedial nucleus, periventricular nucleus, and dorsomedial nucleus are located in

67

this area and known to have a very high level of hormonal regulation.[50-52] Neuronal mRNA sampled from VMN neurons showed colocalized expression of ERα and H_1, H_2, and H_3 receptors.[23] Indeed the regulation of lordosis has been shown to be dependent on the interplay of histaminergic neurons and estrogens through histamine and estrogen receptors.[23, 34, 53]

We conduct our histamine measurements in a specifically targeted region of the posterior hypothalamus where we are able to detect both evoked histamine and the resulting inhibition of serotonin. This has been shown to be an H_3R mediated process by our lab and others.[1, 24, 26-27] After confirming no statistical differences in evoked histamine between male and female mice and throughout the estrous cycle, we analyzed the level of serotonin inhibition resulting from histamine release in the same mice. Unsurprisingly, the overall amount of serotonin inhibition is not different between males and females, and the ratio of maximum release to peak inhibition does not differ (**Figure 3.2**). Throughout the estrous cycle serotonin did not vary significantly but a relative trend can be seen between histamine and serotonin amplitudes across cycle stages. As histamine exhibited two release profiles, we also compared the corresponding serotonin data of single and double events. A double peaked histamine release resulted in a larger amount of inhibition, but the difference was not significant (**Figure 3.3**). These results highlight the highly conserved nature of both the histamine and serotonin systems to maintain a homeostatic balance in the brain.

3.4.2 Histamine receptor pharmacology in male and female mice

After determining the evoked release of histamine was conserved between male and female mice, we wanted to explore how different receptor targeting compounds affected the release and reuptake of histamine. Antihistamines are compounds most

commonly prescribed for common allergies and target post-synaptic H_1 or H_2 receptors. First generation antihistamines, like diphenhydramine, readily cross the blood brain barrier and block the H_1 receptor. Histamine is unable to activate the receptor to propagate signaling resulting in the common side effect of drowsiness. In both male and female mice, when H_1 activation is inhibited, a slowing of histamine clearance is observed, presumably to allow histamine to remain in the synapse and activate the receptor after which it would then be reuptaken. Interestingly, these results point to a communication between H_1 and membrane transport proteins.[54] The results of zolantidine administration were unexpected given how H_1 antagonism effected reuptake. Even as a brain penetrating potent H_2 antagonist, zolantidine did not cause any significant changes in the release and reuptake profile of histamine in male or female mice (**Figure 3.4**). This could be due to the difference between diphenhydramine being an inverse agonist and zolantidine being an antagonist.[55] H_2 receptors are widely expressed throughout the hypothalamus just as H_1 receptors but reuptake signaling mechanisms appear not to be linked to H_2 activation and propagation.

There is a substantial amount of literature documenting the neuromodulatory role and autoregulatory role of the H_3 receptor.[1, 5, 26-27] We previously used the H_3R antagonist thioperamide when developing histamine FSCV[24-25] and anticipated seeing robust changes in brain histamine when targeting H_3R. However, when an equivalent dose of thioperamide was administered to female mice, a robust increase in histamine release did not occur. This contrasts with previous work that observed behavior following thioperamide treatment and found similar effects in and male female rats.[56] After confirming there was consistently no change in female mice, we hypothesized that H_3R expression in females possibly is lower

69

and administering a higher dose (50 mg kg^{-1}) would test this notion. The higher dose did not result in a similar elevated release as in male mice and we ruled out receptor expression. We then tested whether immepip, an H$_3$R agonist, would have a differential response in male and female mice. We found that H$_3$R agonism resulted in an overall decrease in evoked histamine in both male and female mice without affecting the clearance slope (**Figure 3.4**). We hypothesized potential evolutionary regulatory mechanisms are present in female mice that do not allow histamine to elevate above a certain threshold. Ferretti *et al.* suggested that stressor-induced increases in histamine release may be lower in females than it is in males.[22] Therefore, we tested this hypothesis by pretreating female mice with immepip to cause a significant decrease in evoked histamine. Following immepip, administration of thioperamide (20 mg kg^{-1}) should now increase histamine to control or above control levels. In **Figure 3.5**, following a significant decrease in evoked histamine, thioperamide was only able to increase histamine back to near control levels, supporting our hypothesis that there are intrinsic mechanisms present in the female immune system that strictly regulate the levels of histamine in the brain. This increased control may have evolutionary underpinnings as it is often thought that female animals exhibit more homeostatic control and that female hormones, estrogens and progesterones, have neuroprotective functions.[57-58]

Studies have shown that females experience an increased risk of developing inflammatory disorders later in life, particularly post-menopause.[40-41] Therefore we wanted to test whether age or circulating hormone levels could influence the female response to thioperamide. There are three potential strategies we identified. 1) perform voltammetry experiments on mice that are undergoing or have undergone menopause (age 9-12+

70

months).[59] 2) chemically or physically eliminate ovaries through ovotoxin administration or ovariectomy. 3) eliminate the influence of estrogens on the immune response through pretreatment with an aromatase inhibitor, letrozole. By pretreating female mice with letrozole and then administering thioperamide, we would be able to view how the female histaminergic system responds to H_3R antagonism in the absence of estrogenic regulation. This is the focus of future experiments.

3.4.3 Vesicular packaging of histamine in male and female mice

Vesicular packaging is a crucial step for monoamine neurotransmission and disruptions can have downstream effects. Brain histamine can originate from neurons, glia, and mast cell degranulation.[5] We targeted VMAT2 with two compounds, tetrabenazine and reserpine and examined their effect on histamine release. Tetrabenazine is selective for VMAT2, while reserpine has affinity for both VMAT1 and VMAT2. However, VMAT2 is responsible for packaging in neurons, while VMAT1 is exclusively located in endocrine cells.[60] Additionally, Erickson *et al.* demonstrated that histamine displayed a 30-fold higher affinity for VMAT2 over VMAT1 and reserpine had about 3x affinity for VMAT2 over VMAT1.[61] Both reserpine and tetrabenazine caused significant decreases in overall evoked histamine in males and females, with females responding the strongest to tetrabenazine (**Figure 3.6 Div**). This could also be due to the initially high control signals obtained in that cohort of mice which makes the decrease appear more robust. We also confirmed that the majority of evoked histamine was neuronal or glia based and most likely not related to mast cell degranulation. This confirmed that histamine has similar prerelease mechanisms to other common neurotransmitters such as dopamine and serotonin and will better help understand the altered mechanisms during inflammatory states.

71

3.4.4 Influence of Enzyme Inhibition on Evoked Histamine

We tested how inhibiting histamine synthesis might affect evocable histamine. Other groups have used FMH to successfully lower histamine and our data are in good agreement with those reports.[62-64] Although the goal of this work was to highlight the male and female response to compounds separately, we combined the sexes' responses in the case of FMH (20 mg kg^{-1}) due to the limited amount of the compound available. Despite the inhibition of synthesis, there still is evocable histamine 60 min after *ip* injection, most likely due to the large aphysiological nature of our electrical stimulation. CNS histamine is metabolized exclusively by HA *N*-methyltransferase which is located intracellularly. By blocking the enzyme, a concentration gradient is created between the intra- and extracellular space and histamine spends a prolonged time in the synapse. The male and female mice responded similarly both having significant slowing of reuptake following tacrine (*ip*; 2 mg kg^{-1}) (**Figure 3.7 Diii, iv**). Tacrine has additional affinity for blocking acetylcholine esterase which has been explored for cognitive boosting abilities in Alzheimer's patients.[65-66] Our data show that the metabolic pathway of histamine, including synthesizing and degrading enzymes, is highly conserved between male and female mice.

What we are currently working towards is using this collection of novel simultaneous histamine and serotonin data to create a mathematical model of the synapse. We have made progress on the serotonin system[49, 67] and have investigated parts of the histamine system[24, 68] but have not fully elucidated the mechanisms regulating the synapse outside of standard H$_3$R mediated inhibition.[24] A model built using these data will capture how changes in histamine receptor functionality, vesicular packaging, and synthesis and

metabolism can affect the transmission of histamine and serotonin, a critical step in understanding the differences between healthy and inflamed immune systems.

3.5 Conclusion

In this study, we investigated the pharmacological response of the male and female histamine system in the brain. We compared control evoked histamine between male and female mice and found no differences between them as well as no influence from the estrous cycle on histamine release. We targeted histamine receptors H_1, H_2, H_3, and H_4, vesicular packaging, synthesis, and metabolism. We found that the histaminergic system is highly conserved between the sexes but females appear to have a stronger regulatory control over increased histamine levels mediated through H_3R. Our data highlight the importance of considering biological sex as a variable when evaluating pharmacology data and that simple extrapolation from male animal models to female should no longer occur.

CHAPTER 4

INVESTIGATING HISTAMINE INACTIVATION USING THE MET172

MOUSE MODEL[1]

---

[1] Berger, SN. Hersey, M., Samaranayake, S., Best, J., Nijhout, HF., Reed, MC., Blakely, RD., Hashemi, P. Investigating histamine inactivation using the Met172 mouse model. In preparation. *Euro. J. Neurosci.*

4.0 Abstract

Histamine is an important mediator of inflammation and immune response in the peripheral nervous system. Much less is known about histamine's functions within the brain and central nervous system. Only one metabolic pathway is available for histamine within the brain through the intracellularly located histamine *N*-methyltransferase, despite there not being a dedicated transport protein for histamine identified. Stimulated histamine exhibits similar release and reuptake kinetics to that of common monoamine systems, thus, we investigated which transporters are responsible for the reuptake of histamine in the brain. We screened six agents to inhibit the serotonin transporter (SERT), norepinephrine transporter (NET), dopamine transporter (DAT), and organic cation transporter (OCT) and found compounds showing appreciable slowing of histamine clearance all have antidepressant activity. We focused on the role of SERT inhibition towards histamine clearance by utilizing a transgenic mouse model, the SERT Met172, which is insensitive to certain selective serotonin reuptake inhibitors (SSRI). The SSRI escitalopram significantly slowed histamine clearance in Met172 mice absent SERT antagonism. Our data rule out SERT's contribution toward histamine reuptake and are in agreement with previous reports that propose OCT as the main transporter responsible for clearance. Our study highlighted key off-target mechanisms of antidepressants and the need to better understand the full spectrum of the mechanisms of these agents to improve their clinical efficacy.

4.1 Introduction

Histamine is an important monoamine in the central nervous system (CNS) and dysregulation can lead to behavioral abnormalities.[1-4] Therapies targeting the histaminergic

system are much less robust than other more common monoamine strategies and have failed to reach clinical relevance for neurological disorders.[3, 5-6] There is a wide gap between understanding histamine's roles in the CNS and developing successful therapies because histamine's role and its interaction with other neurotransmitter systems remain understudied. Histamine controls monoamine release through H_3 receptors on presynaptic terminals but understanding this regulation in the context of CNS disorders is unclear.[7-12]

In the CNS, histamine is exclusively metabolized to *tele*-methylhistamine through histamine *N*-methyltransferase.[13] This metabolic route is only available for central histamine; peripheral histamine undergoes its own specific degradation pathway.[14] There is evidence for partial histamine uptake into astrocytes[15] and synaptosomes[16], but a dedicated histamine transporter has not yet been identified. Previous work from the Hashemi lab reported that the reuptake curve of histamine, as measured by FSCV, was best fit with first order Michaelis-Menten kinetics[17] similar to dopamine and serotonin that have dedicated membrane transporters.[18-19] Therefore, we sought to establish which mechanisms might be responsible for this (suggestively) active reuptake of histamine *in vivo*.

Previous work from Lyn Daws' lab has shown that the monoamine transporters (dopamine transporter (DAT), norepinephrine transporter (NET), serotonin transporter (SERT)) are not particularly selective for their dedicated substrate and regularly will reuptake one another's substrates; a phenomenon she coined 'promiscuous reuptake.'[20] Additionally, there is evidence that the non-specific membrane bound organic cation transporter (OCT2/3) and plasma membrane bound transporter (PMAT) play a significant role in histamine reuptake.[21-22]

76

In this work, we inhibited SERTs (with three separate agents), DATs, NETs, and OCTs and found that all agents, with the exception of the DAT inhibitor, slowed the reuptake of histamine. In agreement with previous findings, OCT inhibition resulted in the strongest inhibition of histamine reuptake.[21-23] However, due to promiscuous reuptake, our results do not definitively identify which transporter is responsible for histamine uptake. To hone in better on the reuptake mechanism involved, we utilized a transgenic mouse model, the SERT Met172, generated by Randy Blakely at Florida Atlantic University. In Met172 mice, the SERT protein coding has a single amino acid substitution (isoleucine172 → methionine172) that renders these mice insensitive to several SSRIs including escitalopram, which was included in the initial reuptake screening.[24] Importantly, this substitution does not affect the function of the SERT.[25] We found that administration of escitalopram to both Met172 and wild-type (WT) mice results in the inhibition of histamine reuptake, despite escitalopram not inhibiting the SERT, suggesting that SERTs do not play a major role in histamine reuptake. These results suggest that there exists an active reuptake mechanism for histamine, primarily through OCTs and negligible uptake through SERTs. This information is critical for improving the efficacy of CNS targeting pharmaceuticals.

4.2 Materials and Methods

Chemicals and Reagents

Escitalopram oxalate (Sigma Aldrich, St. Louis, MO, USA) at 10 mg kg^{-1}, GBR 12909 (Sigma Aldrich) at 15 mg kg^{-1}, desipramine hydrochloride (Sigma Aldrich) at 15 mg kg^{-1}, citalopram hydrobromide (Sigma Aldrich) at 5 mg kg^{-1}, sertraline hydrochloride (Sigma Aldrich) at 10 mg kg^{-1}, and decynium-22 (Sigma Aldrich) at 0.1 mg kg^{-1} were individually dissolved in sterile saline (0.9% NaCl solution, Hospira, Lake Forest, IL,

77

USA) and administered *via* intraperitoneal (*ip*) injection at a volume of 5 mL kg^{-1} body weight. Urethane (Sigma Aldrich, St. Louis, MO, USA) was dissolved in sterile saline at 25% w/v and administered *ip* at 7 µL/g mouse body weight for surgical anesthesia.

Electrode Fabrication

All electrodes are made in house. A single carbon fiber is aspirated into a borosilicate capillary (0.6 mm x 0.4 mm x 10 cm; OD x ID x L) (A-M Systems, Sequim WA, USA) and sealed under gravity and heat by a vertical pipette puller (Narishige, Amityville, NY, USA) to create two separate electrodes. The protruding fiber is then trimmed under light microscope to ~150 µm by scalpel. An electrical connection is forged with the fiber through a stainless-steel connecting wire and silver epoxy. Finally, a thin layer of Nafion (LQ-1105, Ion Power, New Castle, DE, USA) is electrodeposited onto the fiber surface at 1 V for 30 s; the coated fiber is dried for 10 min at 70 °C.[26]

Data Collection and Analysis

Fast-scan cyclic voltammetry was performed on anesthetized mice using a Dagan potentiostat (Dagan Corp., Minneapolis, MN, USA) and custom built hardware interfaced with PCIe 6341 & PCI 6221 DAC/ADC cards (National Instruments, Austin, TX) and a Pine Research headstage (Pine Research Instruments, Durham, NC, USA). WCCV 3.06 software (Knowmad Technologies LLC, Tucson, AZ, USA) was used to control the hardware and perform data analysis. The histamine waveform (-0.5 V to -0.7 V to +1.1 V to -0.5 V at 600 V s^{-1}) was applied at 60 Hz for 10 min, then at 10 Hz for min prior to data collection. Data were collected at 10 Hz. Histamine was evoked *via* biphasic stimulation applied through a linear constant current stimulus isolator (NL800A Neurolog, Digitimer

North America LLC, Fort Lauderdale, FL, USA) with stimulations at 60 Hz, 360 µA, 2 ms in width, and 2 s in length.

Data were collected and filtered on WCCV software (zero phase, Butterworth, 3 kHz low pass filter). Four control evoked files, 10 min apart, were averaged for the control evoked histamine signal after which drug was administered and files were collected at 0 min, 5 min, 10 min, and every 10 min thereafter until 120 min. Currents obtained were converted to concentrations through previously generated calibration factors for both histamine (2.825 µM nA^{-1}) and serotonin (11 µM nA^{-1}).[17, 27] Mathematical modeling was *via* a previous model for histamine cells in MatLab.[28]

Statistical Analyses

Average control response was generated from four current vs time traces per animal and averaged to create an overall group average. Exclusion criteria were based on outliers (*via* Grubbs test) and animals that did not survive the experimental paradigm. Standard error of the mean (SEM) was calculated using the average response of each animal (n = # animals). Significance between two points was determined by student's t-test and taken as $p < 0.05$. All error bars represent the standard error of the mean (SEM).

Animals and Surgical Procedure

Animal procedures and protocols were in accordance with the regulations of the Institutional Animal Care and Use Committee (IACUC) at the University of South Carolina, accredited through the Association for Assessment and Accreditation of Laboratory Animal Care (AAALAC). Male and female SERT Met 172 knock in mice on a 129S6/S4 background were backcrossed with C57BL/6J mice and wild type mice (WT; C57 mice with 129 wildtype SERT gene (Ile172)) aged 6-20 weeks were used. Animals

were group housed with *ad libitum* access to food and water and were kept on a 12 h light/12 h dark cycle (lights on 0700/lights off 1900).

Stereotaxic surgery (David Kopf Instruments, Tujunga, CA, USA) followed induction of deep and sustained anesthesia from an intraperitoneal injection of urethane. Mouse body temperature was maintained using a thermal heating pad (Braintree Scientific, Braintree, MA, USA). All surgical coordinates were taken in reference to bregma.[29] A Nafion coated CFM was lowered into the posterior hypothalamus (AP: -2.45, ML: 0.50, DV: -5.45 to -5.55) and a stimulating electrode (insulated stainless-steel, diameter: 0.2 mm, untwisted, Plastics One, Roanoke, VA, USA) was placed into the medial forebrain bundle (AP: -1.07, ML: +1.10, DV: -5.00).[27] A pseudo-Ag/AgCl reference electrode, created by chloridizing a polished silver wire in HCl (15 s in 1 M HCl at 5 V), was placed in the contralateral hemisphere.

4.3 Results

To screen potential monoamine transporters responsible for histamine reuptake, we tested the effects of monoamine transport inhibitors on histamine reuptake. In **Figure 4.1**, we measured evoked histamine (control, blue) and then pharmacologically inhibited the following transporter proteins (post-drug, green): dopamine transporters (DATs), serotonin transporters (SERTs), and norepinephrine transporters (NETs) with the following agents (*ip*; n = 5 each): GBR 12909 (DAT inhibitor, 15 mg kg^{-1}), escitalopram (SERT inhibitor, 10 mg kg^{-1}), citalopram (SERT inhibitor, 5 mg kg^{-1}), sertraline (SERT inhibitor, 10 mg kg^{-1}), and desipramine (NET inhibitor, 15 mg kg^{-1}). We found that in all cases except for DAT inhibition, there was slowing of the rate of histamine reuptake that peaked at 60 min. The ability of both SERT and NET inhibitors to slow histamine clearance suggests a less

selective transporter might be involved. We therefore turned towards organic cation transporters (OCTs) and plasma membrane monoamine transporters (PMATs) which were inhibited with decynium-22 (OCT and PMAT inhibitor, 0.1 mg kg^{-1}), providing evidence that this agent also slowed histamine clearance.
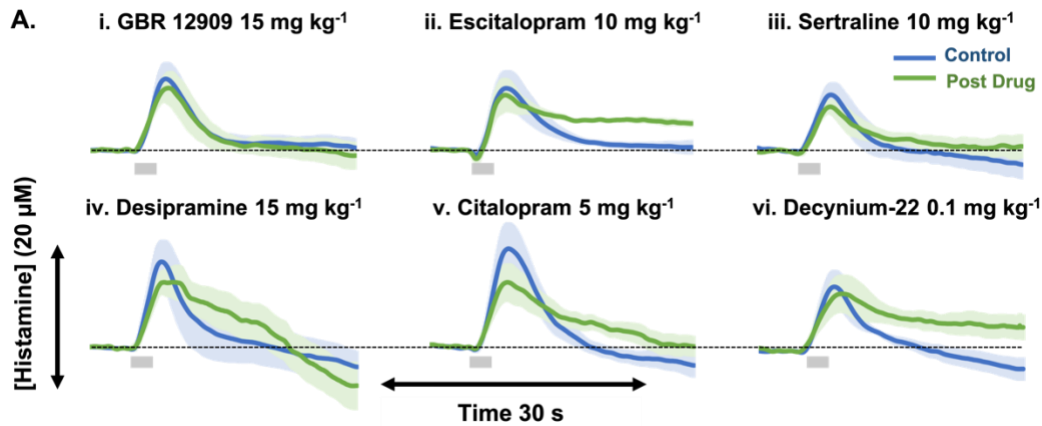
Figure 4.1: Histamine reuptake is inhibited by monoamine transporter inhibitors. (**A**) Control hypothalamic histamine (blue) and 60 min post (**i**) GBR 12909 (*ip*, 15 mg kg^{-1}), (**ii**) escitalopram (10 mg kg^{-1}), (**iii**) sertraline (10 mg kg^{-1}), (**iv**) desipramine (15 mg kg^{-1}), (**v**) citalopram (5 mg kg^{-1}), and (**vi**) decynium-22 (0.1 mg kg^{-1}) (green; n=5, each) Stimulation marked by grey box at 5-7 s. Error ($\pm$ standard error of the mean) is a shaded region around traces. Doses were reported in prior work to create behavioral shifts or neurochemical changes.[26, 30-34]

Instead of only examining $t_{1/2}$ here, we took a more sophisticated kinetic approach. We used a previously developed mathematical model for histamine dynamics[28] to investigate how physiological parameters could be adjusted to best capture curves for escitalopram, citalopram, sertraline, and decynium-22. Model curves (dashed lines) are compared to experimental curves (solid lines) in **Figure 4.2**. In all four cases, we found that the major parameter change was a 50% reduction in the transport of extracellular histamine back into the cell, consistent with the inhibition of histamine reuptake. To further

81

narrow down which transporters are the largest contributor to histamine reuptake we used the SERT Met172 mouse.
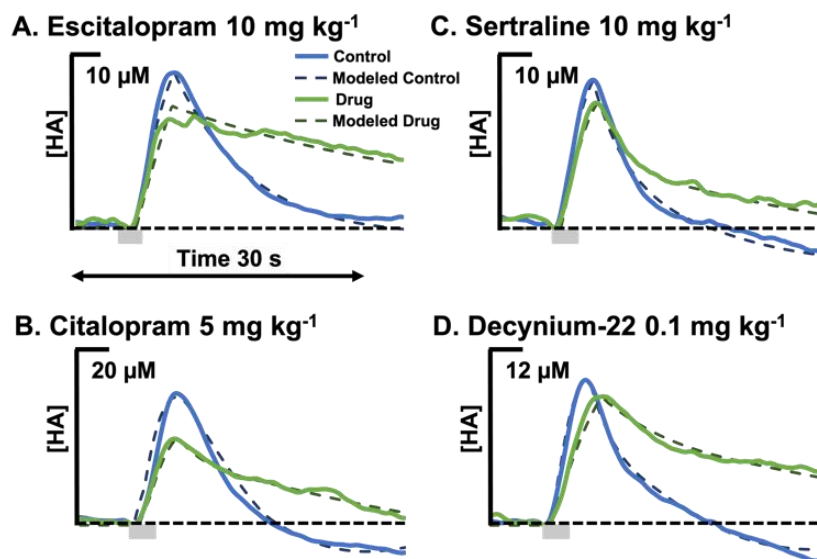
Figure 4.2: Modeled transporter data. Each panel shows the experimental curves (solid lines) and model predictions (dashed lines) both pre- and post-drug for the three different SSRIs and decynium-22. The main difference between the pre-drug and post-drug model curves was a 50% decrease in the reuptake of histamine from the extracellular space into the histamine varicosity. In the cases of escitalopram and decynium-22, the uptake into glial cells was partially blocked, which is consistent with the fact that the post-drug experimental curves are higher and flatter in those two cases.

This mouse bears a single amino acid substitution (Ile172 is encoded in humans and mice and here are converted to Met172) that impairs the binding of high affinity antagonists, such as the SSRIs, without impacting serotonin uptake activity or *in vivo* serotonin clearance (**Fig. 4.3A**).[24-25, 35-36] In **Figure 4.3,** we show the effects of escitalopram on changes in extracellular histamine and serotonin using this mouse. In **Figure 4.3Bi and ii**, escitalopram administration inhibited histamine clearance in Met172 mice ($t_{1/2}$: control: 3.65 ± 0.813 s; escitalopram: 5.35 ± 0.31 s; p=0.048) in a manner comparable to wild type

mice. These data effectively rule out a role for SERT in histamine clearance or in the actions of SSRIs to potentiate extracellular histamine levels but nonetheless show that SSRIs inhibit histamine reuptake. In **Figure 4.3Ci and ii,** we monitored the effects of escitalopram administration on extracellular hippocampal serotonin levels and confirmed previous findings that escitalopram is ineffective at blocking serotonin clearance in Met172 mice.[24] In wild type mice, escitalopram increased evoked hippocampal serotonin (Amp_{max}: 29.19 ± 4.25 nM to 63.30 ± 5.33 nM; p= 0.008) and slowed extracellular clearance ($t_{1/2}$: 1.50 ± 0.07 s; 7.98 ± 1.67 s; p=0.03) after 50 min.
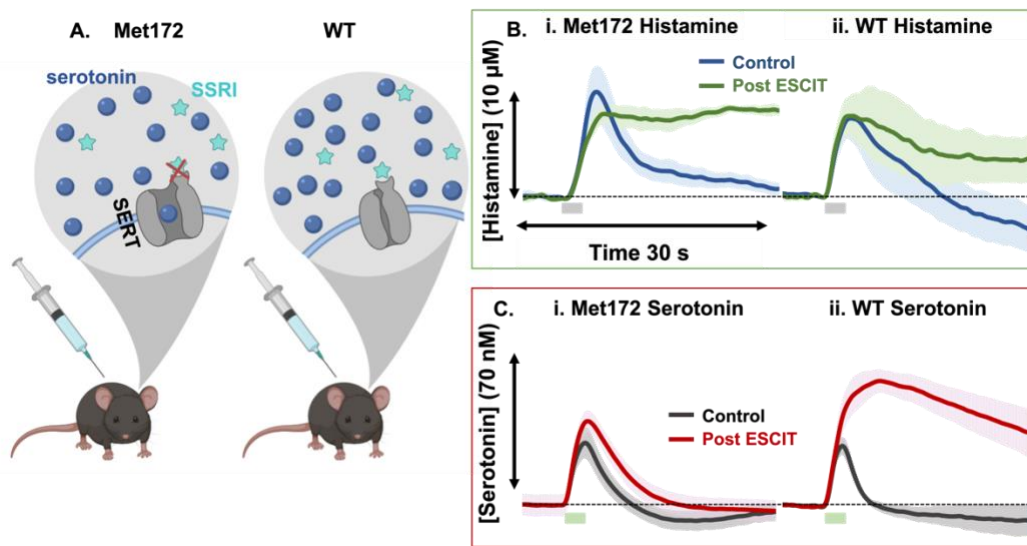
Figure 4.3: Histamine reuptake is inhibited by monoamine transporter inhibitors**.** (**A**) Cartoon schematic depicting SSRIs inability to bind to SERTs and prevent serotonin reuptake in Met172 mouse. (**B**) Evoked hypothalamic histamine control (blue) and 50 min post escitalopram (green, 10 mg kg^{-1}) in (**i**) Met172 and (**ii**) WT mice (n=4, each). (**C**) Evoked hippocampal serotonin control (grey) and 70+ min post escitalopram (red, 10 mg kg^{-1}) in (**i**) Met172 (n=5) and (**ii**) WT mice (n=4). The grey and green bars represent the electrical stimulation from 5-7 s. Error ($\pm$ standard error of the mean) is a shaded region around traces.

4.4 Discussion

Commonly prescribed SSRIs, citalopram, escitalopram, and sertraline all inhibited the reuptake of histamine following electrical stimulation (**Figure 4.1**). In addition to their

high affinity for SERT, SSRIs do possess some off-target affinity for OCT.[37-38] This is particularly important to highlight in terms of antidepressant therapies. Serotonin is thought to be decreased in the extracellular space in depressed patients and the goal of antidepressants is to return serotonin to a healthy level.[39] In fact in the next chapter we provide unequivocal evidence for this lowered serotonin level. Studies have documented the comorbidity of inflammation and depression[40-42] and elevated levels of proinflammatory cytokines has spawned a new hypothesis on the underlying causes of depression.[43] However, pharmacological targeting of inflammatory biomarkers has yielded inconsistent results.[44-46] Histamine is a peripheral marker of inflammation and in Chapter 5 we show that histamine is also a maker of neuroinflammation. Given that during inflammation (i.e. depression) brain histamine is increased and this histamine is at least partially responsible for inhibiting serotonin levels, the compounds ostensibly prescribed to alleviate depressive symptoms may in fact have detrimental effects through keeping histamine present in the synapse and *inhibiting* the release of serotonin; antithetical to their prescribed role. Antidepressants are prescribed to a substantial percentage of the population and patients often take several weeks for symptom alleviation.[47] We highlight the critical need for a comprehensive understanding of the molecular mechanisms of antidepressants to improve clinical efficacy.

A histamine specific transporter has not yet been identified despite histamine having reuptake kinetics similar to other rapidly cleared monoamines and histamine *N*-methyltransferase being located intracellularly.[13, 18-19] Indeed, in Samaranayake *et al.* where we first described FSCV dual histamine-serotonin measurement, when mathematically describing the responses, the models necessitated an active reuptake term

84

to fit the histamine curves.[17] Thus, we pharmacologically tested whether inhibition of other monoamine transporters affected histamine reuptake. We inhibited SERTs (with three different agents), DATs, and NETs and found that SERT and NET inhibition slowed the clearance of histamine. Next we turned towards OCTs and PMATs. OCTs and PMATs are low affinity transporters with the notable ability to non-selectively transport biogenic amines.[48-49] Gasser and colleagues recently showed that OCT and PMAT reuptake histamine (and other monoamines) with varying affinities.[22] Our results are in agreement and show that OCT/PMAT inhibition *via* decynium-22 slowed the clearance of histamine *in vivo*. However, these results do not definitively identify which transporter is responsible for histamine reuptake because the different agents we administered have affinity for the different monoamine transporters.[20] Importantly, we show that histamine clearance was inhibited by several compounds that all possess antidepressant activity in **Figure 4.1** (sertraline, escitalopram, citalopram, desipramine, and decynium-22).[50-51]

To narrow down a histamine reuptake transporter, we utilized a transgenic mouse model, the SERT Met172. SERT Met172 mice are a genetic knock-in strain which bear a single amino acid substitution that renders their SERT insensitive to several SSRIs.[24, 35-36] Importantly, this model allows the SERT to remain intact and functioning, which is arguably more physiologically relevant rather than removing SERT function entirely as in a SERT knockout mouse.[35, 52] Using this mouse, we observed that escitalopram no longer antagonized serotonin reuptake (**Figure 4.3C**), yet still slowed histamine clearance, strongly suggesting that a transporter other than SERT which escitalopram has affinity for[53] dictates escitalopram-mediated clearance. Moreover, a NET-specific tricyclic antidepressant (desipramine) with little SERT activity also delayed histamine clearance.

85

Given the ability of the OCT/PMAT inhibitor decynium-22 to inhibit evoked histamine clearance, it seems likely that SERT-independent effects of SSRIs and the tricyclic antidepressant may be mediated by these transporters. This is a reasonable assumption given that OCTs are located most densely on glial cells that mediate the brain's immune reactions.[54-55]

It is important to remember the greater implications of this finding. During depression and chronic stress, elevated levels of histamine are contributing to decreased serotonin levels through H_3 modulation. Antidepressants are prescribed with the intention to raise serotonin in the extracellular space and increase receptor activation. However, these very prescriptions may result in sustained histamine presence in the synapse decreasing overall serotonin levels. Future work should be aimed at mitigating antidepressant affinity for OCT and aimed at designing therapeutic targets with neuromodulation in mind.

4.5 Conclusion

Histamine is an understudied neuromodulator, but its reuptake mechanism is not fully elucidated. We pharmacologically inhibited serotonin transporters (SERT), dopamine transporters (DAT), norepinephrine transporters (NET), organic cation transporters (OCT), and plasma membrane monoamine transporters (PMAT) and found all agents that inhibited histamine clearance exhibited antidepressant effects. We then used the transgenic mouse model SERT Met172 to rule out SERT's contribution to histamine reuptake in the brain. Our data are in agreement with the conclusion that high efficiency, low affinity OCT are responsible for the bulk of histamine reuptake. PMATs still remain to be studied more extensively, but currently the only selective PMAT inhibitors are HIV protease inhibitors

and present their own confounding factors. Antidepressants target the different monoamine transporters to block reuptake in an effort to extend the amount of time that molecules spend in the synapse. However, we have shown evidence that common SSRIs may have off target effects on a chemical level that are opposite to their intended purpose.

CHAPTER 5

HISTAMINE'S ROLES IN MEDIATING SEROTONIN DURING

NEUROINFLAMMATION[1]

5.0 Abstract

Depression is the leading cause of disability worldwide and current treatments are variable with even the most efficacious selective serotonin reuptake inhibitors (SSRIs) only benefitting ~30% of patients. The low efficacy is in part due to serotonin's role in depression remaining undefined. New research highlights a potential role for inflammation in the low efficacy of antidepressants, further stressing the need to understand the complex relationship between the brain, serotonin, antidepressants, and inflammation. Here we used a chronic mild stress (CMS) paradigm, that is associated with depression phenotypes and neuroinflammation. We analyzed the effect of CMS on the neurotransmission of histamine and serotonin in the hypothalamus and hippocampus, respectively, with fast electrochemical techniques. We found that CMS increased evoked histamine compared to age matched control mice and decreased the extracellular levels of hippocampal serotonin. Additionally, CMS induced inflammation impaired the ability of escitalopram, an SSRI, to raise serotonin levels compared to control. Finally, we co-administered escitalopram with a histamine synthesis inhibitor and found that alleviating histamine's influence on serotonin allows for escitalopram to increase serotonin in a similar fashion to non-stressed control mice. These results suggest that histamine plays a crucial role in modulating serotonin during inflammation and provides a novel therapeutic target as well as insight into the neurochemical basis of depression.

5.1 Introduction

Depression is a debilitating disease that presents itself through a myriad of symptoms and severities patient to patient.[1-3] Rates of depression among the global population have been steadily growing in recent decades, one reason being a decreased

stigma surrounding mental health diagnoses. Health professionals warned about the looming global mental health crisis associated with extensive isolation and feelings of hopelessness during the unprecedented worldwide COVID-19.[4-5] Despite increased prevalence and reduced stigma around depression, treatments have remained stagnant with only a few new therapies introduced in the last two decades.[6]

Traditional antidepressants focus on three main monoamine neurotransmitters that underpin the monoamine hypothesis of depression – dopamine, norepinephrine, and serotonin.[7] The theory hypothesizes that one, two, or all of these monoamines are dysregulated, and their concentrations are lowered in the synaptic area.[8] The majority of antidepressants have focused on the serotonergic system, specifically aiming to block the reuptake of serotonin through the serotonin transporter (SERT). This class of compounds, selective serotonin reuptake inhibitors, has undergone thorough investigation since the 1970s balancing high affinity for SERT and minimal off-target effects.[9] Despite decades of research, treatments remain ineffective, with only ~30% of patients responding to their first or second prescribed antidepressants and those who do respond typically experience several weeks of delayed onset.[10] Ultimately, treatment shortcomings stem from the fact that there has not been a clearly identified chemical marker for depression that can be 'corrected' to restore a patient's heath.

There is growing evidence that depression and inflammation, specifically neuroinflammation, are comorbid but it is unclear which precipitates the other.[11-12] Neuroinflammation is the CNS analogue of peripheral inflammation and is evidenced by similar biochemical markers.[13-14] What remains unclear during cases of neuroinflammation, is how histamine in the brain is reacting to the immune processes.

90

Knowing that histamine is able to negatively modulate serotonin release in the brain *via* H_3Rs[15] and common SSRIs inhibit the reuptake of histamine in the brain (**Chapter 4**), it is critical to understand how histamine behaves in the brain during inflammation. Interestingly, a strong link between inflammatory markers in serum and SSRI resistance has been identified.[16-17] Additionally, antidepressant treatment has been shown to reduce inflammation and recent evidence suggests inhibiting proinflammatory cytokines can alleviate depressive symptoms[18-21] and increase SSRI efficacy.[22-23] Studies have suggested an important role for brain histamine in antidepressant treatment, therefore, we explored this connection between histamine and serotonin during neuroinflammation.[24-25]

In this study, we utilize an established behavior paradigm (unpredictable chronic mild stress; CMS) that is known to induce depression-like phenotypes and inflammation in mice. [26-29] While we did not find strong significance in the depression phenotypes or inflammation markers in these mice, using voltammetry we found that histamine was significantly elevated. As such, CMS-treated mice displayed a decreased level of extracellular serotonin and an impaired response to SSRI when compared to non-stressed controls. We have shown that the CMS-treated mice response to SSRI can be restored when histamine's inhibitory action was eliminated by co-administering a histamine synthesis blocker with the SSRI. These results highlight the importance of the histamine system and inflammation in the underlying mechanisms of depression.

5.2 Materials and Methods

Chemicals and Reagents

Escitalopram oxalate (10 mg kg^{-1}) (Sigma Aldrich, St. Louis, MO, USA) and α-fluoromethylhistidine dihydrochloride (20 mg kg^{-1}) (Toronto Research Chemicals Inc.,

Toronoto, CAN) were individually dissolved in sterile saline (0.9% NaCl solution, Hospira, Mountainside Medical Equipment, Marcy, NY, USA) and administered *via* intraperitoneal (*ip*) injection at a volume of 5 mL kg^{-1} body weight. Urethane (Sigma Aldrich, St. Louis, MO, USA) was dissolved in sterile saline at 25% w/v and administered at 7 µL/g mouse body weight for surgical anesthesia.

Calibration solutions were prepared by dissolving serotonin hydrochloride (Sigma Aldrich, St. Louis, MO, USA) in Tris buffer to produce solution concentration of 10, 25, 50, and 100 nM. Tris buffer consisted of 15 mM $H_2NC(CH_2OH)_2$ HCl, 140 mM NaCl, 3.25 mM KCl, 1.2 mM $CaCl_2$, 1.25 mM NaH_2PO_4 H_2O, 1.2 mM $MgCl_2$, and 2.0 mM Na_2SO_4 (Sigma Aldrich, St. Louis, MO, USA) in deionized water and pH adjusted to 7.4.

Electrode Fabrication

All electrodes are made in house. A single carbon fiber is aspirated into a borosilicate capillary (0.6 mm x 0.4 mm x 10 cm; OD x ID x L) (A-M Systems, Sequim WA, USA) and sealed under gravity and heat by a vertical pipette puller (Narishige, Amityville, NY, USA) to create two separate electrodes. The protruding fiber is then trimmed under light microscope to ~150 µm by scalpel. An electrical connection is forged with the fiber through a stainless-steel connecting wire and silver epoxy. Finally, a thin layer of Nafion (LQ-1105, Ion Power, New Castle, DE, USA) is electrodeposited onto the fiber surface at 1 V for 30 s; the coated fiber is dried for 10 min at 70 °C.[15, 30]

Data Collection and Analysis

Fast-scan cyclic voltammetry and fast-scan controlled adsorption voltammetry (FSCAV) were performed on anesthetized mice using a Dagan potentiostat (Dagan Corp., Minneapolis, MN, USA) and custom built hardware interfaced with PCIe 6341 & PCI 6221

DAC/ADC cards (National Instruments, Austin, TX) and a Pine Research headstage (Pine Research Instruments, Durham, NC, USA). WCCV 3.06 software (Knowmad Technologies LLC, Tucson, AZ, USA) was used to control the hardware and perform data analysis. For FSCV collection, the "Jackson" serotonin waveform[31] was applied at 60 Hz for 10 min, then at 10 Hz for 10 min prior to data collection or the histamine waveform (-0.5 V to -0.7 V to +1.1 V to -0.5 V at 600 V s^{-1}) was applied at 60 Hz for 10 min, then at 10 Hz for min prior to data collection. Data were collected at 10 Hz. Neurotransmitter release was evoked *via* biphasic stimulation applied through a linear constant current stimulus isolator (NL800A Neurolog, Digitimer North America LLC, Fort Lauderdale, FL, USA) with stimulations at 60 Hz, 360 µA, 2 ms in width, and 2 s in length.

Data were collected and filtered on WCCV software (zero phase, Butterworth, 3 kHz low pass filter for histamine; 5kHz low pass filter for serotonin). For FSCV analysis, the cyclic voltammogram (CV) was used to identify histamine and serotonin and the current vs. time (IT) was extracted to visualize release and reuptake. Currents obtained were converted to concentrations through previously generated calibration factors for both histamine (2.825 µM nA^{-1}) and serotonin (11 µM nA^{-1})[15, 32] and hippocampal serotonin (49.5 ± 10.2 nA/µM).[30]

For basal experiments, control evoked files were collected followed by the methodology being switched to FSCAV. FSCAV was performed using a CMOS precision analog switch, ADG419 (Analog Devices). For FSCAV collection, the serotonin waveform was applied at 100 Hz for 2 s followed by a period of controlled adsorption where the potential was held at 0.2 V for 10 s and then the serotonin waveform was reapplied at 100 Hz, as described in Abdalla *et al*.[33] Thirty files (at one file min^{-1}) were collected as control

93

files. Following control files, an *ip* injection of saline was administered and 30 more files of FSCAV were collected. Animals were then administered escitalopram (10 mg kg^{-1}; *ip*) and 60 files post-escitalopram were collected. The system was then switched back to traditional FSCV and four post-basal stimulation files were collected. Electrodes were removed from the animal and underwent post-calibration in which 10 files were collected with the electrode in solutions of 10, 25, 50, and 100 nM serotonin.

For FSCV data, four IT curves were averaged for each animal to establish a control signal. The average for each individual animal was then averaged throughout the group to create an overall group average.

For FSCAV data, the first characteristic CV following waveform reapplication was selected for quantification, and the peak occurring approximately between 0.4 and 0.85 V was integrated to determine the charge (pC). Post-calibrations of each electrode, plotting charge (pC) vs. [serotonin] (nM), were used to determine basal concentration.

Statistical Analyses

Exclusion criteria were based on outliers (*via* Grubbs test) and animals that did not survive the experimental paradigm. To determine the $t_{1/2}$, a code was custom written in Excel to fit the reuptake component of the curve and calculate the time taken to reach half the maximum amplitude. Standard error of the mean (SEM) was calculated using the average response of each animal (n = # animals). Significance between two points was determined by 2-tailed paired t-test and taken as $p < 0.05$. Two-way ANOVA was used to determine significance between control max amplitude and the time course of drug max amplitude. All error bars represent the standard error of the mean (SEM). Area under the curve (AUC) was measured using Simpson's rule of histamine release from time 0 s to the

first intercept of the x axis; in the case of two peaks, only the first peak was analyzed. The Shapiro-Wilk test was used to determine AUC data distribution. The Wilcoxon rank-sum test was applied between control and CMS. Significance was taken as $p < 0.05$.

Animals and Surgical Procedure

Animal procedures and protocols were in accordance with the regulations of the Institutional Animal Care and Use Committee (IACUC) at the University of South Carolina, accredited through the Association for Assessment and Accreditation of Laboratory Animal Care (AAALAC). Male and female C57BL/6J mice (Jackson Laboratory, Bar Harbor, ME, USA) arrived at 6-7 weeks old group housed, with *ad libitum* access to food and water, and were kept on a 12 h light/12 h dark cycle (lights off 0700; light on 1900). An unpredictable chronic mild stress (CMS) paradigm was conducted over a 16-week period and based on previously documented models.[34-37] Two to three mild stressors were performed a day. Stressors included: food or water deprivation, confinement, cage tilt, soiled cage, light during dark cycle, bedding removal, novel object, and handling. All stressors were stopped during behavior testing and 12 h leading up to neurochemical studies.

Stereotaxic surgery (David Kopf Instruments, Tujunga, CA, USA) followed induction of deep and sustained anesthesia from an *ip* injection of urethane. Mouse body temperature was maintained using a thermal heating pad (Braintree Scientific, Braintree, MA, USA). All surgical coordinates were taken in reference to bregma.[38] For serotonin analysis, a Nafion coated CFM was lowered into the CA2 region of the hippocampus (AP: -2.91, ML: +3.35, DV: -2.5 to -3.0) and a stimulating electrode (insulated stainless-steel, diameter: 0.2 mm, untwisted, Plastics One, Roanoke, VA, USA) was placed into the medial

95

forebrain bundle (AP: -1.58, ML: +1.00, DV: -4.8). For histamine analysis, a Nafion coated CFM was lowered into the posterior hypothalamus (AP: -2.45, ML: 0.50, DV: -5.45 to -5.55) and a stimulating electrode was placed into the medial forebrain bundle (AP: -1.07, ML: +1.10, DV: -5.00). A pseudo-Ag/AgCl reference electrode, created by chloridizing a polished silver wire in HCl (15 s in 1 M HCl at 5 V), was placed in the contralateral hemisphere.

Behavioral Analyses

Following the CMS behavioral paradigm, mice underwent behavioral testing for anxiety- and depressive-like phenotypes. Sucrose preference test (SPT) was conducted as previously described.[39] Briefly, mice were given access to water and 1% sucrose solution for 24 h and the difference in consumption amounts was recorded. Elevated zero maze (EZM) was conducted as previously described.[40] Each mouse was placed into the closed arm of the apparatus (Maze Engineers, Boston, MA, USA) and allowed to explore for 5 min. Time spent in the closed arm was measured as an indicator of anxiety-like behavior. Tail suspension test (TST) was completed as previously described.[41] Mice were attached *via* tape to a supported metal rod and a small plastic, flexible tube was placed on the tail to limit climbing behavior within the apparatus (Maze Engineers, Boston, MA, USA) for the duration of the 6 min test. Percent immobility was measured in the first two min (as pre-test) and the remaining 4 min (test period) as an indicator of depressive-like behavior. Forced swim test (FST) was conducted as previously described.[42] Briefly, mice were individually placed in 4 L beakers filled with ~30 °C water for 5 min and the latency to float and duration of floating (immobility) was recorded.

Biochemical Analyses

BioPlex immunoassays (Bio-Rad Laboratories, Hercules, CA, USA) were used according to manufacturer instructions to analyze cytokines in plasma at sacrifice.

5.3 Results

5.3.1 Behavioral and cytokine analyses

Following the stress paradigm, we analyzed behavioral tests for anxiety (elevated zero maze) and depression through SPT, TST and FST. For the SPT (**Figure 5.1B**), significantly less preference was only found in male mice after 12 h (control: $88.31 \pm 0.92\%$; CMS: $83.33 \pm 1.42\%$; p= 0.013). For the EZM **(Figure 5.1C)**, CMS-treated mice spent significantly more time in the closed arm of the maze than control mice (249.83 ± 2.76 s, 230.09 ± 3.79 s respectively; $p < 0.001$). For the FST, only male mice showed less active behaviors after CMS (Con: $41.36 \pm 8.05\%$; CMS: $66.14 \pm 9.13\%$; p=0.035) (**Figure 5.1D**). There were no significant differences between control and CMS mice in the TST despite a clear trend (65.64 ± 4.17 %, 70.50 ± 3.57 % respectively; $p = 0.38$) (**Figure 5.1E**). While there is some significance in this data, in our hands CMS does not robustly (*i.e.* in every animal) create depression-like phenotypes.

Similarly, we performed plasma cytokines analyses from these mice and found that differences were weakly significant. There was no difference in peripheral cytokine concentration between these two groups, however, when the ratios of proinflammatory cytokines to anti-inflammatory cytokines were compared, for example with TNF-α / IL-4 in females, significance was apparent (control: 15.18 ± 0.93 pg/mL; CMS: 19.30 ± 1.30 pg/mL; $p = 0.016$) (**Figure 5.1F**). CMS-treated mice also trended towards an increase in IL-6/IL-4 ratios (p =0.21 and 0.24 in male and female mice) (**Figure 5.1F**). Overall,

behavioral and plasma cytokine analysis yielded mild significance for the 16-week chronic stress paradigm.
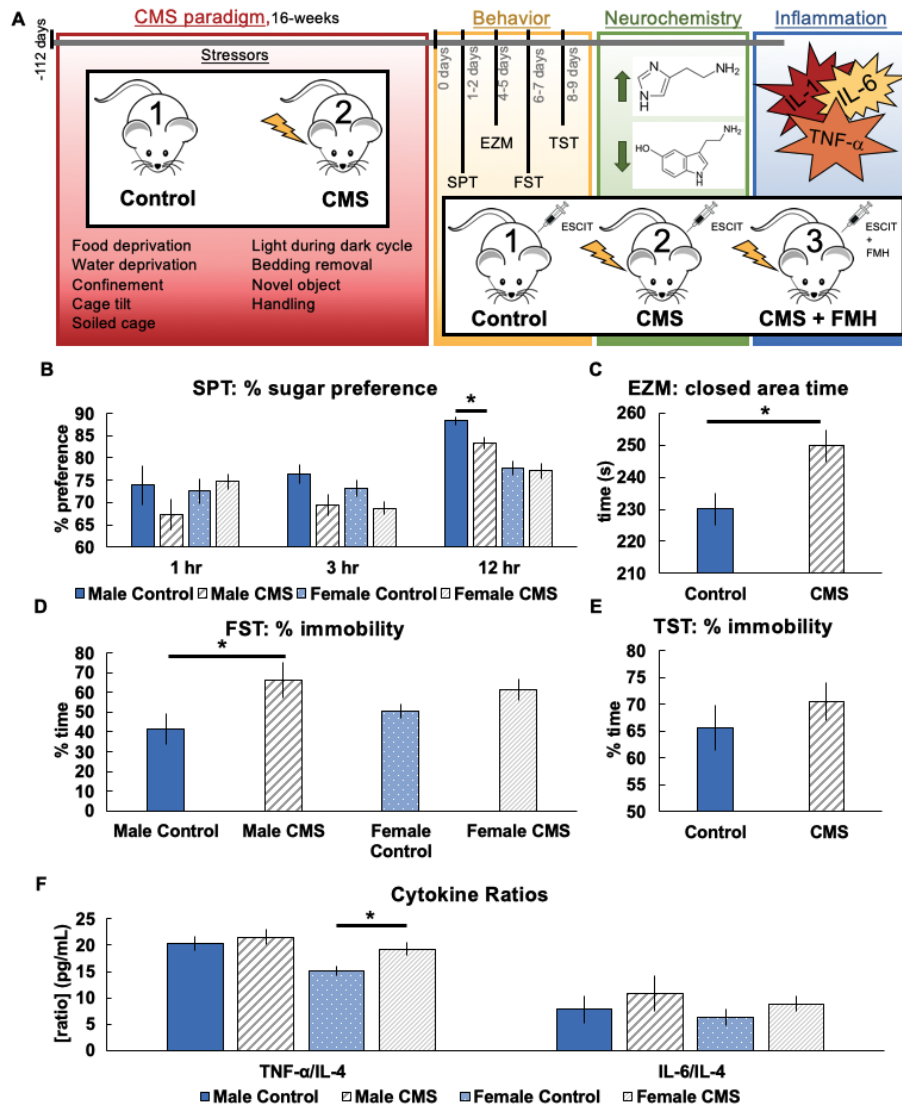
Figure 5.1: Behavioral and inflammatory changes following CMS treatment**. (A)** A schematic is shown for the 16-week CMS paradigm used as well as behavior, neurochemical, and inflammation studies that followed. (**B**) Average sucrose preference (sucrose water consumed - water consumed / total water consumed) in the SPT for non-stress control (bue; n=40) and CMS (gray; n=39) mice (t-test, p <0.001). (**C**) Average time spent in the closed sections of the EZM is shown for control (blue; n=37) and CMS (gray; n=36) mice. (**D**) Average percentage of time immobile in the FST for male (blue) and female (light blue) control mice and male (gray) and female (light gray) CMS mice. (**E**) Average percentage of time

98

immobile in the TST is shown for control (blue) and CMS (gray) mice. (**F**) Analysis of cytokine ratios (TNF-α/IL-4 and IL-6/IL4 respectively). Significance was defined as $p < 0.05$ in a student's t-test.

5.3.2 Hippocampal serotonin is decreased in CMS mice

In these mice we next measured evoked and ambient serotonin with fast-scan cyclic voltammetry (FSCV) and fast-scan controlled adsorption voltammetry (FSCAV). We developed these tools in our lab for minimally invasive, highly reproducible serotonin measures on the neurotransmission temporal and spatial scale. There was no difference in evoked serotonin in the hippocampus between control and CMS mice (Amp$_{max}$: Control: 19.02 ± 3.2 nM; CMS: 19.29 ± 3.71 nM; $p = 0.804$) or reuptake of serotonin ($t_{1/2}$: Control: 2.31 ± 0.27 s; CMS: 2.29 ± 0.26 s; $p = 0.953$) (**Figure 2A-E**). However, using FSCAV we were able to show a robust difference in basal or ambient serotonin. In this region (**Figure 2F-H**), every single mouse that underwent the chronic stress paradigm had decreased ambient serotonin (C$_{max}$: control: 63.17 ± 2.67 nM, CMS: 46.70 ± 0.72 nM; t-test, $p < 0.001$), despite weakly correlated behavioral and cytokine analysis.

5.3.3 Hypothalamic histamine is increased in CMS mice

Fast-scan cyclic voltammetry analysis of histamine was performed in the posterior hypothalamus of the mice. In **Figure 5.3A**, a representative FSCV color plot is shown. The [HA] vs time and [5HT] vs time is shown in **Figure 5.3B** for non-stressed control (blue) and CMS-treated mice (green). There was no apparent change in the reuptake of histamine between CMS and non-stressed control mice ($t_{1/2}$: control: 2.5 ± 0.7 s; CMS: 3.2 ± 0.6 s; $p=0.23$) The peak inhibition of serotonin following histamine release was increased in

CMS mice, however this effect was not significant (Amp$_{max}$: control: 24.02 ± 6.30 nM; CMS: 26.34 ± 4.32 nM; p=0.77).
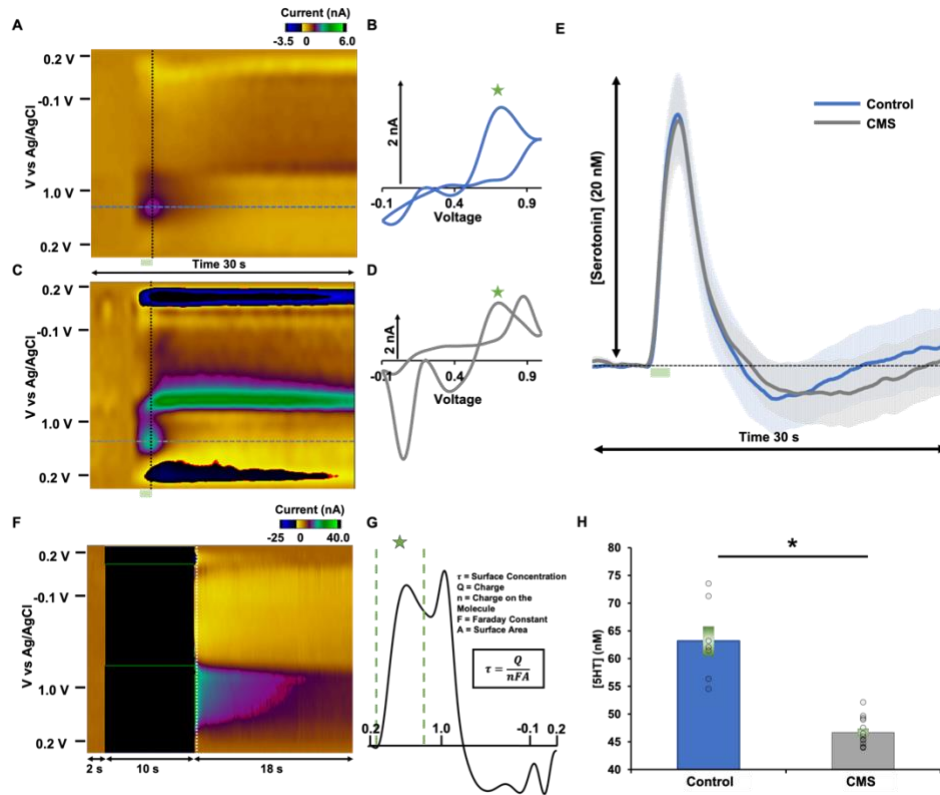
Figure 5.2: Decreased extracellular serotonin predicts stress. (**A,C**) Example 5HT color plots from control and CMS mice respectively. (**B,D**) Example 5HT cyclic voltammograms from control and CMS mice respectively. (**E**) Evoked hippocampal serotonin in control (blue) and CMS (gray) mice. (**F**) An example of a basal serotonin color plot. (**G**) An example of a basal serotonin cyclic voltammogram from which basal serotonin was calculated using the equation shown (τ = Surface Concentration, Q = Charge, n = Charge on the Molecule, F = Faraday Constant, and A = Surface Area). (**H**) Average basal serotonin in control (blue) and CMS (gray) mice is shown in a bar graph and individual animals are denoted by circles. Error is shown as SEM and a student's t-test was performed and significance defined as $p < 0.05$

100

Figure 5.3 Chronic mild stress treatment elevates histamine. (**A**) Representative color plot of evoked histamine and serotonin inhibition with an inset cyclic voltammogram confirming the el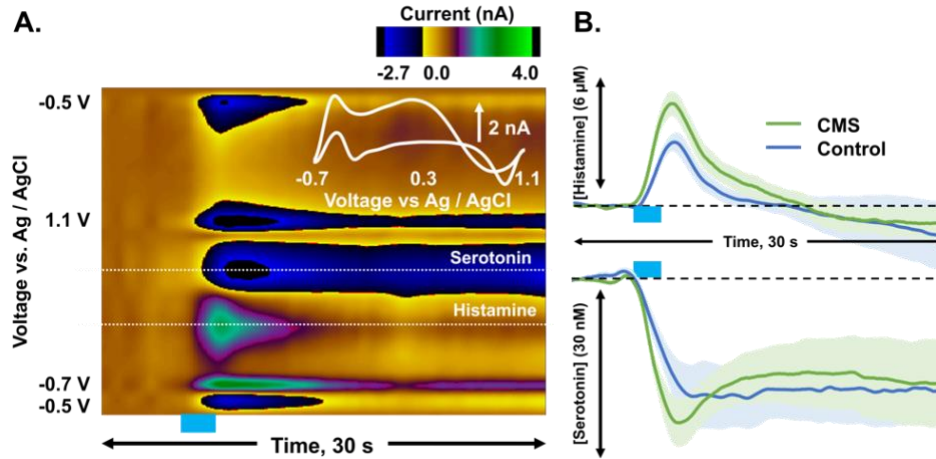ectrochemical identities of histamine and serotonin. The blue bar represents electrical stimulation from 5 - 7 s. (**B**) Average CMS (green, n=5) and non-stressed control (blue, n=6) evoked [histamine] and [serotonin] inhibition vs time profiles. Error (± standard error of the mean) is shown as the shaded region around traces.

We hypothesized that the serotonin levels in CMS mice are low due to elevated histamine in the hypothalamus **Figure 5.3B**, thus, we tested this notion and found in CMS mice there is a non-significant increase in histamine release (control: 4.28 ± 0.51 μM; CMS: 5.64 ± 0.66 μM; p=0.13) and a significant increase in area under the curve of histamine release (AUC control: 14.51 ± 2.35 μM•s; CMS: 25.50 ± 2.80 μM•s; Wilcoxon rank-sum test, p=0.02) (**Figure C1**).

The increased histamine explains the decreased ambient serotonin seen in **Figure 5.2H**. Therefore, we designed an experiment in which three groups of animals would receive escitalopram under different treatments: non-stressed control (escitalopram; 10 mg kg^{-1}), CMS mice (escitalopram; 10 mg kg^{-1}), and CMS mice co-administered escitalopram (10 mg kg^{-1}) and a histamine synthesis inhibitor (FMH; 20 mg kg^{-1}) (**Figure 5.4**).
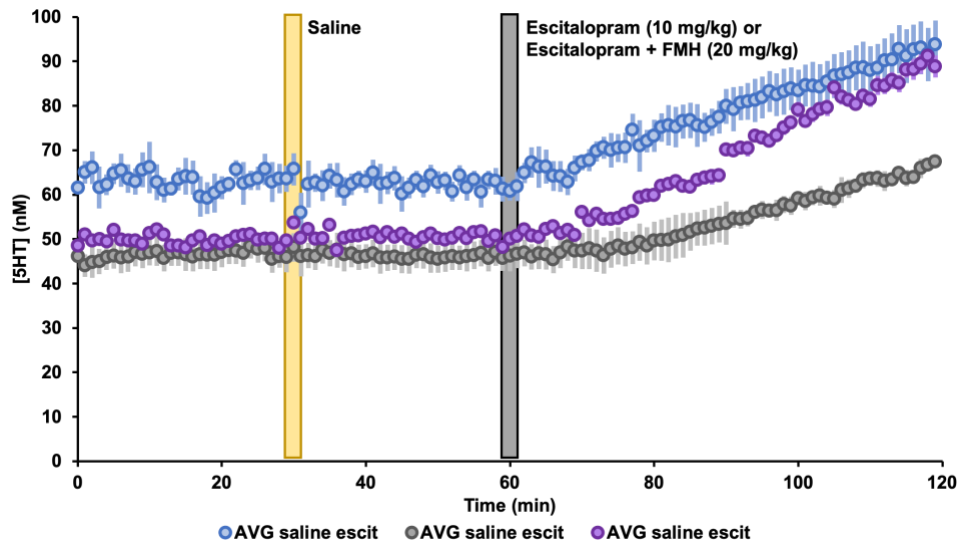
101

Figure 5.4: Dual targeting of histamine and serotonin effects on hippocampal serotonin in CMS-treated mice. Basal serotonin measurements are shown for control mice given saline and then escitalopram (*ip,* 10 mg kg^{-1}, n=5, blue), CMS-treated mice given saline and then escitalopram (*ip*, 10 mg kg^{-1}, n=5, grey), and CMS-treated mice given saline and then escitalopram (*ip*, 10 mg kg^{-1}) and FMH (*ip*, 20 mg kg^{-1}, purple, n=5).

5.4 Discussion

5.4.1 Brain Serotonin is Lower in Response to Chronic Inflammation

The CMS treatment protocol is a model to induce depression-like phenotypes in rodents that also results in associated neuroinflammation.[26-29] Therefore, we used this model to induce chronic inflammation in a cohort of mice to study the effects on brain serotonin and histamine levels. While we found weak significance between this paradigm and depression-like phenotypes and inflammation, using FSCV and FSCAV, developed in our lab, to measure serotonin we found that CMS-treated mice exhibited a significantly lower amount of ambient serotonin in the brain compared to control (**Figure 5.4**). This phenomenon has been hypothesized and studied for some time.[43-44] CMS has been said to decrease brain serotonin levels[45-47], a finding that has also been contradicted[48] while acute stress has been shown to increase serotonin.[49-50] Importantly, CMS has also been associated

www.manaraa.com

with chronic inflammation.[27, 51] Thus, agreement had not been reached in the community about whether serotonin levels were actually lower during depression. Here for the first time, we show that stress robustly decreases serotonin. Knowing histamine's modulatory control of serotonin, we next aimed to determine if histamine is altered in CMS-treated mice.

5.4.2 Brain Histamine is Elevated during CMS Induced Neuroinflammation

Behaviorally depressed mice had higher levels of evoked histamine as analyzed by fast scan cyclic voltammetry (**Figure 5.3/C1**). We contribute our small sample size to unfortunate animal loss as behaviorally depressed mice are known to respond poorly to anesthesia.[52-54] Histamine has been shown to be a crucial signaling molecule for the immune system[55-56] and the connection between depression and altered immune system functionality has been explored.[57] Activated microglia and mast cells can regulate local levels of histamine, which directly respond to immune reactions within the brain.[58-62] Additionally, microglia and mast cell activation is thought to be linked to the induction of anxiety and stress behaviors through inflammatory signaling.[63-65] The role of histamine in inflammatory communication in the brain has not yet been definitively determined, but regulation appears to be complimentary in that histamine receptors can also affect cell recruitment[66-67] Here, we have shown that CMS-induced neuroinflammation increased histamine and decreased serotonin levels in the brain. Previously, we showed that this inverse modulation of histamine on serotonin was due to activation of H_3 receptors present on presynaptic serotonin terminals.[15] We next sought to investigate the implication of this relationship further.

103

5.4.3 Dual pharmacological targeting of serotonin and histamine restores SSRI efficacy during chronic inflammation

Our measurements of serotonin and histamine are in two distinctly different brain regions, the hippocampus and the hypothalamus. We hypothesized that elevated inflammation (thus elevated basal histamine levels) could mediate the lower extracellular levels of serotonin observed in the hippocampus. We intended to remove the inhibitory effect of histamine on H_3 heteroreceptors on serotonin terminals to observe whether we could return serotonin levels to pre-stress levels. Employing an antihistamine is enticing but as covered in Chapter 3, those agents target post-synaptic H_1 and H_2, not H_3 receptors, and actually would result in sustained extracellular histamine. In fact, H_3R are not the ideal pharmacological targets either as administering an agonist or antagonist would have confounding effects (immepip or thioperamide; Chapter 3). Thus, we chose to globally lower histamine levels by inhibiting the overall synthesis of histamine. We accomplish this through α-fluoromethylhistidine (FMH), a suicide inhibitor of histidine decarboxylase (sole enzymatic route of histamine synthesis). Studies have shown this compound dramatically decreased both peripheral and central histamine.[68-70] Co-administration of escitalopram and FMH induced robust increases in ambient serotonin (**Figure 5.4**). We postulated that dual targeting of histamine and serotonin could increase extracellular serotonin and ameliorate the impaired SSRI-induced increases in serotonin seen in CMS-treated mice. In CMS-treated mice, we observed ambient serotonin increased faster and to a level comparable to control mice receiving escitalopram. Importantly, we suggest that histamine may play a crucial role in serotonin dynamics as well as response to SSRI in inflammatory states.

104

5.5 Conclusion

Depression and inflammation are two inextricably linked phenomena that cause debilitating effects in patients. We used an unpredictable chronic mild stress paradigm to induce a depression-like phenotype and associated neuroinflammation in mice. We have shown that serotonin levels are functionally lowered in chronically stressed mice and confirm the notion that brain histamine levels are elevated during neuroinflammatory states using *in vivo* fast-scan cyclic voltammetry. We postulated that elevated histamine is at least partially responsible for decreased serotonin as we were able to restore escitalopram's ability to increase hippocampal serotonin in the absence of histaminergic control. Our results highlight the importance of considering the histaminergic system and the role it plays at the intersection of depression and inflammation.

CHAPTER 6

AN *IN VIVO* ANALYSIS OF KETAMINE'S HISTAMINERGIC

MODULATION OF SEROTONIN IN THE POSTERIOR

HYPOTHALAMUS[1]

---

[1] Berger, SN., Witt, CE., Baumberger Altirriba, BM., Hashemi, P. An *in vivo* analysis of ketamine's histaminergic modulation of serotonin in the posterior hypothalamus. In preparation. *Neurosci. Lett.*

6.0 Abstract

Ketamine is a dissociative anesthetic that has recently been highlighted for its potential role as a rapid acting antidepressant in patients with major depressive and treatment resistant depression. Despite the clinical rush to approve a treatment paradigm utilizing ketamine, a large portion of ketamine's antidepressant effects remain unknown. We used fast voltammetric methods to investigate ketamine's effects on monoamine transmission in the hypothalamus and hippocampus of mice. We found ketamine caused a robust decrease in electrically evoked histamine in the hypothalamus and increased ambient serotonin levels in the hippocampus. We attributed these results to activation of metabotropic glutamate receptors 2 & 3 and glutamatergic modulation of monoamine transmission. Our data reveal new biochemical impacts of ketamine on the brain and will aid in understanding ketamine's antidepressant mechanisms.

6.1 Introduction

Ketamine is an important anesthetic, used primarily in veterinary medicine and recognized as an essential medicine by the World Health Organization.[1] Ketamine has recently been proposed as a new sensational treatment for major depressive disorder despite its storied history as a recreational drug of abuse.[2] While the clinical data on ketamine treatment seems to show net positive effects on patients' outcomes, benefits have variable duration and require repeated injections.[3-9] Exactly how ketamine exerts its effects remains unknown. Ketamine is functionally different than 'classical' antidepressants in that it doesn't directly target one of the major monoaminergic systems *eg*. dopamine, serotonin, or norepinephrine. Acting mainly as an *N*-methyl-D-aspartate (NMDA) receptor antagonist, ketamine's primary effects are on the glutamatergic and GABAergic systems.

107

A substantial body of work has been dedicated to teasing apart which functional changes are responsible for ketamine's antidepressant effects. Metabolism of (*R*/*S*)-ketamine to (2*R*,6*R*;2*S*,6*S*)-hydroxynorketamine appears to be essential for antidepressant effects.[10] Interestingly, the *S* enantiomer is the more potent inhibitor of the NMDA receptors while the *R* enantiomer metabolite appears significantly responsible for antidepressant effects without the psychosis associated with the *S* enantiomer.[11-12] These results, in conjunction with the low clinical efficacy found in clinical trials, are curious considering the recent Food and Drug Administration (FDA) approval of Johnson & Johnson's Spravato, which is an enantiomerically pure *S*-ketamine nasal spray.[13]

Much of the focus on understanding ketamine's antidepressant effects has centered around glutamate, GABA, and serotonin. Based on the known comorbidity of depression and inflammation, in this work, we explored the role that histamine plays in this emerging depression treatment. We previously observed that common selective serotonin reuptake inhibitors (SSRIs) inhibit the reuptake of histamine from the synaptic cleft (**Chapter 4**) and histamine levels are elevated in behaviorally depressed mice (**Chapter 5**). Histamine remains an understudied molecule in the context of depression, therefore, our goal was to expand the understanding of ketamine's effects on the central nervous system by monitoring how hypothalamic histamine responded to a sub-anesthetic dose of ketamine. Additionally, we analyzed how the modulation of serotonin *via* histamine was altered following ketamine exposure. We found that systemic administration of ketamine causes rapid and sustained inhibition of hypothalamic histamine and attenuates histaminergic inhibition of serotonin. As such, ketamine increases the ambient levels of serotonin in a manner synonymous to standard SSRIs. Our results highlight critical mechanistic

108

differences between rapid-acting and slow-acting antidepressants on key neurotransmitter systems.

6.2 Methods and Materials

Chemicals and Reagents

Ketamine hydrochloride (Vet One, MWI Animal Health, Boise, ID, USA) and escitalopram oxalate (Sigma Aldrich, St. Louis, MO, USA) were individually dissolved in sterile saline (0.9% NaCl solution, Hospira, Mountainside Medical Equipment, Marcy, NY, USA) and administered *via* intraperitoneal injection at 10 mg kg^{-1} and a volume of 5 mL kg^{-1} body weight. Urethane (Sigma Aldrich, St. Louis, MO, USA) was dissolved in sterile saline at 25% w/v and administered at 7 µL/g mouse body weight for surgical anesthesia.

Electrode Fabrication

All electrodes are made in house. A single carbon fiber is aspirated into a borosilicate capillary (0.6 mm x 0.4 mm x 10 cm; OD x ID x L) (A-M Systems, Sequim WA, USA) and sealed under gravity and heat by a vertical pipette puller (Narishige, Amityville, NY, USA) to create two separate electrodes. The protruding fiber is then trimmed under light microscope to ~150 µm by scalpel. An electrical connection is forged with the fiber through a stainless-steel connecting wire and silver epoxy. Finally, a thin layer of Nafion (LQ-1105, Ion Power, New Castle, DE, USA) is electrodeposited onto the fiber surface at 1 V for 30 s; the coated fiber is dried for 10 min at 70 °C.[14-16]

Data Collection and Analysis

Fast-scan cyclic voltammetry was performed on anesthetized mice using a Dagan potentiostat (Dagan Corp., Minneapolis, MN, USA), WCCV 3.06 software (Knowmad

109

Technologies LLC, Tucson, AZ, USA), and a Pine Research headstage (Pine Research Instruments, Durham, NC, USA). The histamine waveform (-0.5 V to -0.7 V to +1.1 V to -0.5 V at 600 V s^{-1}) was applied at 60 Hz for 10 min, then at 10 Hz for min prior to data collection. Data were collected at 10 Hz. Histamine was evoked *via* biphasic stimulation applied through a linear constant current stimulus isolator (NL800A Neurolog, Digitimer North America LLC, Fort Lauderdale, FL, USA) with stimulations at 60 Hz, 360 µA, 2 ms in width, and 2 s in length.

Data were collected and filtered on WCCV software (zero phase, Butterworth, 3 kHz low pass filter). Four control evoked files, 10 min apart, were averaged for the control evoked histamine signal after which ketamine was administered and files were collected at 0 min, 5 min, 10 min, and every 10 min thereafter until 100 min. Currents obtained were converted to concentrations through previously generated calibration factors for both histamine (2.825 µM nA^{-1}) and serotonin (11 µM nA^{-1}).[15-16]

For basal experiments, control evoked files were collected followed by the methodology being switched to FSCAV. For FSCAV collection, the serotonin waveform was applied at 100 Hz for 2 s followed by a period of controlled adsorption where the potential was held at 0.2 V for 10 s and then the serotonin waveform was reapplied at 100 Hz, as described in Abdalla *et al*.[17] Thirty files (at one file min^{-1}) were collected as control files. Following control files, an *ip* injection of saline was administered and 30 more files of FSCAV were collected. Animals were then administered escitalopram (10 mg kg^{-1}) *ip* and 60 files post-drug were collected. The system was then switched back to traditional FSCV and four post-basal stimulation files were collected. Electrodes were removed from the animal and underwent post-calibration in which 10 files were collected with the

110

electrode in solutions of 10, 25, 50, and 100 nM serotonin. For FSCAV data, the first characteristic CV following waveform reapplication was selected for quantification, and the peak occurring approximately between 0.4 and 0.85 V was integrated to determine the charge (pC). Post-calibrations of each electrode, plotting charge (pC) vs. [serotonin] (nM), were used to determine basal concentration.

Statistical Analyses

Average control response was generated from four current vs time traces per animal and averaged to create an overall group average. Exclusion criteria were based on outliers (*via* Grubbs test) and animals that did not survive the experimental paradigm. Standard error of the mean (SEM) was calculated using the average response of each animal (n = # animals). Significance between two points was determined by 2-tailed paired t-test and taken as $p < 0.05$.

Animals and Surgical Procedure

Animal procedures and protocols were in accordance with the regulations of the Institutional Animal Care and Use Committee (IACUC) at the University of South Carolina, accredited through the Association for Assessment and Accreditation of Laboratory Animal Care (AAALAC). Male and female C57BL/6J mice (Jackson Laboratory, Bar Harbor, ME, USA) 8-14 weeks of age weighing 20 to 29 g were used.

Stereotaxic surgery (David Kopf Instruments, Tujunga, CA, USA) followed induction of deep and sustained anesthesia from an intraperitoneal injection of urethane (below). Mouse body temperature was maintained using a thermal heating pad (Braintree Scientific, Braintree, MA, USA). All surgical coordinates were taken in reference to bregma.[18] A Nafion coated CFM was lowered into the posterior hypothalamus (AP: -2.45,

111

ML: 0.50, DV: -5.45 to -5.55) and a stimulating electrode (insulated stainless-steel, diameter: 0.2 mm, untwisted, Plastics One, Roanoke, VA, USA) was placed into the medial forebrain bundle (AP: -1.07, ML: +1.10, DV: -5.00). A pseudo-Ag/AgCl reference electrode, created by chloridizing a polished silver wire in HCl (15 s in 1 M HCl at 5 V), was placed in the contralateral hemisphere.

6.3 Results

Administration of 10 mg kg^{-1} ketamine *ip* resulted in a significant decrease in the overall amplitude of stimulated hypothalamic histamine (n=5; 2 male, 3 female; Amp$_{max}$: control: 8.92 ± 1.80 µM; ketamine: 6.09 ± 1.61 µM; p = 0.005) while having no effect on the clearance rate (t$_{1/2}$: control: 4.1 ± 1.1 s; ketamine: 3.3 ± 0.8 s; p = 0.23) after 10 min (**Figure 6.1B**).
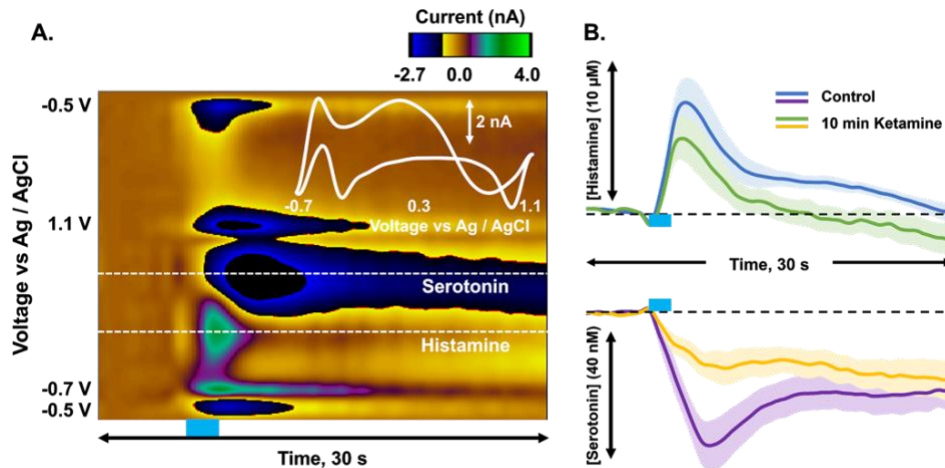
Figure 6.1: Ketamine caused rapid inhibition of histamine release and alleviates serotonin inhibition. (**A**) Representative color plot of stimulated histamine and serotonin inhibition. Inset: CV showing oxidation peaks of histamine and serotonin. (**B**) Top: evoked histamine control (blue, n=5) and 10 min following 10 mg kg^{-1} ketamine (green, n=5) (Amp$_{max}$: control: 8.92 ± 1.80 µM; ketamine: 6.09 ± 1.61 µM; p=0.005 paired t-test). Bottom: [serotonin] vs time profiles for control (purple, n=5) and 10 min following 10 mg kg^{-1} ketamine (yellow) (Amp$_{max}$: control: 44.70 ± 7.91 nM; ketamine: 20.12 ± 4.88 nM; p=0.013 paired t-test). Error (± standard error of the mean) is shown as a shaded region around traces.

112

Ketamine administration had a rapid and sustained effect on suppressed histamine release and alleviated serotonin inhibition throughout the duration (100 min) of data collection (**Figure 6.2A,B**)

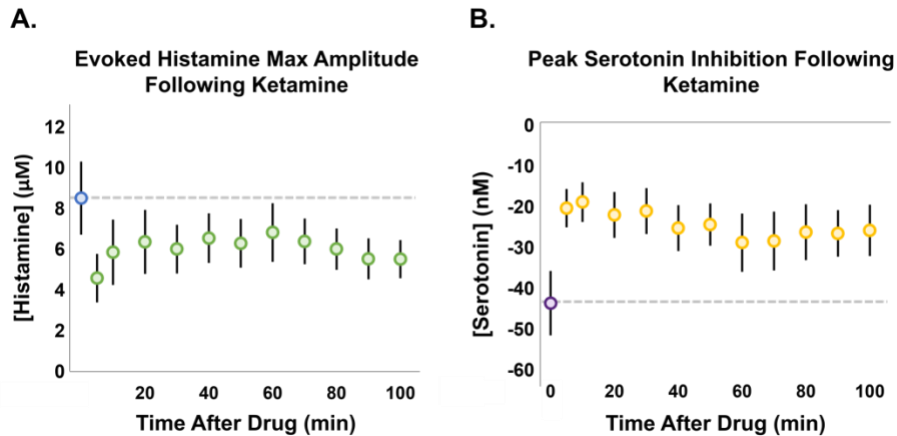**Figure 6.2:** Ketamine caused prolonged suppression of histamine release and serotonin inhibition. (**A**) Control evoked histamine maximum amplitude (blue) and max amplitude for minutes 5, 10, 20, to 100 min (green) following 10 mg kg^{-1} ketamine. (**B**) Control serotonin inhibition minimum amplitude (purple) and inhibition amplitude for minutes 5, 10, 20, to 100 min (yellow) following 10 mg kg^{-1} ketamine. Error bars represent ± standard error of the mean.

There was no significant change in the reuptake curves ($t_{1/2}$) of histamine control (blue) or post-ketamine (green). Due to the inhibition profile of serotonin post-ketamine, it was challenging to determine the reuptake kinetics associated with it. Qualitatively, it can be seen that the overall amplitude of serotonin following ketamine is similar to the post-inhibition (~25 s mark) amount in control signals.

We next investigated ketamine's effect on ambient hippocampal serotonin. Control serotonin levels were collected for 30 min prior to vehicle (saline; 30 to 60 min) injection. Ketamine (blue; 0.66 nM/min) raised extracellular serotonin rapidly following *ip* administration (60 to 120 min) in a similar fashion to escitalopram (orange; 0.482 ± 0.057

113

nM/min), a classical antidepressant that inhibits the serotonin transporter. Saline vehicle did not have an effect on serotonin for either compound (escitalopram, n=10 ; control: 63.68 ± 3.00 nM; saline: 63.53 ± 3.21 nM; p=0.68) (ketamine, n=2; control: 60.03 nM; saline: 59.34 nM). Ketamine increased extracellular serotonin 60 min following injection (control: 60.03 nM to 94.49 nM) similar to how escitalopram increased serotonin levels (control: 63.68 ± 3.00 nM to 91.27 ± 4.64 nM).
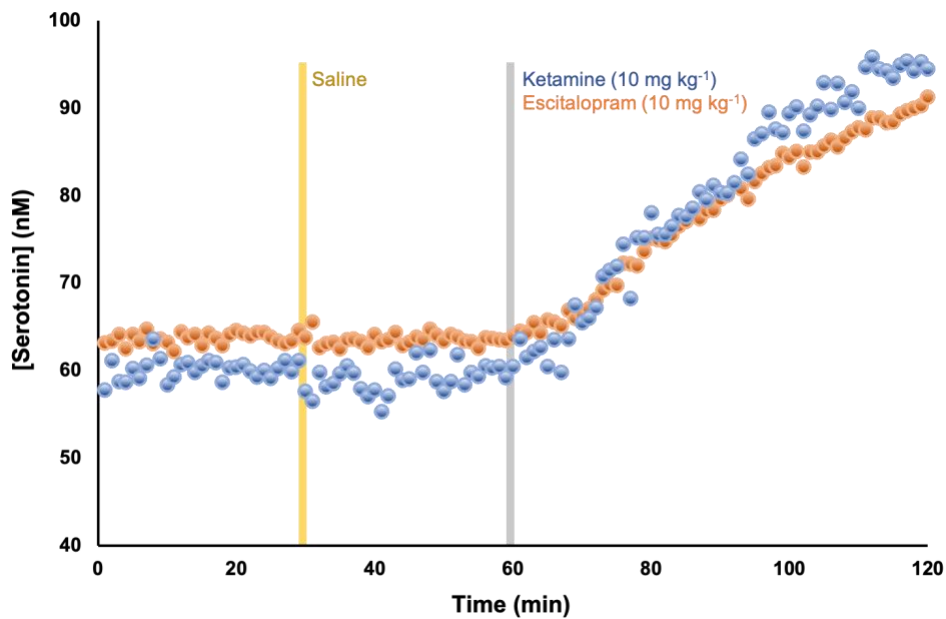
Figure 6.3: Ketamine elevated ambient serotonin similar to escitalopram. FSCAV data for mice receiving escitalopram (*ip*; 10 mg kg^{-1}, orange, n=10) or ketamine (*ip*; 10 mg kg^{-1}, blue, n=2). Ambient serotonin concentration is collected for 30 min, followed by 30 min of vehicle (saline), followed by administration of ketamine (blue) or escitalopram (orange) for 60 min. Ketamine (blue; 0.66 nM/min) raised extracellular serotonin rapidly following *ip* administration (60 to 120 min) in a similar fashion to escitalopram (orange; 0.482 ± 0.057 nM/min). Error bars have been omitted for clarity.

6.4 Discussion

We have shown that administration of ketamine (10 mg kg^{-1}; *ip*) caused rapid and sustained inhibition of histamine release in the mouse posterior hypothalamus. Ketamine

114

has not been shown to act directly on the histaminergic system, but most likely regulates histamine through glutamatergic and GABAergic routes. GABAergic transmission is inhibited by ketamine through NMDA receptor antagonism which leads to excess glutamate release. The presence of histamine and GABA in tuberomammillary nucleus neurons has been confirmed through immunohistochemistry[19] and endogenous GABA has been shown to modulate the release of histamine in the hypothalamus.[20] Excess glutamate release has been shown to influence the release of histamine and activate TMN neurons which express both AMPA and NMDA receptors.[21] NMDA receptor antagonists increased the synthesis and turnover of histamine, which already occurs more frequently than other monoamines in the brain.[22-23] Infusions of glutamate in the anterior hypothalamus resulted in a 150% increase in histamine with respect to baseline measured by microdialysis.[24] Okakura *et al.* noted that glutamate-evoked histamine release was completely blocked by the NMDA receptor specific antagonist AP5, and AP5 alone reduced histamine release to around 60% of basal levels.[24] These results are in agreement with our data in that ketamine caused a robust decrease in histamine release. Fell *et al.* reported that pretreatment with the mGlu2 receptor agonist, LY379268, significantly attenuated histamine release and concluded that hypothalamic histamine is modulated by glutamate through mGlu2 receptors.[25-26] Glutamate is a highly potent endogenous agonist of mGlu2 receptors.[27-28] The mGlu2 are located both pre- and post-synaptically and function as auto- and heteroreceptors controlling the release of glutamate, GABA and other neurotransmitters.[29] The control of histamine release through glutamate activation of mGlu2/3 is a likely effect from ketamine administration. Indeed, immunostaining has confirmed mGlu2 presence in the premammillary nucleus[30] and mGlu3 presence in TMN.[30-31]

115

The antidepressant effects of ketamine are thought to stem from synaptic plasticity as a result of glutamate activated AMPA (alpha-amino-3-hydroxy-5-methyl-4-isoxazoepropionic acid) receptors, increased BDNF (brain derived neurotrophic factor), activation of mTOR (mammalian target of rapamycin), inhibition of glycogen synthase kinase-3 or likely a combination of each.[32-34] The importance of mTOR activation is disputed as Li *et al.* reported inhibition of mTOR signaling blocked ketamine's antidepressant effects[35] while Abdallah *et al.* recently reported that rapamycin pretreatment (the inhibitor of mTOR) actually prolonged the antidepressant effects of ketamine for 2 weeks following initial ketamine treatment.[36] The antagonism of NMDARs is not required for antidepressant effects, but rather an increased level of cyclic adenosine monophosphate (cAMP) that results in increased expression of BDNF.[37-38] Activation of the AMPA receptor is also thought to play an important role in the therapeutic effects of ketamine through increased activation of mTOR, part of a signaling pathway that results in increased BDNF that then increases synaptic plasticity.[39] Antagonism of AMPA receptors significantly blocked the beneficial effects of ketamine in rodents undergoing learned helplessness, tail suspension, and forced swim tests (tests of depressive-like phenotypes).[40-41] The perisynaptically located metabotropic glutamate receptors 2&3 (mGlu2/mGlu3) have also been highlighted for their role in the therapeutic effects of ketamine.[42-43] 2*R*,6*R*-hydroxynorketamine functions as an antagonist of mGlu2/3 receptor.[44] A combination of ketamine and an mGlu2/3 receptor antagonist was shown to activate serotonin neurons in the dorsal raphe nucleus.[45]

In addition to its anesthetic and antidepressant properties, ketamine bears analgesic and anti-inflammatory effects. Ketamine's ability to modulate the body's immune response

116

arose from observations of improved outcomes in critically ill patients[46] and experimental septic shock.[47] Ketamine has been shown to mitigate the inflammatory challenge of lipopolysaccharide and decrease the production of pro-inflammatory cytokines during immune response.[48-51] The immunomodulatory role of ketamine was reviewed thoroughly by De Kock and colleagues.[52] In **Chapter 5** we covered the influence of chronic mild stress and neuroinflammation on brain histamine. In a similar chronic stress behavior model, ketamine (10 mg kg^{-1}) induced a rapid antidepressant effect and decreased expression of hippocampal proinflammatory cytokines interleukin-6 (IL-6) and tumor necrosis factor alpha (TNFα).[53] Interestingly, ketamine's inflammatory response may be dose dependent as higher doses (50 mg kg^{-1} and above) have been shown to increase expression of inflammatory proteins.[54-55] Antidepressant benefits of ketamine involve sub-anesthetic doses, therefore, the increased inflammatory signaling observed with high doses of ketamine will generally not be expected.[56] Overall, ketamine's anti-inflammatory effects function as a pretreatment to immune challenge rather than a response[49] and ketamine has no effect on cytokine production without an immune stimulus.[52]

We have shown that ketamine caused a robust and persistent decrease in evoked histamine. Ketamine has been shown to elevated glutamate transmission while also functioning as an anti-inflammatory agent. Previous reports are in agreement with our data and concluded that ketamine, through glutamate activation inhibiting histamine release through mGlu2/3 receptors and immunomodulatory abilities, could result in the decrease of stimulated histamine. Most interestingly, the overall effect is on serotonin, in a manner synonymous to SSRIs.

6.5 Conclusion

In this report we investigated the effect of acute ketamine administration on histamine and serotonin *in vivo*. In the posterior hypothalamus, we found that ketamine caused a rapid and sustained decrease in histamine amplitude and lessened histamine's inhibition of serotonin 100 min following administration. Additionally, we confirmed the increase in ambient serotonin by showing ketamine increased basal hippocampal serotonin in a similar fashion to the SSRI escitalopram, despite its completely different mode of action. The therapeutic effects of rapid acting antidepressants like ketamine are still being uncovered. Our data provide new insights into the effects of rapid acting antidepressants and how compounds targeting the glutamatergic system influence monoamine neurotransmission.

CHAPTER 7

CONCLUSIONS & PROSPECTS

The relationship of chemicals in the brain is delicate and dynamic. Histamine and serotonin are two important bioamines that regulate many different processes within the brain and body. Their actions and modulation are still being studied to fully understand the impact histamine and serotonin have on brain disorders. However, analyzing the underlying neurochemical changes of these two molecules has been challenging due to the lack of robust analytical tools. This work continued previous Hashemi lab investigations to uncover the intricate relationship histamine and serotonin have in the brain.

In this dissertation, I first reviewed the currently available tools for neurochemical analysis and their respective advantages and drawbacks in Chapter 2. I then used FSCV to investigate how CNS histamine responded to pharmacological challenge in male and female mice in Chapter 3. I found that the histamine system is highly conserved between male and female mice, owing to the brain's homeostatic regulation. However, I determined that female mice appear to have a higher level of immune regulation mediated by H_3 receptors. Next, I used a genetically modified mouse model to investigate the transport mechanisms of histamine clearance in the brain and rule out SERT's contribution to histamine uptake in Chapter 4. With a better understanding of the male and female and transport systems, I applied histamine FSCV to a model of chronic stress and chronic inflammation (chronic mild stress behavioral paradigm) in Chapter 5. I showed that brain histamine is elevated in this model of chronic stress/inflammation which is important in

119

the context of histamine's ability to inhibit serotonin release through H$_3$ receptors. Finally, I studied the effects of the newly approved antidepressant, ketamine in Chapter 6. Ketamine's antidepressant effects are rapid, relatively short lived requiring repeated injections, and broadly not well understood. Unlike common antidepressants that target traditional monoamines, ketamine targets the glutamatergic system and is thought to modulate monoamines through glutamate and GABA. Knowing how histamine is changed during depression and inflammation, and that in addition to its antidepressant effects, ketamine has been shown to be anti-inflammatory, understanding how ketamine affected histaminergic transmission provided novel information on its neurochemical mechanism.

This dissertation pushed our understanding of the co-modulation of histamine and serotonin and how these two neurotransmitters respond to pharmaceutical targeting. Future studies will have to further investigate the ability of female mice to regulate histamine levels in the brain and the influence of cycling hormones on that regulation. Studies using post-menopausal mice, ovariectomized mice, or mice given estrogen blocking compounds should yield a clearer understanding of female H$_3$ receptor control.

I applied histamine FSCV to a model of behaviorally induced chronic stress. In the future, we plan to expand the application of histamine FSCV to other models of chronic inflammation, neuroinflammation, and neurodegeneration. One such model is the chemically induced Parkinson's disease model MPTP (1-methyl-4-phenyl-1,2,3,6-tetrahydropyridine) mouse. Additionally, due to the increased prevalence and risk posed by environmental toxins in today's world, we are in a unique position to study how environmental exposures (*eg*. heavy metals, pesticides, polyaromatic hydrocarbons) affect fundamental neurochemistry.

120

Chapter 3 investigated a substantial amount of pharmacology of the histamine system. We plan to collaborate with mathematicians to create a mathematical model representing the physiological function of a histamine synapse. The model will encompass both male and female aspects as well as the modulation of histamine and serotonin to create a more complete picture than two separate systems. Ultimately, the product would be applied to data obtained from neurodegenerative or inflammation animal models to highlight key criteria (*eg*. release, reuptake, vesicular packaging) causing deficits.

Overall, this dissertation showcased the power of simultaneous, real-time neurochemical measurements *via* FSCV. The continued advancement of our understanding of the intricate relationships neurotransmitter systems have with one another will aid in the development of novel strategies and therapies to manage the enormous burden psychiatric disorders have on our populations.

121

REFERENCES

Chapter 1 References

1.   Carlsson, A., *Science* **2001,** *294* (5544), 1021.
2.   Fakhoury, M., *Molecular Neurobiology* **2016,** *53* (5), 2778-2786.
3.   Gardner, A.; Boles, R. G., *Progress in Neuro-Psychopharmacology and Biological Psychiatry* **2011,** *35* (3), 730-743.
4.   Mayeux, R.; Stern, Y.; Sano, M.; Williams, J. B. W.; Cote, L. J., *Movement Disorders* **1988,** *3* (3), 237-244.
5.   Zlomuzica, A.; Dere, D.; Binder, S.; De Souza Silva, M. A.; Huston, J. P.; Dere, E., *Neuropharmacology* **2016,** *106*, 135-145.
6.   Haas, H. L.; Sergeeva, O. A.; Selbach, O., *Physiological Reviews* **2008,** *88* (3), 1183-1241.
7.   Brown, R. E.; Stevens, D. R.; Haas, H. L., *Progress in Neurobiology* **2001,** *63* (6), 637-672.
8.   Tashiro, M.; Mochizuki, H.; Iwabuchi, K.; Sakurada, Y.; Itoh, M.; Watanabe, T.; Yanai, K., *Life Sciences* **2002,** *72* (4), 409-414.
9.   Morimoto, T.; Yamamoto, Y.; Yamatodani, A., *Behavioural Brain Research* **2001,** *124* (2), 145-150.
10.   Diewald, L.; Heimrich, B.; Busselberg, D.; Watanabe, T.; Haas, H. L., *European Journal of Neuroscience* **1997,** *9* (11), 2406-2413.
11.   Hayashi, H.; Takagi, H.; Takeda, N.; Kubota, Y.; Tohyama, M.; Watanabe, T.; Wada, H., *Journal of Comparative Neurology* **1984,** *229* (2), 233-241.
12.   Kuhar, M. J.; Taylor, K. M.; Snyder, S. H., *Journal of Neurochemistry* **1971,** *18* (8), 1515-1527.
13.   Merickel, A.; Edwards, R. H., *Neuropharmacology* **1995,** *34* (11), 1543-1547.
14.   G D Prell, a.; Green, J. P., *Annual Review of Neuroscience* **1986,** *9* (1), 209-254.
15.   Neame, K. D., *Journal of Neurochemistry* **1964,** *11* (9), 655-662.
16.   Schwartz, J. C.; Arrang, J. M.; Garbarg, M.; Pollard, H.; Ruat, M., *Physiological Reviews* **1991,** *71* (1), 1-51.
17.   Schwartz, J.-C.; Baudry, M.; Chast, F.; Pollard, H.; Bischoff, S.; Krishnamoorthy, M. S., Histamine in the Brain: Importance of Transmethylation Processes and Their Regulation. In *Central Nervous System: Studies on Metabolic Regulation and Function*, Genazzani, E.; Herken, H., Eds. Springer Berlin Heidelberg: Berlin, Heidelberg, 1974; pp 172-184.
18.   Hough, L. B.; Domino, E. F., *Journal of Pharmacology and Experimental Therapeutics* **1979,** *208* (3), 422.
19.   Lin, J. S.; Fort, P.; Kitahama, K.; Panula, P.; Denney, R. M.; Jouvet, M., *Neuroscience Letters* **1991,** *128* (1), 61-65.

20. Panula, P.; Pirvola, U.; Auvinen, S.; Airaksinen, M. S., *Neuroscience* **1989,** *28* (3), 585-610.

21. Panula, P.; Yang, H. Y.; Costa, E., *Proceedings of the National Academy of Sciences* **1984,** *81* (8), 2572.

22. Jutel, M.; Akdis, M.; Akdis, C. A., *Clinical & Experimental Allergy* **2009,** *39* (12), 1786-1800.

23. Strakhova, M. I.; Nikkel, A. L.; Manelli, A. M.; Hsieh, G. C.; Esbenshade, T. A.; Brioni, J. D.; Bitner, R. S., *Brain Research* **2009,** *1250*, 41-48.

24. Schneider, E. H.; Seifert, R., *Neuropharmacology* **2016,** *106*, 116-128.

25. Dong, H.; Zhang, W.; Zeng, X.; Hu, G.; Zhang, H.; He, S.; Zhang, S., *Molecular Neurobiology* **2014,** *49* (3), 1487-1500.

26. Esposito, P.; Gheorghe, D.; Kandere, K.; Pang, X.; Connolly, R.; Jacobson, S.; Theoharides, T. C., *Brain Research* **2001,** *888* (1), 117-127.

27. Zhuang, X.; Silverman, A.-J.; Silver, R., *Journal of Neurobiology* **1996,** *31* (4), 393-403.

28. Tasaka, K.; Chung, Y. H.; Sawada, K.; Mio, M., *Brain Research Bulletin* **1989,** *22* (2), 271-275.

29. Zlomuzica, A.; Viggiano, D.; De Souza Silva, M. A.; Ishizuka, T.; Carnevale, U. A. G.; Ruocco, L. A.; Watanabe, T.; Sadile, A. G.; Huston, J. P.; Dere, E., *European Journal of Neuroscience* **2008,** *27* (6), 1461-1474.

30. Parmentier, R.; Zhao, Y.; Perier, M.; Akaoka, H.; Lintunen, M.; Hou, Y.; Panula, P.; Watanabe, T.; Franco, P.; Lin, J.-S., *Neuropharmacology* **2016,** *106*, 20-34.

31. Sakata, T.; Ookuma, K.; Fukagawa, K.; Fujimoto, K.; Yoshimatsu, H.; Shiraishi, T.; Wada, H., *Brain Research* **1988,** *441* (1), 403-407.

32. Yanai, K.; Son, L. Z.; Endou, M.; Sakurai, E.; Nakagawasai, O.; Tadano, T.; Kisara, K.; Inoue, I.; Watanabe, T.; Watanabe, T., *Neuroscience* **1998,** *87* (2), 479-487.

33. Ruat, M.; Traiffort, E.; Bouthenet, M. L.; Schwartz, J. C.; Hirschfeld, J.; Buschauer, A.; Schunack, W., *Proceedings of the National Academy of Sciences* **1990,** *87* (5), 1658.

34. Vizuete, M. L.; Traiffort, E.; Bouthenet, M. L.; Ruat, M.; Souil, E.; Tardivel-Lacombe, J.; Schwartz, J. C., *Neuroscience* **1997,** *80* (2), 321-343.

35. Dai, H.; Kaneko, K.; Kato, H.; Fujii, S.; Jing, Y.; Xu, A.; Sakurai, E.; Kato, M.; Okamura, N.; Kuramasu, A.; Yanai, K., *Neuroscience Research* **2007,** *57* (2), 306-313.

36. FURR, M. O.; MURRAY, M. J., *Equine Veterinary Journal* **1989,** *21* (S7), 77-79.

37. Blum, A. L., *Digestion* **1990,** *47(suppl 1)* (Suppl. 1), 3-10.

38. Arrang, J.-M.; Garbarg, M.; Schwartz, J.-C., *Nature* **1983,** *302* (5911), 832-837.

39. Lovenberg, T. W.; Roland, B. L.; Wilson, S. J.; Jiang, X.; Pyati, J.; Huvar, A.; Jackson, M. R.; Erlander, M. G., *Molecular Pharmacology* **1999,** *55* (6), 1101-1107.

40. Arrang, J. M.; Garbarg, M.; Lancelo, J. C.; Lecomte, J. M.; Pollard, H.; Robba, M.; Schunack, W.; Schwartz, J. C., *Nature* **1987,** *327* (6118), 117-123.

41. Torrent, A.; Moreno-Delgado, D.; Gómez-Ramírez, J.; Rodríguez-Agudo, D.; Rodríguez-Caso, C.; Sánchez-Jiménez, F.; Blanco, I.; Ortiz, J., *Molecular Pharmacology* **2005,** *67* (1), 195.

42. Schlicker, E.; Betz, R.; Göthert, M., *Naunyn-Schmiedeberg's Archives of Pharmacology* **1988,** *337* (5), 588-590.

43. Schlicker, E.; Fink, K.; Detzner, M.; Göthert, M., *Journal of Neural Transmission / General Section JNT* **1993,** *93* (1), 1-10.

123

44. Schlicker, E.; Werthwein, S.; Zentner, J., *Fundamental & Clinical Pharmacology* **1999,** *13* (1), 120-122.

45. Brown, R. E.; Reymann, K. G., *The Journal of Physiology* **1996,** *496* (1), 175-184.

46. Jang, I. S.; Rhee, J. S.; Watanabe, T.; Akaike, N.; Akaike, N., *The Journal of physiology* **2001,** *534* (Pt 3), 791-803.

47. Blandina, P.; Giorgetti, M.; Bartolini, L.; Cecchi, M.; Timmerman, H.; Leurs, R.; Pepeu, G.; Giovannini, M. G., *Br J Pharmacol* **1996,** *119* (8), 1656-1664.

48. Leurs, R.; Bakker, R. A.; Timmerman, H.; de Esch, I. J. P., *Nature Reviews Drug Discovery* **2005,** *4* (2), 107-120.

49. Gemkow, M. J.; Davenport, A. J.; Harich, S.; Ellenbroek, B. A.; Cesura, A.; Hallett, D., *Drug Discovery Today* **2009,** *14* (9), 509-515.

50. Passani, M. B.; Lin, J.-S.; Hancock, A.; Crochet, S.; Blandina, P., *Trends in Pharmacological Sciences* **2004,** *25* (12), 618-625.

51. Teuscher, C.; Subramanian, M.; Noubade, R.; Gao, J. F.; Offner, H.; Zachary, J. F.; Blankenhorn, E. P., *Proceedings of the National Academy of Sciences* **2007,** *104* (24), 10146.

52. Toyota, H.; Dugovic, C.; Koehl, M.; Laposky, A. D.; Weber, C.; Ngo, K.; Wu, Y.; Lee, D. H.; Yanai, K.; Sakurai, E.; Watanabe, T.; Liu, C.; Chen, J.; Barbier, A. J.; Turek, F. W.; Fung-Leung, W.-P.; Lovenberg, T. W., *Molecular Pharmacology* **2002,** *62* (2), 389.

53. Oda, T.; Morikawa, N.; Saito, Y.; Masuho, Y.; Matsumoto, S., *J Biol Chem* **2000,** *275* (47), 36781-6.

54. Nakamura, T.; Itadani, H.; Hidaka, Y.; Ohta, M.; Tanaka, K., *Biochemical and Biophysical Research Communications* **2000,** *279* (2), 615-620.

55. Zhu, Y.; Michalovich, D.; Wu, H.-L.; Tan, K. B.; Dytko, G. M.; Mannan, I. J.; Boyce, R.; Alston, J.; Tierney, L. A.; Li, X.; Herrity, N. C.; Vawter, L.; Sarau, H. M.; Ames, R. S.; Davenport, C. M.; Hieble, J. P.; Wilson, S.; Bergsma, D. J.; Fitzgerald, L. R., *Molecular Pharmacology* **2001,** *59* (3), 434.

56. Zampeli, E.; Tiligada, E., *Br J Pharmacol* **2009,** *157* (1), 24-33.

57. Goodchild, R. E.; Court, J. A.; Hobson, I.; Piggott, M. A.; Perry, R. H.; Ince, P.; Jaros, E.; Perry, E. K., *European Journal of Neuroscience* **1999,** *11* (2), 449-456.

58. Nakamura, S.; Takemura, M.; Ohnishi, K.; Suenaga, T.; Nishimura, M.; Akiguchi, I.; Kimura, J.; Kimura, T., *Neuroscience Letters* **1993,** *151* (2), 196-199.

59. Panula, P.; Rinne, J.; Kuokkanen, K.; Eriksson, K. S.; Sallmen, T.; Kalimo, H.; Relja, M., *Neuroscience* **1997,** *82* (4), 993-997.

60. Higuchi, M.; Yanai, K.; Okamura, N.; Meguro, K.; Arai, H.; Itoh, M.; Iwata, R.; Ido, T.; Watanabe, T.; Sasaki, H., *Neuroscience* **2000,** *99* (4), 721-729.

61. Ambrée, O.; Buschert, J.; Zhang, W.; Arolt, V.; Dere, E.; Zlomuzica, A., *European Neuropsychopharmacology* **2014,** *24* (8), 1394-1404.

62. Anichtchik, O. V.; Peitsaro, N.; Rinne, J. O.; Kalimo, H.; Panula, P., *Neurobiology of Disease* **2001,** *8* (4), 707-716.

63. Rinne, J. O.; Anichtchik, O. V.; Eriksson, K. S.; Kaslin, J.; Tuomisto, L.; Kalimo, H.; Röyttä, M.; Panula, P., *Journal of Neurochemistry* **2002,** *81* (5), 954-960.

64. Anichtchik, O. V.; Huotari, M.; Peitsaro, N.; Haycock, J. W.; Männistö, P. T.; Panula, P., *European Journal of Neuroscience* **2000,** *12* (11), 3823-3832.

65. Nowak, P.; Noras, Ł.; Jochem, J.; Szkilnik, R.; Brus, H.; Körőssy, E.; Drab, J.; Kostrzewa, R. M.; Brus, R., *Neurotoxicity Research* **2009,** *15* (3), 246-251.

124

66.   Kano, M.; Fukudo, S.; Tashiro, A.; Utsumi, A.; Tamura, D.; Itoh, M.; Iwata, R.; Tashiro, M.; Mochizuki, H.; Funaki, Y.; Kato, M.; Hongo, M.; Yanai, K., *European Journal of Neuroscience* **2004,** *20* (3), 803-810.

67.   Yamada, Y.; Yoshikawa, T.; Naganuma, F.; Kikkawa, T.; Osumi, N.; Yanai, K., *Neuropharmacology* **2020,** *175*, 108179.

68.   Anderson, J. M.; Rodriguez, A.; Chang, D. T., *Seminars in Immunology* **2008,** *20* (2), 86-100.

69.   Hoogland, I. C. M.; Houbolt, C.; van Westerloo, D. J.; van Gool, W. A.; van de Beek, D., *Journal of Neuroinflammation* **2015,** *12* (1), 114.

70.   Health, N. I. o., Consideration of Sex as a Biological Variable in NIH-Funded Research: NOT-OD-15-102. 2015.

71.   Beery, A. K.; Zucker, I., *Neurosci Biobehav Rev* **2011,** *35* (3), 565-572.

72.   Bracken, M. B., *J R Soc Med* **2009,** *102* (3), 120-122.

73.   Dupré, C.; Lovett-Barron, M.; Pfaff, D. W.; Kow, L.-M., *Proceedings of the National Academy of Sciences* **2010,** *107* (27), 12311.

74.   Lund, T. D.; Rovis, T.; Chung, W. C. J.; Handa, R. J., *Endocrinology* **2005,** *146* (2), 797-807.

75.   Musatov, S.; Chen, W.; Pfaff, D. W.; Mobbs, C. V.; Yang, X.-J.; Clegg, D. J.; Kaplitt, M. G.; Ogawa, S., *Proceedings of the National Academy of Sciences* **2007,** *104* (7), 2501.

76.   Mori, H.; Matsuda, K.-I.; Yamawaki, M.; Kawata, M., *PLoS One* **2014,** *9* (5), e96232.

77.   Gotoh, K.; Masaki, T.; Chiba, S.; Higuchi, K.; Kakuma, T.; Shimizu, H.; Mori, M.; Sakata, T.; Yoshimatsu, H., *Journal of Neurochemistry* **2009,** *110* (6), 1796-1805.

78.   Baker, A. E.; Brautigam, V. M.; Watters, J. J., *Endocrinology* **2004,** *145* (11), 5021-5032.

79.   Deshpande, R.; Khalili, H.; Pergolizzi, R. G.; Michael, S. D.; Chang, M.-D. Y., *American Journal of Reproductive Immunology* **1997,** *38* (1), 46-54.

80.   Lei, B.; Mace, B.; Dawson, H. N.; Warner, D. S.; Laskowitz, D. T.; James, M. L., *PLoS One* **2014,** *9* (7), e103969.

81.   Vegeto, E.; Bonincontro, C.; Pollio, G.; Sala, A.; Viappiani, S.; Nardi, F.; Brusadelli, A.; Viviani, B.; Ciana, P.; Maggi, A., *The Journal of Neuroscience* **2001,** *21* (6), 1809.

82.   Fish, E. N., *Nature Reviews Immunology* **2008,** *8* (9), 737-744.

83.   Reckelhoff, J. F., *Hypertension* **2001,** *37* (5), 1199-1208.

84.   López-Muñoz, F.; Alamo, C., *Current pharmaceutical design* **2009,** *15* (14), 1563-1586.

85.   Krystal, J. H.; Abdallah, C. G.; Sanacora, G.; Charney, D. S.; Duman, R. S., *Neuron* **2019,** *101* (5), 774-778.

86.   Wong, M.-L.; Licinio, J., *Nature Reviews Drug Discovery* **2004,** *3* (2), 136-151.

87.   Pereira, V. S.; Hiroaki-Sato, V. A., *Acta Neuropsiatrica* **2018,** *30* (6), 307-322.

88.   Kendell, S. F.; Krystal, J. H.; Sanacora, G., *Expert Opinion on Therapeutic Targets* **2005,** *9* (1), 153-168.

89.   Berman, R. M.; Cappiello, A.; Anand, A.; Oren, D. A.; Heninger, G. R.; Charney, D. S.; Krystal, J. H., *Biological Psychiatry* **2000,** *47* (4), 351-354.

90.   Wray, N. H.; Schappi, J. M.; Singh, H.; Senese, N. B.; Rasenick, M. M., *Molecular Psychiatry* **2019,** *24* (12), 1833-1843.

91.   Yang, C.; Shirayama, Y.; Zhang, J. c.; Ren, Q.; Yao, W.; Ma, M.; Dong, C.; Hashimoto, K., *Translational Psychiatry* **2015,** *5* (9), e632-e632.

92.   Zanos, P.; Highland, J. N.; Stewart, B. W.; Georgiou, P.; Jenne, C. E.; Lovett, J.; Morris, P. J.; Thomas, C. J.; Moaddel, R.; Zarate, C. A.; Gould, T. D., *Proceedings of the National Academy of Sciences* **2019,** *116* (13), 6441.

93.   Zanos, P.; Moaddel, R.; Morris, P. J.; Georgiou, P.; Fischell, J.; Elmer, G. I.; Alkondon, M.; Yuan, P.; Pribut, H. J.; Singh, N. S.; Dossou, K. S. S.; Fang, Y.; Huang, X.-P.; Mayo, C. L.; Wainer, I. W.; Albuquerque, E. X.; Thompson, S. M.; Thomas, C. J.; Zarate Jr, C. A.; Gould, T. D., *Nature* **2016,** *533* (7604), 481-486.

94.   Zhang, J.-c.; Li, S.-x.; Hashimoto, K., *Pharmacology Biochemistry and Behavior* **2014,** *116*, 137-141.

95.   Zhou, W.; Wang, N.; Yang, C.; Li, X. M.; Zhou, Z. Q.; Yang, J. J., *European Psychiatry* **2014,** *29* (7), 419-423.

96.   Berger, S. N. H., P., Brain Chemistry | Neurotransmitters. In *Encyclopedia of Analytical Science*, 3rd ed.; Worsfold, P. P., C.; Townshend, A.; Miro, M., Ed. Elsevier: 2019; Vol. 1, pp 316-331.

97.   Hersey, M.; Berger, S. N.; Holmes, J.; West, A.; Hashemi, P., *Analytical Chemistry* **2019,** *91* (1), 27-43.

98.   Wightman, R. M., *Science* **2006,** *311* (5767), 1570.

99.   Heien, M. L. A. V.; Phillips, P. E. M.; Stuber, G. D.; Seipel, A. T.; Wightman, R. M., *Analyst* **2003,** *128* (12), 1413-1419.

100.   Roberts, J. G.; Sombers, L. A., *Analytical Chemistry* **2018,** *90* (1), 490-504.

101.   Hawley, M. D.; Tatawawadi, S. V.; Piekarski, S.; Adams, R. N., *Journal of the American Chemical Society* **1967,** *89* (2), 447-450.

102.   Kissinger, P. T.; Hart, J. B.; Adams, R. N., *Brain Research* **1973,** *55* (1), 209-213.

103.   Zhang, B.; Heien, M. L. A. V.; Santillo, M. F.; Mellander, L.; Ewing, A. G., *Analytical Chemistry* **2011,** *83* (2), 571-577.

104.   Fathali, H.; Cans, A.-S., *Pflügers Archiv - European Journal of Physiology* **2018,** *470* (1), 125-134.

105.   Zhang, B.; Adams, K. L.; Luber, S. J.; Eves, D. J.; Heien, M. L.; Ewing, A. G., *Analytical Chemistry* **2008,** *80* (5), 1394-1400.

106.   Amatore, C.; Arbault, S.; Guille, M.; Lemaître, F., *Chemical Reviews* **2008,** *108* (7), 2585-2621.

107.   Phan, N. T. N.; Li, X.; Ewing, A. G., *Nature Reviews Chemistry* **2017,** *1* (6), 0048.

108.   Wiedholz, L. M.; Owens, W. A.; Horton, R. E.; Feyder, M.; Karlsson, R. M.; Hefner, K.; Sprengel, R.; Celikel, T.; Daws, L. C.; Holmes, A., *Molecular Psychiatry* **2008,** *13* (6), 631-640.

109.   Daws, L. C.; Montañez, S.; Owens, W. A.; Gould, G. G.; Frazer, A.; Toney, G. M.; Gerhardt, G. A., *Journal of Neuroscience Methods* **2005,** *143* (1), 49-62.

110.   Perez, X. A.; Andrews, A. M., *Analytical Chemistry* **2005,** *77* (3), 818-826.

111.   Willuhn, I.; Wanat, M. J.; Clark, J. J.; Phillips, P. E. M., Dopamine Signaling in the Nucleus Accumbens of Animals Self-Administering Drugs of Abuse. In *Behavioral Neuroscience of Drug Addiction*, Self, D. W.; Staley Gottschalk, J. K., Eds. Springer Berlin Heidelberg: Berlin, Heidelberg, 2010; pp 29-71.

112. Millar, J.; Stamford, J. A.; Kruk, Z. L.; Wightman, R. M., *European Journal of Pharmacology* **1985,** *109* (3), 341-348.

113. Stamford, J. A.; Kruk, Z. L.; Millar, J.; Wightman, R. M., *Neuroscience Letters* **1984,** *51* (1), 133-138.

114. Hashemi, P.; Dankoski, E. C.; Lama, R.; Wood, K. M.; Takmakov, P.; Wightman, R. M., *Proceedings of the National Academy of Sciences* **2012,** *109* (29), 11510.

115. Tsai, H.-C.; Zhang, F.; Adamantidis, A.; Stuber, G. D.; Bonci, A.; de Lecea, L.; Deisseroth, K., *Science* **2009,** *324* (5930), 1080.

116. Venton, B. J.; Wightman, R. M., *Synapse* **2007,** *61* (1), 37-39.

117. Johnson, J. A.; Hobbs, C. N.; Wightman, R. M., *Analytical Chemistry* **2017,** *89* (11), 6166-6174.

118. Norton, J. D.; White, H. S.; Feldberg, S. W., *The Journal of Physical Chemistry* **1990,** *94* (17), 6772-6780.

119. Hashemi, P.; Dankoski, E. C.; Petrovic, J.; Keithley, R. B.; Wightman, R. M., *Analytical Chemistry* **2009,** *81* (22), 9462-9471.

120. Michael, D.; Travis, E. R.; Wightman, R. M., *Analytical Chemistry* **1998,** *70* (17), 586A-592A.

121. Samaranayake, S.; Abdalla, A.; Robke, R.; Wood, K. M.; Zeqja, A.; Hashemi, P., *Analyst* **2015,** *140* (11), 3759-3765.

122. Samaranayake, S.; Abdalla, A.; Robke, R.; Nijhout, H. F.; Reed, M. C.; Best, J.; Hashemi, P., *Journal of Neurochemistry* **2016,** *138* (3), 374-383.

Chapter 2 References

1. Anderson, J. M.; Rodriguez, A.; Chang, D. T., *Seminars in Immunology* **2008,** *20* (2), 86-100.

2. Khan, A. S.; Michael, A. C., *TrAC Trends in Analytical Chemistry* **2003,** *22* (8), 503-508.

3. Egorova, K. S.; Ananikov, V. P., *Organometallics* **2017,** *36* (21), 4071-4090.

4. Liu, W.; Wu, Y.; Wang, C.; Li, H. C.; Wang, T.; Liao, C. Y.; Cui, L.; Zhou, Q. F.; Yan, B.; Jiang, G. B., *Nanotoxicology* **2010,** *4* (3), 319-330.

5. Soto, R. J.; Merricks, E. P.; Bellinger, D. A.; Nichols, T. C.; Schoenfisch, M. H., *Biomaterials* **2018,** *157*, 76-85.

6. Soto, R. J.; Privett, B. J.; Schoenfisch, M. H., *Analytical Chemistry* **2014,** *86* (14), 7141-7149.

7. Storm, W. L.; Schoenfisch, M. H., *ACS Applied Materials & Interfaces* **2013,** *5* (11), 4904-4912.

8. Clark, J. J.; Sandberg, S. G.; Wanat, M. J.; Gan, J. O.; Horne, E. A.; Hart, A. S.; Akers, C. A.; Parker, J. G.; Willuhn, I.; Martinez, V.; Evans, S. B.; Stella, N.; Phillips, P. E. M., *Nature Methods* **2010,** *7* (2), 126-129.

9. Amatore, C.; Delacotte, J.; Guille-Collignon, M.; Lemaître, F., *Analyst* **2015,** *140* (11), 3687-3695.

10. Bucher, E. S.; Wightman, R. M., *Annual Review of Analytical Chemistry* **2015,** *8* (1), 239-261.

11. Hashemi, P.; Dankoski, E. C.; Petrovic, J.; Keithley, R. B.; Wightman, R. M., *Analytical Chemistry* **2009,** *81* (22), 9462-9471.

12.   Ross, A. E.; Venton, B. J., *Analyst* **2012,** *137* (13), 3045-3051.

13.   Vreeland, R. F.; Atcherley, C. W.; Russell, W. S.; Xie, J. Y.; Lu, D.; Laude, N. D.; Porreca, F.; Heien, M. L., *Analytical Chemistry* **2015,** *87* (5), 2600-2607.

14.   Yang, C.; Jacobs, C. B.; Nguyen, M. D.; Ganesana, M.; Zestos, A. G.; Ivanov, I. N.; Puretzky, A. A.; Rouleau, C. M.; Geohegan, D. B.; Venton, B. J., *Analytical Chemistry* **2016,** *88* (1), 645-652.

15.   Yang, C.; Wang, Y.; Jacobs, C. B.; Ivanov, I. N.; Venton, B. J., *Analytical Chemistry* **2017,** *89* (10), 5605-5611.

16.   Meyer, E. P.; Ulmann-Schuler, A.; Staufenbiel, M.; Krucker, T., *Proceedings of the National Academy of Sciences* **2008,** *105* (9), 3587.

17.   Silvani, A.; Bojic, T.; Cianci, T.; Franzini, C.; Lenzi, P.; Lucchi, M. L.; Zoccoli, G., *Experimental Brain Research* **2004,** *154* (1), 44-49.

18.   Lee, W. H.; Ngernsutivorakul, T.; Mabrouk, O. S.; Wong, J.-M. T.; Dugan, C. E.; Pappas, S. S.; Yoon, H. J.; Kennedy, R. T., *Analytical Chemistry* **2016,** *88* (2), 1230-1237.

19.   Lee, W. H.; Slaney, T. R.; Hower, R. W.; Kennedy, R. T., *Analytical Chemistry* **2013,** *85* (8), 3828-3831.

20.   Jaquins-Gerstl, A.; Shu, Z.; Zhang, J.; Liu, Y.; Weber, S. G.; Michael, A. C., *Analytical Chemistry* **2011,** *83* (20), 7662-7667.

21.   Abdalla, A.; Atcherley, C. W.; Pathirathna, P.; Samaranayake, S.; Qiang, B.; Peña, E.; Morgan, S. L.; Heien, M. L.; Hashemi, P., *Analytical Chemistry* **2017,** *89* (18), 9703-9711.

22.   Atcherley, C. W.; Laude, N. D.; Parent, K. L.; Heien, M. L., *Langmuir* **2013,** *29* (48), 14885-14892.

23.   Atcherley, C. W.; Wood, K. M.; Parent, K. L.; Hashemi, P.; Heien, M. L., *Chemical Communications* **2015,** *51* (12), 2235-2238.

24.   Brindley, R. L.; Bauer, M. B.; Blakely, R. D.; Currie, K. P. M., *Neuropharmacology* **2016,** *110*, 438-448.

25.   Fathali, H.; Dunevall, J.; Majdi, S.; Cans, A.-S., *ACS Chemical Neuroscience* **2017,** *8* (2), 368-375.

26.   Ren, L.; Mellander, L. J.; Keighron, J.; Cans, A.-S.; Kurczy, M. E.; Svir, I.; Oleinick, A.; Amatore, C.; Ewing, A. G., *Quarterly Reviews of Biophysics* **2016,** *49*, e12.

27.   Ye, D.; Gu, C.; Ewing, A., *ACS Chemical Neuroscience* **2018,** *9* (12), 2941-2947.

28.   Day, B. K.; Pomerleau, F.; Burmeister, J. J.; Huettl, P.; Gerhardt, G. A., *Journal of Neurochemistry* **2006,** *96* (6), 1626-1635.

29.   Mabrouk, O. S.; Han, J. L.; Wong, J.-M. T.; Akil, H.; Kennedy, R. T.; Flagel, S. B., *ACS Chemical Neuroscience* **2018,** *9* (4), 715-724.

30.   Hensley, A. L.; Colley, A. R.; Ross, A. E., *Analytical Chemistry* **2018,** *90* (14), 8642-8650.

31.   Hobbs, C. N.; Johnson, J. A.; Verber, M. D.; Mark Wightman, R., *Analyst* **2017,** *142* (16), 2912-2920.

32.   Samaranayake, S.; Abdalla, A.; Robke, R.; Nijhout, H. F.; Reed, M. C.; Best, J.; Hashemi, P., *Journal of Neurochemistry* **2016,** *138* (3), 374-383.

33.   Sanford, A. L.; Morton, S. W.; Whitehouse, K. L.; Oara, H. M.; Lugo-Morales, L. Z.; Roberts, J. G.; Sombers, L. A., *Analytical Chemistry* **2010,** *82* (12), 5205-5210.

34.   Dahlin, A. P.; Purins, K.; Clausen, F.; Chu, J.; Sedigh, A.; Lorant, T.; Enblad, P.; Lewén, A.; Hillered, L., *Analytical Chemistry* **2014,** *86* (17), 8671-8679.

128

35.   Ferris, M. J.; España, R. A.; Locke, J. L.; Konstantopoulos, J. K.; Rose, J. H.; Chen, R.; Jones, S. R., *Proceedings of the National Academy of Sciences* **2014,** *111* (26), E2751.

36.   Greco, S.; Danysz, W.; Zivkovic, A.; Gross, R.; Stark, H., *Analytica Chimica Acta* **2013,** *771*, 65-72.

37.   Kim, M.; Lee, J.-g.; Yang, C. H.; Lee, S., *Analytica Chimica Acta* **2016,** *923*, 55-65.

38.   Gowers, S. A. N.; Hamaoui, K.; Cunnea, P.; Anastasova, S.; Curto, V. F.; Vadgama, P.; Yang, G. Z.; Papalois, V.; Drakakis, E. M.; Fotopoulou, C.; Weber, S. G.; Boutelle, M. G., *Analyst* **2018,** *143* (3), 715-724.

39.   Lin, Y.; Yu, P.; Mao, L., *Analyst* **2015,** *140* (11), 3781-3787.

40.   Rogers, M. L.; Brennan, P. A.; Leong, C. L.; Gowers, S. A. N.; Aldridge, T.; Mellor, T. K.; Boutelle, M. G., *Analytical and Bioanalytical Chemistry* **2013,** *405* (11), 3881-3888.

41.   Justice, J. B., *Journal of Neuroscience Methods* **1993,** *48* (3), 263-276.

42.   Kendrick, K. M., *Journal of Neuroscience Methods* **1990,** *34* (1), 35-46.

43.   Sandberg, M.; Lindström, S., *Journal of Neuroscience Methods* **1983,** *9* (1), 65-74.

44.   TOSSMAN, U.; UNGERSTEDT, U., *Acta Physiologica Scandinavica* **1986,** *128* (1), 9-14.

45.   Kozai, T. D. Y.; Jaquins-Gerstl, A. S.; Vazquez, A. L.; Michael, A. C.; Cui, X. T., *ACS Chemical Neuroscience* **2015,** *6* (1), 48-67.

46.   Cepeda, D. E.; Hains, L.; Li, D.; Bull, J.; Lentz, S. I.; Kennedy, R. T., *Journal of Neuroscience Methods* **2015,** *242*, 97-105.

47.   Ngo, K. T.; Varner, E. L.; Michael, A. C.; Weber, S. G., *ACS Chemical Neuroscience* **2017,** *8* (2), 329-338.

48.   Nesbitt, K. M.; Varner, E. L.; Jaquins-Gerstl, A.; Michael, A. C., *ACS Chemical Neuroscience* **2015,** *6* (1), 163-173.

49.   Varner, E. L.; Leong, C. L.; Jaquins-Gerstl, A.; Nesbitt, K. M.; Boutelle, M. G.; Michael, A. C., *ACS Chemical Neuroscience* **2017,** *8* (8), 1779-1788.

50.   Nesbitt, K. M.; Jaquins-Gerstl, A.; Skoda, E. M.; Wipf, P.; Michael, A. C., *Analytical Chemistry* **2013,** *85* (17), 8173-8179.

51.   Varner, E. L.; Jaquins-Gerstl, A.; Michael, A. C., *ACS Chemical Neuroscience* **2016,** *7* (6), 728-736.

52.   Yang, H.; Thompson, A. B.; McIntosh, B. J.; Altieri, S. C.; Andrews, A. M., *ACS Chemical Neuroscience* **2013,** *4* (5), 790-798.

53.   Gu, H.; Varner, E. L.; Groskreutz, S. R.; Michael, A. C.; Weber, S. G., *Analytical Chemistry* **2015,** *87* (12), 6088-6094.

54.   Yang, H.; Sampson, M. M.; Senturk, D.; Andrews, A. M., *ACS Chemical Neuroscience* **2015,** *6* (8), 1487-1501.

55.   Zhang, J.; Jaquins-Gerstl, A.; Nesbitt, K. M.; Rutan, S. C.; Michael, A. C.; Weber, S. G., *Analytical Chemistry* **2013,** *85* (20), 9889-9897.

56.   Zhang, J.; Liu, Y.; Jaquins-Gerstl, A.; Shu, Z.; Michael, A. C.; Weber, S. G., *Journal of Chromatography A* **2012,** *1251*, 54-62.

57.   Harrison, D. J.; Fluri, K.; Seiler, K.; Fan, Z.; Effenhauser, C. S.; Manz, A., *Science* **1993,** *261* (5123), 895.

58.   Sloan, C. D. K.; Nandi, P.; Linz, T. H.; Aldrich, J. V.; Audus, K. L.; Lunte, S. M., *Annual Review of Analytical Chemistry* **2012,** *5* (1), 505-531.

129

59. Manz, A.; Harrison, D. J.; Verpoorte, E. M. J.; Fettinger, J. C.; Paulus, A.; Lüdi, H.; Widmer, H. M., *Journal of Chromatography A* **1992,** *593* (1), 253-258.

60. Saylor, R. A.; Lunte, S. M., *Journal of Chromatography A* **2015,** *1382*, 48-64.

61. Scott, D. E.; Grigsby, R. J.; Lunte, S. M., *ChemPhysChem* **2013,** *14* (10), 2288-2294.

62. Shou, M.; Ferrario, C. R.; Schultz, K. N.; Robinson, T. E.; Kennedy, R. T., *Analytical Chemistry* **2006,** *78* (19), 6717-6725.

63. Wang, M.; Roman, G. T.; Perry, M. L.; Kennedy, R. T., *Analytical Chemistry* **2009,** *81* (21), 9072-9078.

64. Bert, L.; Parrot, S.; Robert, F.; Desvignes, C.; Denoroy, L.; Suaud-Chagny, M. F.; Renaud, B., *Neuropharmacology* **2002,** *43* (5), 825-835.

65. Lada, M. W.; Vickroy, T. W.; Kennedy, R. T., *Analytical Chemistry* **1997,** *69* (22), 4560-4565.

66. Saylor, R. A.; Lunte, S. M., *ELECTROPHORESIS* **2018,** *39* (3), 462-469.

67. Tucci, S.; Rada, P.; Sepúlveda, M. J.; Hernandez, L., *Journal of Chromatography B: Biomedical Sciences and Applications* **1997,** *694* (2), 343-349.

68. Wang, M.; Roman, G. T.; Schultz, K.; Jennings, C.; Kennedy, R. T., *Analytical Chemistry* **2008,** *80* (14), 5607-5615.

69. Song, P.; Hershey, N. D.; Mabrouk, O. S.; Slaney, T. R.; Kennedy, R. T., *Analytical Chemistry* **2012,** *84* (11), 4659-4664.

70. Ngernsutivorakul, T.; Steyer, D. J.; Valenta, A. C.; Kennedy, R. T., *Analytical Chemistry* **2018,** *90* (18), 10943-10950.

71. Rogers, M. L.; Leong, C. L.; Gowers, S. A.; Samper, I. C.; Jewell, S. L.; Khan, A.; McCarthy, L.; Pahl, C.; Tolias, C. M.; Walsh, D. C.; Strong, A. J.; Boutelle, M. G., *Journal of Cerebral Blood Flow & Metabolism* **2017,** *37* (5), 1883-1895.

72. Clay, M.; Monbouquette, H. G., *ACS Chemical Neuroscience* **2018,** *9* (2), 241-251.

73. Koshy Cherian, A.; Gritton, H.; Johnson, D. E.; Young, D.; Kozak, R.; Sarter, M., *Neuropharmacology* **2014,** *82*, 41-48.

74. Malvaez, M.; Greenfield, V. Y.; Wang, A. S.; Yorita, A. M.; Feng, L.; Linker, K. E.; Monbouquette, H. G.; Wassum, K. M., *Scientific Reports* **2015,** *5* (1), 12511.

75. Thomas, T. C.; Beitchman, J. A.; Pomerleau, F.; Noel, T.; Jungsuwadee, P.; Butterfield, D. A.; Clair, D. K. S.; Vore, M.; Gerhardt, G. A., *Brain Research* **2017,** *1672*, 10-17.

76. Guilbault, G. G.; Lubrano, G. J., *Analytica Chimica Acta* **1972,** *60* (1), 254-256.

77. Navera, E. N.; Sode, K.; Tamiya, E.; Karube, I., *Biosensors and Bioelectronics* **1991,** *6* (8), 675-680.

78. Updike, S. J.; Hicks, G. P., *Science* **1967,** *158* (3798), 270.

79. Villarta, R. L.; Cunningham, D. D.; Guilbault, G. G., *Talanta* **1991,** *38* (1), 49-55.

80. Silber, A.; Hampp, N.; Schuhmann, W., *Biosensors and Bioelectronics* **1996,** *11* (3), 215-223.

81. Wickramasinghe, Y.; Yang, Y.; Spencer, S. A., *Journal of Fluorescence* **2004,** *14* (5), 513-520.

82. Burmeister, J. J.; Gerhardt, G. A., *Analytical Chemistry* **2001,** *73* (5), 1037-1042.

83. Burmeister, J. J.; Moxon, K.; Gerhardt, G. A., *Analytical Chemistry* **2000,** *72* (1), 187-192.

84.   Teles-Grilo Ruivo, L. M.; Baker, K. L.; Conway, M. W.; Kinsley, P. J.; Gilmour, G.; Phillips, K. G.; Isaac, J. T. R.; Lowry, J. P.; Mellor, J. R., *Cell Reports* **2017,** *18* (4), 905-917.

85.   Wassum, K. M.; Tolosa, V. M.; Wang, J.; Walker, E.; Monbouquette, H. G.; Maidment, N. T., *Sensors* **2008,** *8* (8), 5023-5036.

86.   Wang, Y.; Vaddiraju, S.; Gu, B.; Papadimitrakopoulos, F.; Burgess, D. J., *Journal of Diabetes Science and Technology* **2015,** *9* (5), 966-977.

87.   Lugo-Morales, L. Z.; Loziuk, P. L.; Corder, A. K.; Toups, J. V.; Roberts, J. G.; McCaffrey, K. A.; Sombers, L. A., *Analytical Chemistry* **2013,** *85* (18), 8780-8786.

88.   Smith, S. K.; Lee, C. A.; Dausch, M. E.; Horman, B. M.; Patisaul, H. B.; McCarty, G. S.; Sombers, L. A., *ACS Chemical Neuroscience* **2017,** *8* (2), 272-280.

89.   Soto, R. J.; Schofield, J. B.; Walter, S. E.; Malone-Povolny, M. J.; Schoenfisch, M. H., *ACS Sensors* **2017,** *2* (1), 140-150.

90.   Bergman, J.; Wang, Y.; Wigström, J.; Cans, A.-S., *Analytical and Bioanalytical Chemistry* **2018,** *410* (6), 1775-1783.

91.   Datta, S.; Christena, L. R.; Rajaram, Y. R. S., *3 Biotech* **2013,** *3* (1), 1-9.

92.   Mohamad, N. R.; Marzuki, N. H. C.; Buang, N. A.; Huyop, F.; Wahab, R. A., *Biotechnology & Biotechnological Equipment* **2015,** *29* (2), 205-220.

93.   Grupe, M.; Paolone, G.; Jensen, A. A.; Sandager-Nielsen, K.; Sarter, M.; Grunnet, M., *Biochemical Pharmacology* **2013,** *86* (10), 1487-1496.

94.   Miller, E. M.; Quintero, J. E.; Pomerleau, F.; Huettl, P.; Gerhardt, G. A.; Glaser, P. E. A., *Journal of Neuroscience Methods* **2015,** *252*, 75-79.

95.   Lenoir, M.; Kiyatkin, E. A., *Journal of Neurochemistry* **2013,** *127* (4), 541-551.

96.   Hinzman, J. M.; Gibson, J. L.; Tackla, R. D.; Costello, M. S.; Burmeister, J. J.; Quintero, J. E.; Gerhardt, G. A.; Hartings, J. A., *Biosensors and Bioelectronics* **2015,** *74*, 512-517.

97.   Gritton, H. J.; Howe, W. M.; Mallory, C. S.; Hetrick, V. L.; Berke, J. D.; Sarter, M., *Proceedings of the National Academy of Sciences* **2016,** *113* (8), E1089.

98.   Howe, W. M.; Gritton, H. J.; Lusk, N. A.; Roberts, E. A.; Hetrick, V. L.; Berke, J. D.; Sarter, M., *The Journal of Neuroscience* **2017,** *37* (12), 3215.

99.   Fathali, H.; Cans, A.-S., *Pflügers Archiv - European Journal of Physiology* **2018,** *470* (1), 125-134.

100.   Amatore, C.; Arbault, S.; Bouret, Y.; Guille, M.; Lemaître, F.; Verchier, Y., *Analytical Chemistry* **2009,** *81* (8), 3087-3093.

101.   Barlow, S. T.; Louie, M.; Hao, R.; Defnet, P. A.; Zhang, B., *Analytical Chemistry* **2018,** *90* (16), 10049-10055.

102.   Li, X.; Dunevall, J.; Ewing, A. G., *Accounts of Chemical Research* **2016,** *49* (10), 2347-2354.

103.   Li, X.; Dunevall, J.; Ren, L.; Ewing, A. G., *Analytical Chemistry* **2017,** *89* (17), 9416-9423.

104.   Li, X.; Ren, L.; Dunevall, J.; Ye, D.; White, H. S.; Edwards, M. A.; Ewing, A. G., *ACS Nano* **2018,** *12* (3), 3010-3019.

105.   Zhang, B.; Adams, K. L.; Luber, S. J.; Eves, D. J.; Heien, M. L.; Ewing, A. G., *Analytical Chemistry* **2008,** *80* (5), 1394-1400.

106.   Zhang, B.; Heien, M. L. A. V.; Santillo, M. F.; Mellander, L.; Ewing, A. G., *Analytical Chemistry* **2011,** *83* (2), 571-577.

131

107. Wang, J.; Trouillon, R.; Dunevall, J.; Ewing, A. G., *Analytical Chemistry* **2014,** *86* (9), 4515-4520.

108. Trouillon, R.; Ewing, A. G., *Chemphyschem : a European journal of chemical physics and physical chemistry* **2013,** *14* (10), 2295-2301.

109. Trouillon, R.; Ewing, A. G., *ACS Chemical Biology* **2014,** *9* (3), 812-820.

110. Logan, T.; Bendor, J.; Toupin, C.; Thorn, K.; Edwards, R. H., *Nature Neuroscience* **2017,** *20* (5), 681-689.

111. Oleinick, A.; Svir, I.; Amatore, C., *Proceedings of the Royal Society A: Mathematical, Physical and Engineering Sciences* **2017,** *473* (2197), 20160684.

112. Mellander, L. J.; Kurczy, M. E.; Najafinobar, N.; Dunevall, J.; Ewing, A. G.; Cans, A.-S., *Scientific Reports* **2014,** *4* (1), 3847.

113. Heien, M. L. A. V.; Phillips, P. E. M.; Stuber, G. D.; Seipel, A. T.; Wightman, R. M., *Analyst* **2003,** *128* (12), 1413-1419.

114. Roberts, J. G.; Moody, B. P.; McCarty, G. S.; Sombers, L. A., *Langmuir* **2010,** *26* (11), 9116-9122.

115. Takmakov, P.; Zachek, M. K.; Keithley, R. B.; Walsh, P. L.; Donley, C.; McCarty, G. S.; Wightman, R. M., *Analytical Chemistry* **2010,** *82* (5), 2020-2028.

116. Jacobs, C. B.; Vickrey, T. L.; Venton, B. J., *Analyst* **2011,** *136* (17), 3557-3565.

117. Swamy, B. E. K.; Venton, B. J., *Analyst* **2007,** *132* (9), 876-884.

118. Johnson, J. A.; Hobbs, C. N.; Wightman, R. M., *Analytical Chemistry* **2017,** *89* (11), 6166-6174.

119. Hashemi, P.; Dankoski, E. C.; Lama, R.; Wood, K. M.; Takmakov, P.; Wightman, R. M., *Proceedings of the National Academy of Sciences* **2012,** *109* (29), 11510.

120. Venton, B. J.; Wightman, R. M., *Synapse* **2007,** *61* (1), 37-39.

121. Tsai, H.-C.; Zhang, F.; Adamantidis, A.; Stuber, G. D.; Bonci, A.; de Lecea, L.; Deisseroth, K., *Science* **2009,** *324* (5930), 1080.

122. Schwerdt, H. N.; Shimazu, H.; Amemori, K.-i.; Amemori, S.; Tierney, P. L.; Gibson, D. J.; Hong, S.; Yoshida, T.; Langer, R.; Cima, M. J.; Graybiel, A. M., *Proceedings of the National Academy of Sciences* **2017,** *114* (50), 13260.

123. Jackson, B. P.; Dietz, S. M.; Wightman, R. M., *Analytical Chemistry* **1995,** *67* (6), 1115-1120.

124. West, A.; Best, J.; Abdalla, A.; Nijhout, H. F.; Reed, M.; Hashemi, P., *Neurochemistry International* **2019,** *123*, 50-58.

125. Wood, K. M.; Zeqja, A.; Nijhout, H. F.; Reed, M. C.; Best, J.; Hashemi, P., *Journal of Neurochemistry* **2014,** *130* (3), 351-359.

126. Roberts, J. G.; Hamilton, K. L.; Sombers, L. A., *Analyst* **2011,** *136* (17), 3550-3556.

127. Wilson, L. R.; Panda, S.; Schmidt, A. C.; Sombers, L. A., *Analytical Chemistry* **2018,** *90* (1), 888-895.

128. Pyakurel, P.; Privman Champaloux, E.; Venton, B. J., *ACS Chemical Neuroscience* **2016,** *7* (8), 1112-1119.

129. Cooper, S. E.; Venton, B. J., *Analytical and Bioanalytical Chemistry* **2009,** *394* (1), 329-336.

130. Samaranayake, S.; Abdalla, A.; Robke, R.; Wood, K. M.; Zeqja, A.; Hashemi, P., *Analyst* **2015,** *140* (11), 3759-3765.

131. Park, J.; Kile, B. M.; Mark Wightman, R., *European Journal of Neuroscience* **2009,** *30* (11), 2121-2133.

132.   Park, J.; Takmakov, P.; Wightman, R. M., *Journal of Neurochemistry* **2011,** *119* (5), 932-944.

133.   Kennedy, R. T.; Jones, S. R.; Wightman, R. M., *Neuroscience* **1992,** *47* (3), 603-612.

134.   Zimmerman, J. B.; Wightman, R. M., *Analytical Chemistry* **1991,** *63* (1), 24-28.

135.   Schmidt, A. C.; Dunaway, L. E.; Roberts, J. G.; McCarty, G. S.; Sombers, L. A., *Analytical Chemistry* **2014,** *86* (15), 7806-7812.

136.   McConnell, E. M.; Ventura, K.; Dwyer, Z.; Hunt, V.; Koudrina, A.; Holahan, M. R.; DeRosa, M. C., *ACS Chemical Neuroscience* **2019,** *10* (1), 371-383.

137.   Taylor, I. M.; Du, Z.; Bigelow, E. T.; Eles, J. R.; Horner, A. R.; Catt, K. A.; Weber, S. G.; Jamieson, B. G.; Cui, X. T., *Journal of Materials Chemistry B* **2017,** *5* (13), 2445-2458.

138.   Nakatsuka, N.; Cao, H. H.; Deshayes, S.; Melkonian, A. L.; Kasko, A. M.; Weiss, P. S.; Andrews, A. M., *ACS Applied Materials & Interfaces* **2018,** *10* (28), 23490-23500.

139.   Nakatsuka, N.; Yang, K.-A.; Abendroth, J. M.; Cheung, K. M.; Xu, X.; Yang, H.; Zhao, C.; Zhu, B.; Rim, Y. S.; Yang, Y.; Weiss, P. S.; Stojanović, M. N.; Andrews, A. M., *Science* **2018,** *362* (6412), 319.

140.   Park, S.; Guo, Y.; Jia, X.; Choe, H. K.; Grena, B.; Kang, J.; Park, J.; Lu, C.; Canales, A.; Chen, R.; Yim, Y. S.; Choi, G. B.; Fink, Y.; Anikeeva, P., *Nature Neuroscience* **2017,** *20* (4), 612-619.

141.   Patriarchi, T.; Cho, J. R.; Merten, K.; Howe, M. W.; Marley, A.; Xiong, W.-H.; Folk, R. W.; Broussard, G. J.; Liang, R.; Jang, M. J.; Zhong, H.; Dombeck, D.; von Zastrow, M.; Nimmerjahn, A.; Gradinaru, V.; Williams, J. T.; Tian, L., *Science* **2018,** *360* (6396), eaat4422.

142.   Colombo, M. L.; Sweedler, J. V.; Shen, M., *Analytical Chemistry* **2015,** *87* (10), 5095-5100.

143.   Iwai, N. T.; Kramaric, M.; Crabbe, D.; Wei, Y.; Chen, R.; Shen, M., *Analytical Chemistry* **2018,** *90* (5), 3067-3072.

Chapter 3 References

1.   Rocha, S. M.; Pires, J.; Esteves, M.; Graça, B.; Bernardino, L., *Frontiers in Cellular Neuroscience* **2014,** *8* (120).

2.   Metcalfe, D. D.; Baram, D.; Mekori, Y. A., *Physiological Reviews* **1997,** *77* (4), 1033-1079.

3.   Ennis, M.; Truneh, A.; White, J. R.; Pearce, F. L., *Nature* **1981,** *289* (5794), 186-187.

4.   Jutel, M.; Watanabe, T.; Klunker, S.; Akdis, M.; Thomet, O. A. R.; Malolepszy, J.; Zak-Nejmark, T.; Koga, R.; Kobayashi, T.; Blaser, K.; Akdis, C. A., *Nature* **2001,** *413* (6854), 420-425.

5.   Haas, H. L.; Sergeeva, O. A.; Selbach, O., *Physiological Reviews* **2008,** *88* (3), 1183-1241.

6.   Panula, P.; Pirvola, U.; Auvinen, S.; Airaksinen, M. S., *Neuroscience* **1989,** *28* (3), 585-610.

7.   Watanabe, T.; Taguchi, Y.; Hayashi, H.; Tanaka, J.; Shiosaka, S.; Tohyama, M.; Kubota, H.; Terano, Y.; Wada, H., *Neuroscience Letters* **1983,** *39* (3), 249-254.

8. Giannoni, P.; Passani, M.-B.; Nosi, D.; Chazot, P. L.; Shenton, F. C.; Medhurst, A. D.; Munari, L.; Blandina, P., *European Journal of Neuroscience* **2009,** *29* (12), 2363-2374.

9. Health, N. I. o., Consideration of Sex as a Biological Variable in NIH-Funded Research: NOT-OD-15-102. 2015.

10. Rainville, J. R.; Tsyglakova, M.; Hodes, G. E., *Frontiers in Neuroendocrinology* **2018,** *50*, 67-90.

11. Mackey, E.; Ayyadurai, S.; Pohl, C. S.; D' Costa, S.; Li, Y.; Moeser, A. J., *Biology of Sex Differences* **2016,** *7* (1), 60.

12. GUSTAFSSON, B.; KAHLSON, G.; ROSENGREN, E., *Acta Physiologica Scandinavica* **1957,** *41* (2-3), 217-228.

13. Kim, K. S., *American Journal of Physiology-Legacy Content* **1959,** *197* (6), 1258-1260.

14. Leitch, J. L.; Debley, V. G.; Haley, T. J., *American Journal of Physiology-Legacy Content* **1956,** *187* (2), 307-311.

15. Taylor, K. M.; Snyder, S. H., *Journal of Neurochemistry* **1972,** *19* (2), 341-354.

16. Björklund, A.; Falck, B.; Owman, C., *Fluorescence Microscopic and Microspectrofluometric Techniques for the Cellular Localization and Characterization of Biogenic Amines*. North-Holland: 1972.

17. Maśliński, C., *Agents and Actions* **1975,** *5* (3), 183-225.

18. ORR, E.; QUAY, W. B., *Endocrinology* **1975,** *96* (4), 941-945.

19. Green, H.; Erickson, R. W., *International Journal of Neuropharmacology* **1964,** *3* (3), 315-320.

20. Flik, G.; Folgering, J. H. A.; Cremers, T. I. H. F.; Westerink, B. H. C.; Dremencov, E., *Journal of Molecular Neuroscience* **2015,** *56* (2), 320-328.

21. Itoh, Y.; Oishi, R.; Nishibori, M.; Saeki, K., *Journal of Neurochemistry* **1991,** *56* (3), 769-774.

22. Ferretti, C.; Blengio, M.; Ghi, P.; Adage, T.; Portaleone, P.; Gamalero, S. R., *Pharmacology Biochemistry and Behavior* **1998,** *59* (1), 255-260.

23. Dupré, C.; Lovett-Barron, M.; Pfaff, D. W.; Kow, L.-M., *Proceedings of the National Academy of Sciences* **2010,** *107* (27), 12311.

24. Samaranayake, S.; Abdalla, A.; Robke, R.; Nijhout, H. F.; Reed, M. C.; Best, J.; Hashemi, P., *Journal of Neurochemistry* **2016,** *138* (3), 374-383.

25. Samaranayake, S.; Abdalla, A.; Robke, R.; Wood, K. M.; Zeqja, A.; Hashemi, P., *Analyst* **2015,** *140* (11), 3759-3765.

26. Schlicker, E.; Betz, R.; Göthert, M., *Naunyn-Schmiedeberg's Archives of Pharmacology* **1988,** *337* (5), 588-590.

27. Threlfell, S.; Cragg, S. J.; Kalló, I.; Turi, G. F.; Coen, C. W.; Greenfield, S. A., *The Journal of Neuroscience* **2004,** *24* (40), 8704.

28. Hashemi, P.; Dankoski, E. C.; Petrovic, J.; Keithley, R. B.; Wightman, R. M., *Analytical Chemistry* **2009,** *81* (22), 9462-9471.

29. Paxinos, G.; Franklin, K. B., *Paxinos and Franklin's the mouse brain in stereotaxic coordinates*. Academic press: 2019.

30. Caligioni, C. S., *Curr Protoc Neurosci* **2009,** *Appendix 4*, Appendix-4I.

31. Bracken, M. B., *J R Soc Med* **2009,** *102* (3), 120-122.

32. Musatov, S.; Chen, W.; Pfaff, D. W.; Mobbs, C. V.; Yang, X.-J.; Clegg, D. J.; Kaplitt, M. G.; Ogawa, S., *Proceedings of the National Academy of Sciences* **2007,** *104* (7), 2501.

33. Lund, T. D.; Rovis, T.; Chung, W. C. J.; Handa, R. J., *Endocrinology* **2005,** *146* (2), 797-807.

34. Mori, H.; Matsuda, K.-I.; Yamawaki, M.; Kawata, M., *PLoS One* **2014,** *9* (5), e96232-e96232.

35. Gotoh, K.; Masaki, T.; Chiba, S.; Higuchi, K.; Kakuma, T.; Shimizu, H.; Mori, M.; Sakata, T.; Yoshimatsu, H., *Journal of Neurochemistry* **2009,** *110* (6), 1796-1805.

36. Baker, A. E.; Brautigam, V. M.; Watters, J. J., *Endocrinology* **2004,** *145* (11), 5021-5032.

37. Deshpande, R.; Khalili, H.; Pergolizzi, R. G.; Michael, S. D.; Chang, M.-D. Y., *American Journal of Reproductive Immunology* **1997,** *38* (1), 46-54.

38. Vegeto, E.; Bonincontro, C.; Pollio, G.; Sala, A.; Viappiani, S.; Nardi, F.; Brusadelli, A.; Viviani, B.; Ciana, P.; Maggi, A., *The Journal of Neuroscience* **2001,** *21* (6), 1809.

39. Lei, B.; Mace, B.; Dawson, H. N.; Warner, D. S.; Laskowitz, D. T.; James, M. L., *PLoS One* **2014,** *9* (7), e103969.

40. Fish, E. N., *Nature Reviews Immunology* **2008,** *8* (9), 737-744.

41. Reckelhoff, J. F., *Hypertension* **2001,** *37* (5), 1199-1208.

42. Saylor, R. A.; Hersey, M.; West, A.; Buchanan, A. M.; Berger, S. N.; Nijhout, H. F.; Reed, M. C.; Best, J.; Hashemi, P., *Frontiers in Neuroscience* **2019,** *13* (362).

43. Prell, G. D.; Green, J. P., *Agents and Actions* **1994,** *41* (1), C5-C8.

44. Ferris, M. J.; Calipari, E. S.; Yorgason, J. T.; Jones, S. R., *ACS Chemical Neuroscience* **2013,** *4* (5), 693-703.

45. Beery, A. K.; Zucker, I., *Neurosci Biobehav Rev* **2011,** *35* (3), 565-572.

46. Muñoz-Cruz, S.; Mendoza-Rodríguez, Y.; Nava-Castro, K. E.; Yepez-Mulia, L.; Morales-Montor, J., *Journal of Immunology Research* **2015,** *2015*, 351829.

47. Krzych, U.; Strausser, H. R.; Bressler, J. P.; Goldstein, A. L., *The Journal of Immunology* **1978,** *121* (4), 1603.

48. Sánchez, C.; Meier, E., *Psychopharmacology* **1997,** *129* (3), 197-205.

49. West, A.; Best, J.; Abdalla, A.; Nijhout, H. F.; Reed, M.; Hashemi, P., *Neurochemistry International* **2019,** *123*, 50-58.

50. Watson, R. E.; Langub, M. C.; Engle, M. G.; Maley, B. E., *Brain Research* **1995,** *689* (2), 254-264.

51. Adachi, S.; Yamada, S.; Takatsu, Y.; Matsui, H.; Kinoshita, M.; Takase, K.; Sugiura, H.; Ohtaki, T.; Matsumoto, H.; Uenoyama, Y.; Tsukamura, H.; Inoue, K.; Maeda, K.-i., *Journal of Reproduction and Development* **2007,** *advpub*, 0701090061-0701090061.

52. RUBIN, B. S.; BARFIELD, R. J., *Endocrinology* **1983,** *113* (2), 797-804.

53. Zhou, J.; Lee, A. W.; Devidze, N.; Zhang, Q.; Kow, L.-M.; Pfaff, D. W., *Journal of Neurophysiology* **2007,** *98* (6), 3143-3152.

54. Oishi, R.; Adachi, N.; Saeki, K., *European Journal of Pharmacology* **1993,** *237* (2), 155-159.

55. Calcutt, C. R.; Ganellin, C. R.; Griffiths, R.; Leigh, B. K.; Maguire, J. P.; Mitchell, R. C.; Mylek, M. E.; Parsons, M. E.; Smith, I. R.; Young, R. C., *Br J Pharmacol* **1988,** *93* (1), 69-78.

135

56.   Ghi, P.; Orsetti, M.; Gamalero, S. R.; Ferretti, C., *Pharmacology Biochemistry and Behavior* **1999,** *64* (4), 761-766.

57.   McEwen, B.; Akama, K.; Alves, S.; Brake, W. G.; Bulloch, K.; Lee, S.; Li, C.; Yuen, G.; Milner, T. A., *Proceedings of the National Academy of Sciences* **2001,** *98* (13), 7093.

58.   Roof, R. L.; Hall, E. D., *Journal of Neurotrauma* **2000,** *17* (5), 367-388.

59.   Diaz Brinton, R., *Endocrinology* **2012,** *153* (8), 3571-3578.

60.   Weihe, E.; Schäfer, M. K. H.; Erickson, J. D.; Eiden, L. E., *Journal of Molecular Neuroscience* **1994,** *5* (3), 149-164.

61.   Erickson, J. D.; Schafer, M. K.; Bonner, T. I.; Eiden, L. E.; Weihe, E., *Proceedings of the National Academy of Sciences* **1996,** *93* (10), 5166.

62.   Garbarg, M.; Barbin, G.; Rodergas, E.; Schwartz, J. C., *Journal of Neurochemistry* **1980,** *35* (5), 1045-1052.

63.   Takehiko, W.; Atsushi, Y.; Kazutaka, M.; Hiroshi, W., *Trends in Pharmacological Sciences* **1990,** *11* (9), 363-367.

64.   Maeyama, K.; Watanabe, T.; Taguchi, Y.; Yamatodani, A.; Wada, H., *Biochemical Pharmacology* **1982,** *31* (14), 2367-2370.

65.   Eagger, S. A.; Levy, R.; Sahakian, B. J., *The Lancet* **1991,** *337* (8748), 989-992.

66.   Farlow, M.; Gracon, S. I.; Hershey, L. A.; Lewis, K. W.; Sadowsky, C. H.; Dolan-Ureno, J.; Asher, S. W.; Beaver, C.; Hamilton, D.; Bergman, S. M.; Roger, L. F.; Black, S. E.; Carr, S.; Winchester, T.; Layne, E.; Clark, C.; Dexter, J.; DuBoff, E. A.; Hendrie, H.; Caress, J.; Shatz, R.; Hanna, G. R.; Brashear, H. R.; Damgaard, P.; Hershey, L. A.; Donnelly, K.; Burch, K.; Homan, R. W.; McSweeney, A. J.; Ann Barczak, M.; Mattes, J. A.; Hermann, A. M.; Mohr, E.; Mendis, T.; Roberts, J.; Begin, L.; Sampson, M.; Ott, B. R.; Lannon, M. C.; Prendergast, J. J.; Madan, S.; Hanning, R.; Martinez, W.; Stone, R.; Winner, P.; Zuniga, J.; Mate, L. J.; Ehlert, B. J.; Lessard, C.; Seltzer, B.; Taylor, J. R.; Calabrese, V. P.; Harkins, S. W.; Weis, S. J.; Slade, W.; Sommer, B. R.; Wichter, M.; Schwartz, M.; Eastman, J.; Thein, S. G., Jr; Williams, G.; Dewar, J. A.; Foster, N. L.; Bluemlein, L. A.; Gelb, D. J.; Berent, S.; Giordani, B.; Baron, B. A.; Myers, S., *JAMA* **1992,** *268* (18), 2523-2529.

67.   Wood, K. M.; Zeqja, A.; Nijhout, H. F.; Reed, M. C.; Best, J.; Hashemi, P., *Journal of Neurochemistry* **2014,** *130* (3), 351-359.

68.   Best, J.; Nijhout, H. F.; Samaranayake, S.; Hashemi, P.; Reed, M., *Theoretical Biology and Medical Modelling* **2017,** *14* (1), 24.

Chapter 4 References

1.   Panula, P.; Nuutinen, S., *Nature Reviews Neuroscience* **2013,** *14* (7), 472-487.

2.   Goodchild, R. E.; Court, J. A.; Hobson, I.; Piggott, M. A.; Perry, R. H.; Ince, P.; Jaros, E.; Perry, E. K., *European Journal of Neuroscience* **1999,** *11* (2), 449-456.

3.   Panula, P.; Rinne, J.; Kuokkanen, K.; Eriksson, K. S.; Sallmen, T.; Kalimo, H.; Relja, M., *Neuroscience* **1997,** *82* (4), 993-997.

4.   Anichtchik, O. V.; Peitsaro, N.; Rinne, J. O.; Kalimo, H.; Panula, P., *Neurobiology of Disease* **2001,** *8* (4), 707-716.

5.   Esbenshade, T. A.; Browman, K. E.; Bitner, R. S.; Strakhova, M.; Cowart, M. D.; Brioni, J. D., *Br J Pharmacol* **2008,** *154* (6), 1166-1181.

6.   Berlin, M.; Boyce, C. W.; de Lera Ruiz, M., *Journal of Medicinal Chemistry* **2011,** *54* (1), 26-53.

7.   Schlicker, E.; Betz, R.; Göthert, M., *Naunyn-Schmiedeberg's Archives of Pharmacology* **1988,** *337* (5), 588-590.

8.   Schlicker, E.; Fink, K.; Detzner, M.; Göthert, M., *Journal of Neural Transmission / General Section JNT* **1993,** *93* (1), 1-10.

9.   Schlicker, E.; Werthwein, S.; Zentner, J., *Fundamental & Clinical Pharmacology* **1999,** *13* (1), 120-122.

10.   Brown, R. E.; Reymann, K. G., *The Journal of Physiology* **1996,** *496* (1), 175-184.

11.   Jang, I. S.; Rhee, J. S.; Watanabe, T.; Akaike, N.; Akaike, N., *The Journal of physiology* **2001,** *534* (Pt 3), 791-803.

12.   Blandina, P.; Giorgetti, M.; Bartolini, L.; Cecchi, M.; Timmerman, H.; Leurs, R.; Pepeu, G.; Giovannini, M. G., *Br J Pharmacol* **1996,** *119* (8), 1656-1664.

13.   Schwartz, J.-C.; Baudry, M.; Chast, F.; Pollard, H.; Bischoff, S.; Krishnamoorthy, M. S., Histamine in the Brain: Importance of Transmethylation Processes and Their Regulation. In *Central Nervous System: Studies on Metabolic Regulation and Function*, Genazzani, E.; Herken, H., Eds. Springer Berlin Heidelberg: Berlin, Heidelberg, 1974; pp 172-184.

14.   G D Prell, a.; Green, J. P., *Annual Review of Neuroscience* **1986,** *9* (1), 209-254.

15.   Huszti, Z.; Prast, H.; Tran, M. H.; Fischer, H.; Philippu, A., *Naunyn-Schmiedeberg's Archives of Pharmacology* **1997,** *357* (1), 49-53.

16.   Barnes, W. G.; Hough, L. B., *Journal of Neurochemistry* **2002,** *82* (5), 1262-1271.

17.   Samaranayake, S.; Abdalla, A.; Robke, R.; Nijhout, H. F.; Reed, M. C.; Best, J.; Hashemi, P., *Journal of Neurochemistry* **2016,** *138* (3), 374-383.

18.   Walters, S. H.; Robbins, E. M.; Michael, A. C., *ACS Chemical Neuroscience* **2015,** *6* (8), 1468-1475.

19.   Wood, K. M.; Zeqja, A.; Nijhout, H. F.; Reed, M. C.; Best, J.; Hashemi, P., *Journal of Neurochemistry* **2014,** *130* (3), 351-359.

20.   Daws, L. C., *Pharmacol Ther* **2009,** *121* (1), 89-99.

21.   Yoshikawa, T.; Naganuma, F.; Iida, T.; Nakamura, T.; Harada, R.; Mohsen, A. S.; Kasajima, A.; Sasano, H.; Yanai, K., *Glia* **2013,** *61* (6), 905-916.

22.   Gasser, P. J.; Lowry, C. A.; Orchinik, M., *The Journal of Neuroscience* **2006,** *26* (34), 8758.

23.   Schneider , E.; Machavoine , F. o.; Pléau , J.-M.; Bertron , A.-F.; Thurmond , R. L.; Ohtsu , H.; Watanabe , T.; Schinkel , A. H.; Dy , M., *Journal of Experimental Medicine* **2005,** *202* (3), 387-393.

24.   Nackenoff, A. G.; Moussa-Tooks, A. B.; McMeekin, A. M.; Veenstra-VanderWeele, J.; Blakely, R. D., *Neuropsychopharmacology* **2016,** *41* (7), 1733-1741.

25.   Nackenoff, A. G.; Simmler, L. D.; Baganz, N. L.; Pehrson, A. L.; Sánchez, C.; Blakely, R. D., *ACS Chemical Neuroscience* **2017,** *8* (5), 1092-1100.

26.   Hashemi, P.; Dankoski, E. C.; Petrovic, J.; Keithley, R. B.; Wightman, R. M., *Analytical Chemistry* **2009,** *81* (22), 9462-9471.

27.   Samaranayake, S.; Abdalla, A.; Robke, R.; Wood, K. M.; Zeqja, A.; Hashemi, P., *Analyst* **2015,** *140* (11), 3759-3765.

28.   Best, J.; Nijhout, H. F.; Samaranayake, S.; Hashemi, P.; Reed, M., *Theoretical Biology and Medical Modelling* **2017,** *14* (1), 24.

137

29.   Paxinos, G.; Franklin, K. B., *Paxinos and Franklin's the mouse brain in stereotaxic coordinates*. Academic press: 2019.

30.   Park, J.; Kile, B. M.; Mark Wightman, R., *European Journal of Neuroscience* **2009,** *30* (11), 2121-2133.

31.   Zomkowski, A. D. E.; Engel, D.; Gabilan, N. H.; Rodrigues, A. L. S., *European Neuropsychopharmacology* **2010,** *20* (11), 793-801.

32.   Kulikov, A. V.; Tikhonova, M. A.; Osipova, D. V.; Kulikov, V. A.; Popova, N. K., *Pharmacology Biochemistry and Behavior* **2011,** *99* (4), 683-687.

33.   Mikail, H. G.; Dalla, C.; Kokras, N.; Kafetzopoulos, V.; Papadopoulou-Daifoti, Z., *Physiology & Behavior* **2012,** *107* (2), 201-206.

34.   Horton, R. E.; Apple, D. M.; Owens, W. A.; Baganz, N. L.; Cano, S.; Mitchell, N. C.; Vitela, M.; Gould, G. G.; Koek, W.; Daws, L. C., *The Journal of Neuroscience* **2013,** *33* (25), 10534.

35.   Henry, L. K.; Field, J. R.; Adkins, E. M.; Parnas, M. L.; Vaughan, R. A.; Zou, M.-F.; Newman, A. H.; Blakely, R. D., *Journal of Biological Chemistry* **2006,** *281* (4), 2012-2023.

36.   Simmler, L. D.; Blakely, R. D., *ACS Chemical Neuroscience* **2019,** *10* (7), 3053-3060.

37.   Bacq, A.; Balasse, L.; Biala, G.; Guiard, B.; Gardier, A. M.; Schinkel, A.; Louis, F.; Vialou, V.; Martres, M. P.; Chevarin, C.; Hamon, M.; Giros, B.; Gautron, S., *Molecular Psychiatry* **2012,** *17* (9), 926-939.

38.   Zhu, H.-J.; Appel, D. I.; Gründemann, D.; Richelson, E.; Markowitz, J. S., *Pharmacological Research* **2012,** *65* (4), 491-496.

39.   Nestler, E. J.; Barrot, M.; DiLeone, R. J.; Eisch, A. J.; Gold, S. J.; Monteggia, L. M., *Neuron* **2002,** *34* (1), 13-25.

40.   Raison, C. L.; Capuron, L.; Miller, A. H., *Trends in Immunology* **2006,** *27* (1), 24-31.

41.   Maes, M.; Yirmyia, R.; Noraberg, J.; Brene, S.; Hibbeln, J.; Perini, G.; Kubera, M.; Bob, P.; Lerer, B.; Maj, M., *Metabolic Brain Disease* **2009,** *24* (1), 27-53.

42.   Dantzer, R., *Biological psychiatry* **2012**.

43.   Schiepers, O. J. G.; Wichers, M. C.; Maes, M., *Progress in Neuro-Psychopharmacology and Biological Psychiatry* **2005,** *29* (2), 201-217.

44.   Raison, C. L.; Rutherford, R. E.; Woolwine, B. J.; Shuo, C.; Schettler, P.; Drake, D. F.; Haroon, E.; Miller, A. H., *JAMA Psychiatry* **2013,** *70* (1), 31-41.

45.   Lee, Y.; Subramaniapillai, M.; Brietzke, E.; Mansur, R. B.; Ho, R. C.; Yim, S. J.; McIntyre, R. S., *Therapeutic Advances in Psychopharmacology* **2018,** *8* (12), 337-348.

46.   Shariq, A. S.; Brietzke, E.; Rosenblat, J. D.; Barendra, V.; Pan, Z.; McIntyre, R. S., *Progress in Neuro-Psychopharmacology and Biological Psychiatry* **2018,** *83*, 86-91.

47.   Krishnan, V.; Nestler, E. J., *Nature* **2008,** *455* (7215), 894-902.

48.   Engel, K.; Zhou, M.; Wang, J., *Journal of Biological Chemistry* **2004,** *279* (48), 50042-50049.

49.   Koepsell, H.; Lips, K.; Volk, C., *Pharmaceutical Research* **2007,** *24* (7), 1227-1251.

50.   Hyttel, J., *Int Clin Psychopharmacol* **1994,** *9*, 19-26.

51.   Fraser-Spears, R.; Krause-Heuer, A. M.; Basiouny, M.; Mayer, F. P.; Manishimwe, R.; Wyatt, N. A.; Dobrowolski, J. C.; Roberts, M. P.; Greguric, I.; Kumar, N.; Koek, W.;

138

Sitte, H. H.; Callaghan, P. D.; Fraser, B. H.; Daws, L. C., *European Journal of Pharmacology* **2019,** *842*, 351-364.

52.   Thompson, B. J.; Jessen, T.; Henry, L. K.; Field, J. R.; Gamble, K. L.; Gresch, P. J.; Carneiro, A. M.; Horton, R. E.; Chisnell, P. J.; Belova, Y.; McMahon, D. G.; Daws, L. C.; Blakely, R. D., *Proceedings of the National Academy of Sciences* **2011,** *108* (9), 3785.

53.   Owens, M. J.; Knight, D. L.; Nemeroff, C. B., *Biological Psychiatry* **2001,** *50* (5), 345-350.

54.   Neumann, H., *Glia* **2001,** *36* (2), 191-199.

55.   Watkins, C. C.; Sawa, A.; Pomper, M. G., *Translational Psychiatry* **2014,** *4* (1), e350-e350.

Chapter 5 References

1.   Goldberg, D., *World Psychiatry* **2011,** *10* (3), 226-228.

2.   Chen, L.-S.; Eaton, W. W.; Gallo, J. J.; Nestadt, G., *Journal of Affective Disorders* **2000,** *59* (1), 1-11.

3.   Ballard, E. D.; Yarrington, J. S.; Farmer, C. A.; Lener, M. S.; Kadriu, B.; Lally, N.; Williams, D.; Machado-Vieira, R.; Niciu, M. J.; Park, L.; Zarate, C. A., *Journal of Affective Disorders* **2018,** *231*, 51-57.

4.   Czeisler, M. E.; Rashon, L. I.; Petrosky, E.; Wiley, J. F.; Christensen, A.; Njai, R.; Weaver, M. D.; Robbins, R.; Facer-Childs, E. R.; Barger, L. K.; Czeisler, C. A.; Howard, M. E.; Rajaratnam, S. M. W., Mental Health, Substance Use, and Suicidal Ideation During the COVID-19 Pandemic - United States, June 24-30, 2020. Prevention, C. f. D. C. a., Ed. 2020; Vol. 69, pp 1049-1057.

5.   Peng, M.; Mo, B.; Liu, Y.; Xu, M.; Song, X.; Liu, L.; Fang, Y.; Guo, T.; Ye, J.; Yu, Z.; Deng, Q.; Zhang, X., *Journal of Affective Disorders* **2020,** *275*, 119-124.

6.   Wong, M.-L.; Licinio, J., *Nature Reviews Drug Discovery* **2004,** *3* (2), 136-151.

7.   Belmaker, R. H.; Agam, G., *New England Journal of Medicine* **2008,** *358* (1), 55-68.

8.   Krishnan, V.; Nestler, E. J., *Nature* **2008,** *455* (7215), 894-902.

9.   Hiemke, C.; Härtter, S., *Pharmacol Ther* **2000,** *85* (1), 11-28.

10.   Artigas, F.; Bortolozzi, A.; Celada, P., *European Neuropsychopharmacology* **2018,** *28* (4), 445-456.

11.   Derry, H. M.; Padin, A. C.; Kuo, J. L.; Hughes, S.; Kiecolt-Glaser, J. K., *Current Psychiatry Reports* **2015,** *17* (10), 78.

12.   Hurley, L. L.; Tizabi, Y., *Neurotoxicity Research* **2013,** *23* (2), 131-144.

13.   Kim, Y.-K.; Na, K.-S.; Myint, A.-M.; Leonard, B. E., *Progress in Neuro-Psychopharmacology and Biological Psychiatry* **2016,** *64*, 277-284.

14.   Kempuraj, D.; Thangavel, R.; Selvakumar, G. P.; Zaheer, S.; Ahmed, M. E.; Raikwar, S. P.; Zahoor, H.; Saeed, D.; Natteru, P. A.; Iyer, S.; Zaheer, A., *Frontiers in Cellular Neuroscience* **2017,** *11* (216).

15.   Samaranayake, S.; Abdalla, A.; Robke, R.; Nijhout, H. F.; Reed, M. C.; Best, J.; Hashemi, P., *Journal of Neurochemistry* **2016,** *138* (3), 374-383.

16.   Eller, T.; Vasar, V.; Shlik, J.; Maron, E., *Progress in Neuro-Psychopharmacology and Biological Psychiatry* **2008,** *32* (2), 445-450.

17.   Haroon, E.; Daguanno, A. W.; Woolwine, B. J.; Goldsmith, D. R.; Baer, W. M.; Wommack, E. C.; Felger, J. C.; Miller, A. H., *Psychoneuroendocrinology* **2018,** *95*, 43-49.

18.   Tyring, S.; Gottlieb, A.; Papp, K.; Gordon, K.; Leonardi, C.; Wang, A.; Lalla, D.; Woolley, M.; Jahreis, A.; Zitnik, R.; Cella, D.; Krishnan, R., *The Lancet* **2006,** *367* (9504), 29-35.

19.   Raison, C. L.; Rutherford, R. E.; Woolwine, B. J.; Shuo, C.; Schettler, P.; Drake, D. F.; Haroon, E.; Miller, A. H., *JAMA Psychiatry* **2013,** *70* (1), 31-41.

20.   Köhler, O.; Benros, M. E.; Nordentoft, M.; Farkouh, M. E.; Iyengar, R. L.; Mors, O.; Krogh, J., *JAMA Psychiatry* **2014,** *71* (12), 1381-1391.

21.   Abbott, R.; Whear, R.; Nikolaou, V.; Bethel, A.; Coon, J. T.; Stein, K.; Dickens, C., *Journal of Psychosomatic Research* **2015,** *79* (3), 175-184.

22.   Mendlewicz, J.; Kriwin, P.; Oswald, P.; Souery, D.; Alboni, S.; Brunello, N., *Int Clin Psychopharmacol* **2006,** *21* (4), 227-231.

23.   Barkin, R. L.; Beckerman, M.; Blum, S. L.; Clark, F. M.; Koh, E.-K.; Wu, D. S., *Drugs & Aging* **2010,** *27* (10), 775-789.

24.   Knigge, U.; Kjær, A.; Jørgensen, H.; Garbarg, M.; Ross, C.; Rouleau, A.; Warberg, J., *Neuroendocrinology* **1994,** *60* (3), 243-251.

25.   Munari, L.; Provensi, G.; Passani, M. B.; Galeotti, N.; Cassano, T.; Benetti, F.; Corradetti, R.; Blandina, P., *International Journal of Neuropsychopharmacology* **2015,** *18* (10).

26.   Willner, P., *Neurobiology of Stress* **2017,** *6*, 78-93.

27.   Wang, Y.-L.; Han, Q.-Q.; Gong, W.-Q.; Pan, D.-H.; Wang, L.-Z.; Hu, W.; Yang, M.; Li, B.; Yu, J.; Liu, Q., *Journal of Neuroinflammation* **2018,** *15* (1), 21.

28.   Farooq, R. K.; Isingrini, E.; Tanti, A.; Le Guisquet, A.-M.; Arlicot, N.; Minier, F.; Leman, S.; Chalon, S.; Belzung, C.; Camus, V., *Behavioural Brain Research* **2012,** *231* (1), 130-137.

29.   Zhang, J.-q.; Wu, X.-h.; Feng, Y.; Xie, X.-f.; Fan, Y.-h.; Yan, S.; Zhao, Q.-y.; Peng, C.; You, Z.-l., *Acta Pharmacologica Sinica* **2016,** *37* (9), 1141-1153.

30.   Hashemi, P.; Dankoski, E. C.; Petrovic, J.; Keithley, R. B.; Wightman, R. M., *Analytical Chemistry* **2009,** *81* (22), 9462-9471.

31.   Jackson, B. P.; Dietz, S. M.; Wightman, R. M., *Analytical Chemistry* **1995,** *67* (6), 1115-1120.

32.   Samaranayake, S.; Abdalla, A.; Robke, R.; Wood, K. M.; Zeqja, A.; Hashemi, P., *Analyst* **2015,** *140* (11), 3759-3765.

33.   Abdalla, A.; Atcherley, C. W.; Pathirathna, P.; Samaranayake, S.; Qiang, B.; Peña, E.; Morgan, S. L.; Heien, M. L.; Hashemi, P., *Analytical Chemistry* **2017,** *89* (18), 9703-9711.

34.   Papp, M.; Willner, P.; Muscat, R., *Psychopharmacology* **1991,** *104* (2), 255-259.

35.   Matthews, K.; Forbes, N.; Reid, I. C., *Physiology & Behavior* **1995,** *57* (2), 241-248.

36.   Forbes, N. F.; Stewart, C. A.; Matthews, K.; Reid, I. C., *Physiology & Behavior* **1996,** *60* (6), 1481-1484.

37.   Mineur, Y. S.; Belzung, C.; Crusio, W. E., *Behavioural Brain Research* **2006,** *175* (1), 43-50.

38.   Paxinos, G.; Franklin, K. B., *Paxinos and Franklin's the mouse brain in stereotaxic coordinates*. Academic press: 2019.

39.   Pothion, S.; Bizot, J.-C.; Trovero, F.; Belzung, C., *Behavioural Brain Research* **2004,** *155* (1), 135-146.
40.   Tucker, L. B.; McCabe, J. T., *Front Behav Neurosci* **2017,** *11*, 13-13.
41.   Sanna, M. D.; Ghelardini, C.; Galeotti, N., *Brain Research Bulletin* **2017,** *128*, 1-6.
42.   Castagné, V.; Moser, P.; Roux, S.; Porsolt, R. D., *Curr Protoc Neurosci* **2011,** *55* (1), 8.10A.1-8.10A.14.
43.   Risch, S. C.; Nemeroff, C. B., *J Clin Psychiatry* **1992**.
44.   Hill, M. N.; Hellemans, K. G. C.; Verma, P.; Gorzalka, B. B.; Weinberg, J., *Neuroscience & Biobehavioral Reviews* **2012,** *36* (9), 2085-2117.
45.   Vancassel, S.; Leman, S.; Hanonick, L.; Denis, S.; Roger, J.; Nollet, M.; Bodard, S.; Kousignian, I.; Belzung, C.; Chalon, S., *Journal of Lipid Research* **2008,** *49* (2), 340-348.
46.   Li, J.-M.; Kong, L.-D.; Wang, Y.-M.; Cheng, C. H. K.; Zhang, W.-Y.; Tan, W.-Z., *Life Sciences* **2003,** *74* (1), 55-73.
47.   Ahmad, A.; Rasheed, N.; Banu, N.; Palit, G., *Stress* **2010,** *13* (4), 356-365.
48.   Bekris, S.; Antoniou, K.; Daskas, S.; Papadopoulou-Daifoti, Z., *Behavioural Brain Research* **2005,** *161* (1), 45-59.
49.   Merali, Z.; Lacosta, S.; Anisman, H., *Brain Research* **1997,** *761* (2), 225-235.
50.   Fujino, K.; Yoshitake, T.; Inoue, O.; Ibii, N.; Kehr, J.; Ishida, J.; Nohta, H.; Yamaguchi, M., *Neuroscience Letters* **2002,** *320* (1), 91-95.
51.   Lu, Y.; Ho, C. S.; Liu, X.; Chua, A. N.; Wang, W.; McIntyre, R. S.; Ho, R. C., *PLoS One* **2017,** *12* (10), e0186700.
52.   Moldestad, O.; Karlsen, P.; Molden, S.; Storm, J. F., *Journal of Neuroscience Methods* **2009,** *176* (2), 57-62.
53.   Stoenica, L.; Senkov, O.; Gerardy-Schahn, R.; Weinhold, B.; Schachner, M.; Dityatev, A., *European Journal of Neuroscience* **2006,** *23* (9), 2255-2264.
54.   Ellrich, J.; Wesselak, M., *Brain Research Protocols* **2003,** *11* (3), 178-188.
55.   Anderson, J. M.; Rodriguez, A.; Chang, D. T., *Seminars in Immunology* **2008,** *20* (2), 86-100.
56.   O'Mahony, L.; Akdis, M.; Akdis, C. A., *Journal of Allergy and Clinical Immunology* **2011,** *128* (6), 1153-1162.
57.   Gold, S. M.; Irwin, M. R., *Immunology and Allergy Clinics of North America* **2009,** *29* (2), 309-320.
58.   Esposito, P.; Gheorghe, D.; Kandere, K.; Pang, X.; Connolly, R.; Jacobson, S.; Theoharides, T. C., *Brain Research* **2001,** *888* (1), 117-127.
59.   Theoharides, T. C., *Life Sciences* **1990,** *46* (9), 607-617.
60.   Rocha, S. M.; Pires, J.; Esteves, M.; Graça, B.; Bernardino, L., *Frontiers in Cellular Neuroscience* **2014,** *8* (120).
61.   Dong, Y.; Zhao, R.; Chen, X. Q.; Yu, A. C. H., *Molecular Neurobiology* **2010,** *41* (2), 218-231.
62.   Huszti, Z.; Prast, H.; Tran, M. H.; Fischer, H.; Philippu, A., *Naunyn-Schmiedeberg's Archives of Pharmacology* **1997,** *357* (1), 49-53.
63.   Nautiyal, K. M.; Ribeiro, A. C.; Pfaff, D. W.; Silver, R., *Proceedings of the National Academy of Sciences* **2008,** *105* (46), 18053.
64.   Ramirez, K.; Fornaguera-Trías, J.; Sheridan, J. F., Stress-Induced Microglia Activation and Monocyte Trafficking to the Brain Underlie the Development of Anxiety

and Depression. In *Inflammation-Associated Depression: Evidence, Mechanisms and Implications*, Dantzer, R.; Capuron, L., Eds. Springer International Publishing: Cham, 2017; pp 155-172.

65.   McKim, D. B.; Weber, M. D.; Niraula, A.; Sawicki, C. M.; Liu, X.; Jarrett, B. L.; Ramirez-Chan, K.; Wang, Y.; Roeth, R. M.; Sucaldito, A. D.; Sobol, C. G.; Quan, N.; Sheridan, J. F.; Godbout, J. P., *Molecular Psychiatry* **2018,** *23* (6), 1421-1431.

66.   Hiraga, N.; Adachi, N.; Liu, K.; Nagaro, T.; Arai, T., *European Journal of Pharmacology* **2007,** *557* (2), 236-244.

67.   Ferreira, R.; Santos, T.; Gonçalves, J.; Baltazar, G.; Ferreira, L.; Agasse, F.; Bernardino, L., *Journal of Neuroinflammation* **2012,** *9* (1), 90.

68.   Garbarg, M.; Barbin, G.; Rodergas, E.; Schwartz, J. C., *Journal of Neurochemistry* **1980,** *35* (5), 1045-1052.

69.   Maeyama, K.; Watanabe, T.; Taguchi, Y.; Yamatodani, A.; Wada, H., *Biochemical Pharmacology* **1982,** *31* (14), 2367-2370.

70.   Takehiko, W.; Atsushi, Y.; Kazutaka, M.; Hiroshi, W., *Trends in Pharmacological Sciences* **1990,** *11* (9), 363-367.

Chapter 6 References

1.   W.H.O. *World Health Organization Model List of Essential Medicines 21st List*; Online, 2019.

2.   Singh, I.; Morgan, C.; Curran, V.; Nutt, D.; Schlag, A.; McShane, R., *The Lancet Psychiatry* **2017,** *4* (5), 419-426.

3.   Berman, R. M.; Cappiello, A.; Anand, A.; Oren, D. A.; Heninger, G. R.; Charney, D. S.; Krystal, J. H., *Biological Psychiatry* **2000,** *47* (4), 351-354.

4.   Michael F. Grunebaum, M.D. ,; Hanga C. Galfalvy, Ph.D. ,; Tse-Hwei Choo, M.P.H. ,; John G. Keilp, Ph.D. ,; Vivek K. Moitra, M.D. ,; Michelle S. Parris, B.A. ,; Julia E. Marver, B.A. ,; Ainsley K. Burke, Ph.D. ,; Matthew S. Milak, M.D. ,; M. Elizabeth Sublette, M.D., Ph.D. ,; Maria A. Oquendo, M.D., Ph.D. ,; J. John Mann, M.D., *American Journal of Psychiatry* **2018,** *175* (4), 327-335.

5.   Lapidus, K. A. B.; Levitch, C. F.; Perez, A. M.; Brallier, J. W.; Parides, M. K.; Soleimani, L.; Feder, A.; Iosifescu, D. V.; Charney, D. S.; Murrough, J. W., *Biological Psychiatry* **2014,** *76* (12), 970-976.

6.   D. Jeffrey Newport, M.D., M.S., M.Div. ,; Linda L. Carpenter, M.D. ,; William M. McDonald, M.D. ,; James B. Potash, M.D., M.P.H. ,; Mauricio Tohen, M.D., Dr.P.H., M.B.A. ,; Charles B. Nemeroff, M.D., Ph.D. ,, *American Journal of Psychiatry* **2015,** *172* (10), 950-966.

7.   aan het Rot, M.; Collins, K. A.; Murrough, J. W.; Perez, A. M.; Reich, D. L.; Charney, D. S.; Mathew, S. J., *Biological Psychiatry* **2010,** *67* (2), 139-145.

8.   Abdallah, C. G.; Roache, J. D.; Averill, L. A.; Young-McCaughan, S.; Martini, B.; Gueorguieva, R.; Amoroso, T.; Southwick, S. M.; Guthmiller, K.; López-Roca, A. L.; Lautenschlager, K.; Mintz, J.; Litz, B. T.; Williamson, D. E.; Keane, T. M.; Peterson, A. L.; Krystal, J. H., *Contemporary Clinical Trials* **2019,** *81*, 11-18.

9.   Phillips, J. L.; Norris, S.; Talbot, J.; Hatchard, T.; Ortiz, A.; Birmingham, M.; Owoeye, O.; Batten, L. A.; Blier, P., *Neuropsychopharmacology* **2020,** *45* (4), 606-612.

10.   Zanos, P.; Moaddel, R.; Morris, P. J.; Georgiou, P.; Fischell, J.; Elmer, G. I.; Alkondon, M.; Yuan, P.; Pribut, H. J.; Singh, N. S.; Dossou, K. S. S.; Fang, Y.; Huang, X.-P.; Mayo, C. L.; Wainer, I. W.; Albuquerque, E. X.; Thompson, S. M.; Thomas, C. J.; Zarate Jr, C. A.; Gould, T. D., *Nature* **2016,** *533* (7604), 481-486.

11.   Zhang, J.-c.; Li, S.-x.; Hashimoto, K., *Pharmacology Biochemistry and Behavior* **2014,** *116*, 137-141.

12.   Yang, C.; Shirayama, Y.; Zhang, J. c.; Ren, Q.; Yao, W.; Ma, M.; Dong, C.; Hashimoto, K., *Translational Psychiatry* **2015,** *5* (9), e632-e632.

13.   Urquhart, L., *Nature Reviews Drug Discovery* **2019**, NA.

14.   Hashemi, P.; Dankoski, E. C.; Petrovic, J.; Keithley, R. B.; Wightman, R. M., *Analytical Chemistry* **2009,** *81* (22), 9462-9471.

15.   Samaranayake, S.; Abdalla, A.; Robke, R.; Nijhout, H. F.; Reed, M. C.; Best, J.; Hashemi, P., *Journal of Neurochemistry* **2016,** *138* (3), 374-383.

16.   Samaranayake, S.; Abdalla, A.; Robke, R.; Wood, K. M.; Zeqja, A.; Hashemi, P., *Analyst* **2015,** *140* (11), 3759-3765.

17.   Abdalla, A.; Atcherley, C. W.; Pathirathna, P.; Samaranayake, S.; Qiang, B.; Peña, E.; Morgan, S. L.; Heien, M. L.; Hashemi, P., *Analytical Chemistry* **2017,** *89* (18), 9703-9711.

18.   Paxinos, G.; Franklin, K. B., *Paxinos and Franklin's the mouse brain in stereotaxic coordinates*. Academic press: 2019.

19.   Takeda, N.; Inagaki, S.; Shiosaka, S.; Taguchi, Y.; Oertel, W. H.; Tohyama, M.; Watanabe, T.; Wada, H., *Proceedings of the National Academy of Sciences* **1984,** *81* (23), 7647.

20.   Okakura-Mochizuki, K.; Mochizuki, T.; Yamamoto, Y.; Horii, A.; Yamatodani, A., *Journal of Neurochemistry* **1996,** *67* (1), 171-176.

21.   Yang, Q. Z.; Hatton, G. I., *Brain Research* **1997,** *773* (1), 162-172.

22.   Faucard, R.; Armand, V.; Héron, A.; Cochois, V.; Schwartz, J.-C.; Arrang, J.-M., *Journal of Neurochemistry* **2006,** *98* (5), 1487-1496.

23.   Haas, H. L.; Sergeeva, O. A.; Selbach, O., *Physiological Reviews* **2008,** *88* (3), 1183-1241.

24.   Okakura, K.; Yamatodani, A.; Mochizuki, T.; Horii, A.; Wada, H., *European Journal of Pharmacology* **1992,** *213* (2), 189-192.

25.   Fell, M. J.; Flik, G.; Dijkman, U.; Folgering, J. H. A.; Perry, K. W.; Johnson, B. J.; Westerink, B. H. C.; Svensson, K. A., *Neuropharmacology* **2015,** *99*, 1-8.

26.   Fell, M. J.; Katner, J. S.; Johnson, B. G.; Khilevich, A.; Schkeryantz, J. M.; Perry, K. W.; Svensson, K. A., *Neuropharmacology* **2010,** *58* (3), 632-639.

27.   Pin, J.-P.; De Colle, C.; Bessis, A.-S.; Acher, F., *European Journal of Pharmacology* **1999,** *375* (1), 277-294.

28.   Schoepp, D. D.; Jane, D. E.; Monn, J. A., *Neuropharmacology* **1999,** *38* (10), 1431-1476.

29.   Nicoletti, F.; Bockaert, J.; Collingridge, G. L.; Conn, P. J.; Ferraguti, F.; Schoepp, D. D.; Wroblewski, J. T.; Pin, J. P., *Neuropharmacology* **2011,** *60* (7), 1017-1041.

30.   Ohishi, H.; Neki, A.; Mizuno, N., *Neuroscience Research* **1998,** *30* (1), 65-82.

31.   Gu, G.; Lorrain, D. S.; Wei, H.; Cole, R. L.; Zhang, X.; Daggett, L. P.; Schaffhauser, H. J.; Bristow, L. J.; Lechner, S. M., *Brain Research* **2008,** *1197*, 47-62.

32. Sattar, Y.; Wilson, J.; Khan, A. M.; Adnan, M.; Azzopardi Larios, D.; Shrestha, S.; Rahman, Q.; Mansuri, Z.; Hassan, A.; Patel, N. B.; Tariq, N.; Latchana, S.; Lopez Pantoja, S. C.; Vargas, S.; Shaikh, N. A.; Syed, F.; Mittal, D.; Rumesa, F., *Cureus* **2018,** *10* (5), e2652-e2652.

33. Beurel, E.; Song, L.; Jope, R. S., *Molecular Psychiatry* **2011,** *16* (11), 1068-1070.

34. Browne, C. A.; Lucki, I., *Frontiers in pharmacology* **2013,** *4*, 161.

35. Li, N.; Lee, B.; Liu, R.-J.; Banasr, M.; Dwyer, J. M.; Iwata, M.; Li, X.-Y.; Aghajanian, G.; Duman, R. S., *Science* **2010,** *329* (5994), 959.

36. Abdallah, C. G.; Averill, L. A.; Gueorguieva, R.; Goktas, S.; Purohit, P.; Ranganathan, M.; Sherif, M.; Ahn, K.-H.; D'Souza, D. C.; Formica, R.; Southwick, S. M.; Duman, R. S.; Sanacora, G.; Krystal, J. H., *Neuropsychopharmacology* **2020,** *45* (6), 990-997.

37. Wray, N. H.; Schappi, J. M.; Singh, H.; Senese, N. B.; Rasenick, M. M., *Molecular Psychiatry* **2019,** *24* (12), 1833-1843.

38. Lepack, A. E.; Fuchikami, M.; Dwyer, J. M.; Banasr, M.; Duman, R. S., *International Journal of Neuropsychopharmacology* **2014,** *18* (1).

39. Zhou, W.; Wang, N.; Yang, C.; Li, X. M.; Zhou, Z. Q.; Yang, J. J., *European Psychiatry* **2014,** *29* (7), 419-423.

40. Koike, H.; Iijima, M.; Chaki, S., *Behavioural Brain Research* **2011,** *224* (1), 107-111.

41. Maeng, S.; Zarate, C. A.; Du, J.; Schloesser, R. J.; McCammon, J.; Chen, G.; Manji, H. K., *Biological Psychiatry* **2008,** *63* (4), 349-352.

42. Chaki, S., *Trends in Pharmacological Sciences* **2017,** *38* (6), 569-580.

43. Chaki, S.; Ago, Y.; Palucha-Paniewiera, A.; Matrisciano, F.; Pilc, A., *Neuropharmacology* **2013,** *66*, 40-52.

44. Zanos, P.; Highland, J. N.; Stewart, B. W.; Georgiou, P.; Jenne, C. E.; Lovett, J.; Morris, P. J.; Thomas, C. J.; Moaddel, R.; Zarate, C. A.; Gould, T. D., *Proceedings of the National Academy of Sciences* **2019,** *116* (13), 6441.

45. Fukumoto, K.; Iijima, M.; Chaki, S., *Neuropsychopharmacology* **2016,** *41* (4), 1046-1056.

46. Yli-Hankala, A.; Kirvelä, M.; Randell, T.; Lindgren, L., *Acta Anaesthesiologica Scandinavica* **1992,** *36* (5), 483-485.

47. Van der Linden, P.; Gilbart, E.; Engelman, E.; Schmartz, D.; Rood, M. d.; Vincent, J.-L., *Anesthesia & Analgesia* **1990,** *70* (6).

48. Takenaka, I.; Ogata, M.; Koga, K.; Matsumoto, T.; Shigematsu, A., *Anesthesiology* **1994,** *80* (2), 402-408.

49. Taniguchi, T.; Shibata, K.; Yamamoto, K., *Anesthesiology* **2001,** *95* (4), 928-932.

50. Lankveld, D. P. K.; Bull, S.; Dijk, P. V.; Fink-Gremmels, J.; Hellebrekers, L. J., *Vet. Res.* **2005,** *36* (2), 257-262.

51. Kawasaki, C.; Kawasaki, T.; Ogata, M.; Nandate, K.; Shigematsu, A., *Canadian Journal of Anesthesia* **2001,** *48* (8), 819-823.

52. De Kock, M.; Loix, S.; Lavand'homme, P., *CNS Neuroscience & Therapeutics* **2013,** *19* (6), 403-410.

53. Wang, N.; Yu, H.-Y.; Shen, X.-F.; Gao, Z.-Q.; Yang, C.; Yang, J.-J.; Zhang, G.-F., *Upsala Journal of Medical Sciences* **2015,** *120* (4), 241-248.

54.   Sun, J.; Li, F.; Chen, J.; Xu, J., *Annals of Clinical & Laboratory Science* **2004,** *34* (2), 181-186.

55.   Meng, C.; Liu, Z.; Liu, G.-l.; Fu, L.-s.; Zhang, M.; Zhang, Z.; Xia, H.-m.; Zhang, S.-h.; Xu, Y.-n., *Journal of Huazhong University of Science and Technology [Medical Sciences]* **2015,** *35* (3), 419-425.

56.   Jennifer L. Phillips, Ph.D. ,; Sandhaya Norris, M.D. ,; Jeanne Talbot, M.D. , Ph.D. ,; Meagan Birmingham, M.A. , M.B.A. ,; Taylor Hatchard, Ph.D. ,; Abigail Ortiz, M.D. ,; Olabisi Owoeye, M.D. ,; Lisa A. Batten, Ph.D. ,; Pierre Blier, M.D. , Ph.D., *American Journal of Psychiatry* **2019,** *176* (5), 401-409.

APPENDIX A

PERMISSION OBTAINED FROM ELSEVIER TO REPRINT THE

ARTICLE IN CHAPTER 2
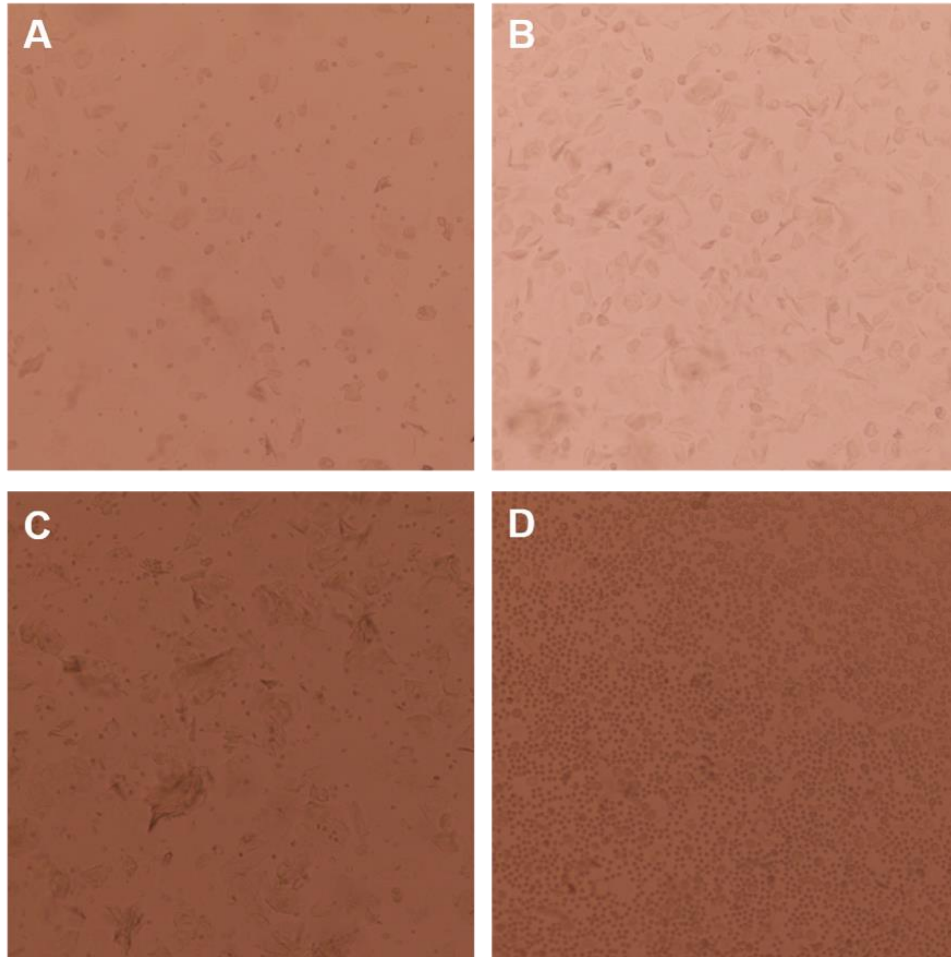
APPENDIX B

SUPPLEMENTAL FIGURES FOR CHAPTER 3

Figure B1: Representative images for estrous cycle determination. (**A**) proestrus (**B**) estrus (**C**) metestrus (**D**) diestrus.
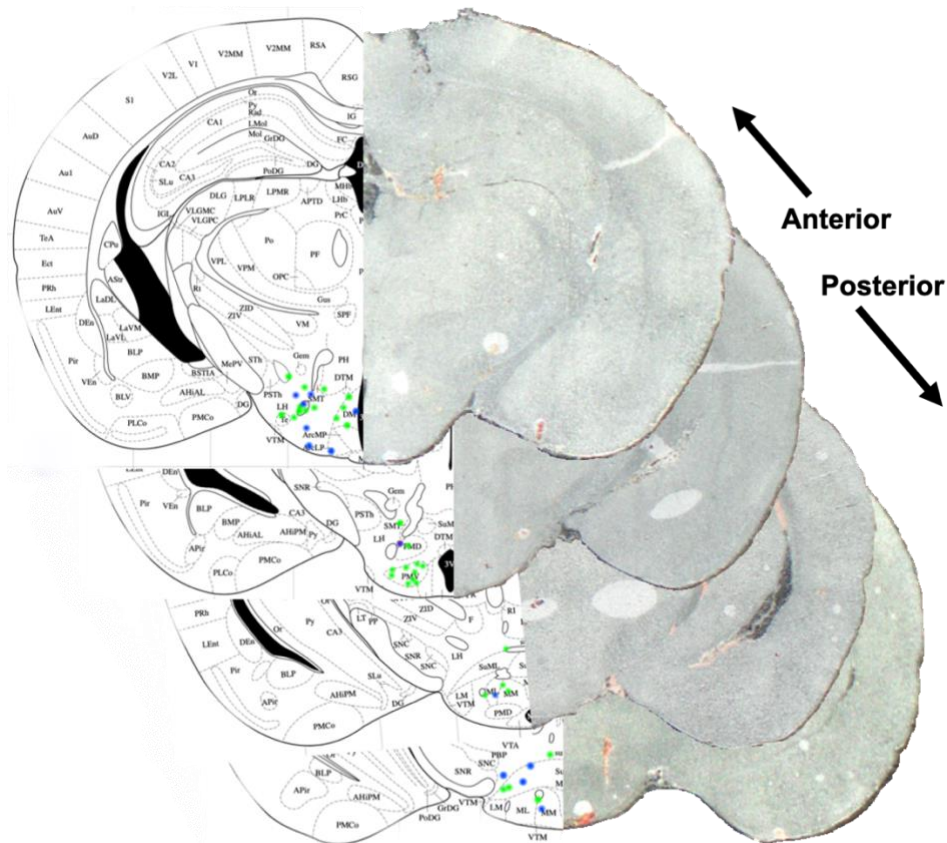
Figure B2: Electrode placement in the posterior hypothalamus. Layered brain slices and brain atlas images show the placement of CFM in hypothalamus for single (green) and double (blue) histamine release events.

APPENDIX C

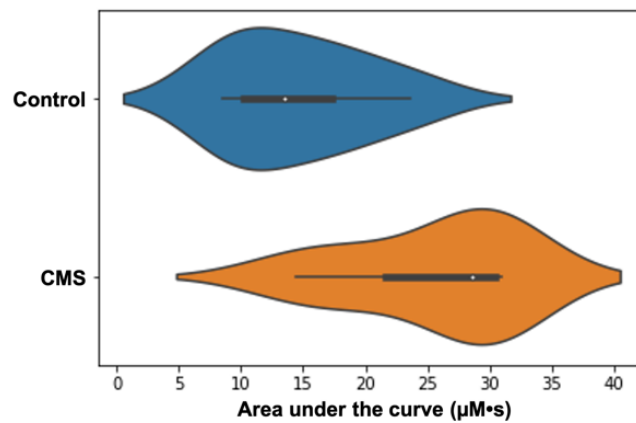SUPPLEMENTAL MATERIAL FOR CHAPTER 5

Figure C1 CMS-treated mice have larger stimulated histamine area under the curve. Violin plot comparing the area under the curve of stimulated histamine between non-stress control mice and CMS-treated mice. (AUC control: 14.51 ± 2.35 μM•s; CMS: 25.50 ± 2.80 μM•s; Wilcoxon rank-sum test, p=0.02)